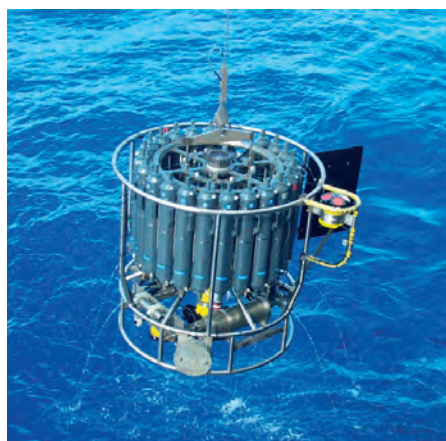




Continental moisture recycling and  
evaporation-precipitation coupling:  
water as passive tracer and as  
active component

Helge Friedrich Gößling



## Hinweis

Die Berichte zur Erdsystemforschung werden vom Max-Planck-Institut für Meteorologie in Hamburg in unregelmäßiger Abfolge herausgegeben.

Sie enthalten wissenschaftliche und technische Beiträge, inklusive Dissertationen.

Die Beiträge geben nicht notwendigerweise die Auffassung des Instituts wieder.

Die "Berichte zur Erdsystemforschung" führen die vorherigen Reihen "Reports" und "Examensarbeiten" weiter.

## Notice

*The Reports on Earth System Science are published by the Max Planck Institute for Meteorology in Hamburg. They appear in irregular intervals.*

*They contain scientific and technical contributions, including Ph. D. theses.*

*The Reports do not necessarily reflect the opinion of the Institute.*

*The "Reports on Earth System Science" continue the former "Reports" and "Examensarbeiten" of the Max Planck Institute.*



## Anschrift / Address

Max-Planck-Institut für Meteorologie  
Bundesstrasse 53  
20146 Hamburg  
Deutschland

Tel.: +49-(0)40-4 11 73-0  
Fax: +49-(0)40-4 11 73-298  
Web: [www.mpimet.mpg.de](http://www.mpimet.mpg.de)

## Layout:

Bettina Diallo, PR & Grafik

Titelfotos:

vorne:

Christian Klepp - Jochem Marotzke - Christian Klepp

hinten:

Clotilde Dubois - Christian Klepp - Katsumasa Tanaka

Continental moisture recycling and  
evaporation-precipitation coupling:  
water as passive tracer and as  
active component

Helge Friedrich Gößling

aus Hamburg

Hamburg 2013

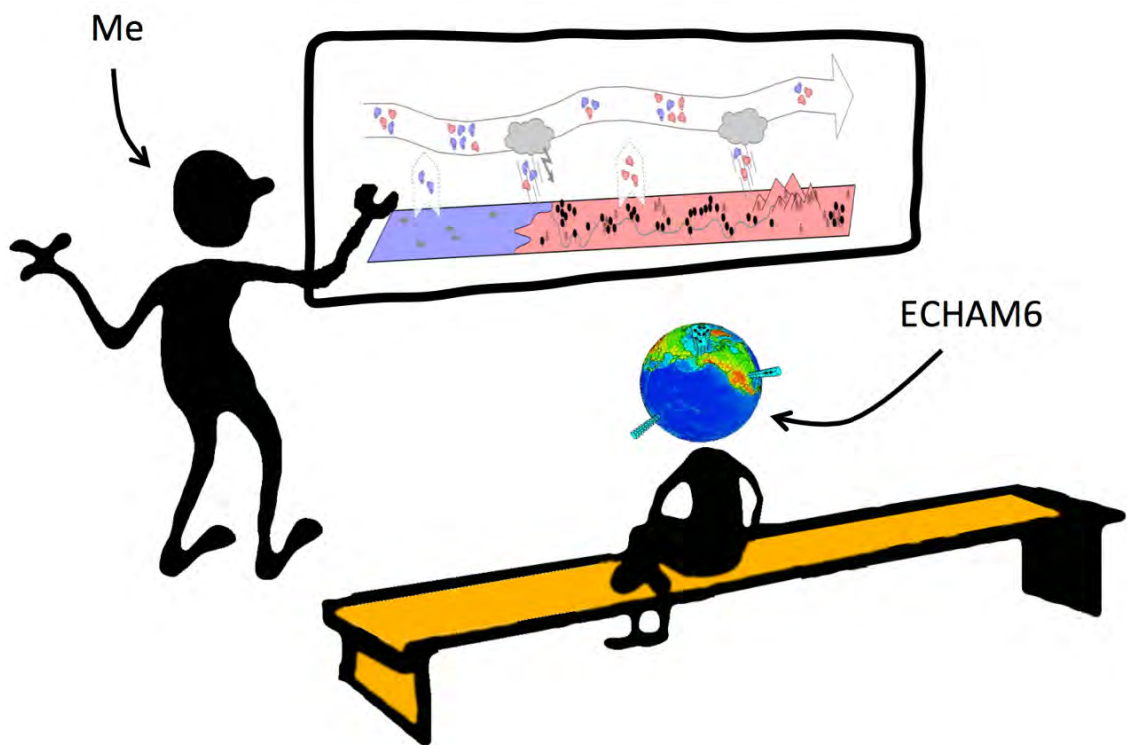
Helge Friedrich Gößling  
Max-Planck-Institut für Meteorologie  
Bundesstrasse 53  
20146 Hamburg

Als Dissertation angenommen  
vom Department Geowissenschaften der Universität Hamburg

auf Grund der Gutachten von  
Prof. Dr. Martin Claussen  
und  
Dr. Christian H. Reick

Hamburg, den 17. Januar 2013  
Prof. Dr. Jürgen Oßenbrügge  
Leiter des Fachbereichs Geowissenschaften

Continental moisture recycling and  
evaporation-precipitation coupling:  
water as passive tracer and as  
active component



Helge Friedrich Gößling

Hamburg 2013



## Thesis abstract

The global distribution of precipitation is strongly influenced by the availability of water at the continental surface. First, the replenishment of atmospheric water by evaporation, known as continental moisture recycling, sustains precipitation in downwind continental regions. This mechanism can be captured by treating moisture as a passive atmospheric tracer. Second, evaporation influences precipitation in various ways because water is, in fact, a very active component of the atmosphere.

In my dissertation I investigate several aspects of continental moisture recycling and evaporation-precipitation coupling: How often are water molecules recycled on their journey across a continent? What determines whether the ‘well-mixed’ assumption – the theoretical basis of 2D moisture tracing – is valid? How large are the errors that arise from applying the 2D approximation? What do source-sink relations of atmospheric moisture, including moisture recycling estimates, tell us about the sensitivity of precipitation to evaporation?

The methods I apply to tackle these questions include purely analytical considerations, sensitivity experiments with an atmospheric general circulation model (AGCM), and numerical tracing of atmospheric moisture. For the purpose of the latter I have implemented a simple offline 2D moisture tracing scheme and supplemented an AGCM with several variants of online water vapour tracing (WVT) schemes.

The most important results are: Continental moisture recycling can be interpreted as a Poisson process. Vertically well-mixed conditions are typically not met, giving rise (I) to a significant degree of fast-recycling that is neglected by 2D moisture tracing and (II) to errors in the horizontal advection term diagnosed by 2D moisture tracing where horizontal winds are sheared vertically. Because the latter is more characteristic of the tropics, 2D moisture tracing gives better results in the extratropics. Finally, moisture recycling estimates are no reliable indicator of the sensitivity of precipitation to evaporation because modified evaporation rates affect the atmosphere also via local coupling and via the large-scale circulation – effects that are due to water’s active role in the atmosphere.



# Contents

<b>Thesis abstract</b>	<b>i</b>
<b>List of Figures</b>	<b>vii</b>
<b>List of Tables</b>	<b>ix</b>
<b>Introduction</b>	<b>1</b>
Motivation and background . . . . .	2
Overview of and relations between the chapters . . . . .	9
Formal remarks . . . . .	10
<b>1 What do moisture recycling estimates tell us? Exploring the extreme case of non-evaporating continents</b>	<b>13</b>
Abstract . . . . .	14
1.1 Introduction . . . . .	15
1.2 Background . . . . .	18
1.2.1 Moisture recycling . . . . .	18
1.2.2 Local coupling . . . . .	20
1.2.3 Circulation . . . . .	23
1.2.4 Scale aspects . . . . .	24
1.3 Methods . . . . .	26
1.3.1 Model experiments . . . . .	26
1.3.2 Moisture tracing . . . . .	27
1.4 Recycling in the reference experiment . . . . .	29
1.5 Response to suppressed continental evaporation . . . . .	32
1.5.1 The moisture-recycling perspective . . . . .	33

1.5.2	Response of the atmospheric circulation . . . . .	40
1.5.3	Effects from local coupling . . . . .	44
1.6	Discussion . . . . .	49
1.7	Summary . . . . .	52
1.8	Conclusions . . . . .	53
<b>2</b>	<b>Atmospheric water vapour tracers and the significance of the vertical dimension</b>	<b>55</b>
	Abstract . . . . .	56
2.1	Introduction . . . . .	57
2.2	The theoretical basis of 2D moisture tracing . . . . .	60
2.3	Relevant characteristics of the atmosphere . . . . .	64
2.4	Atmospheric water vapour tracers in ECHAM6 . . . . .	69
2.4.1	Implementation . . . . .	69
2.4.2	Technical validation . . . . .	74
2.5	On the validity of the ‘well-mixed’ assumption . . . . .	75
2.6	Uncertainties associated with 3D moisture tracing . . . . .	81
2.7	Errors introduced by the 2D approximation . . . . .	85
2.8	Discussion . . . . .	93
2.9	Summary and conclusions . . . . .	98
<b>3</b>	<b>Continental moisture recycling as a Poisson process</b>	<b>101</b>
	Abstract . . . . .	102
3.1	Introduction . . . . .	103
3.2	Theory . . . . .	104
3.2.1	Exact transport equations . . . . .	104
3.2.2	The ‘well-mixed’ assumption . . . . .	105
3.2.3	Species definition and the ‘steady-state’ assumption . . . . .	105
3.2.4	The Poisson distribution as solution over land . . . . .	107
3.2.5	Extension to the ocean (case B) and the high intensity limit . . . . .	108
3.2.6	The geometric distribution as stationary solution in the low intensity limit . . . . .	110
3.3	From idealised to real conditions on Earth . . . . .	111
3.3.1	The intensity limits . . . . .	111
3.3.2	The ‘well-mixed’ assumption . . . . .	112
3.3.3	The ‘steady-state’ assumption . . . . .	113
3.4	Final remarks . . . . .	114

<b>Summary, conclusions, and outlook</b>	<b>117</b>
Summary and conclusions . . . . .	118
Further research opportunities . . . . .	125
What have we learned? . . . . .	128
<b>Bibliography</b>	<b>131</b>
<b>Acknowledgements</b>	<b>139</b>
<b>A Supplementary material for Chapter 1</b>	<b>141</b>
A.1 Effect of different averaging methods on recycling estimates . . . . .	142
A.2 Simulations with an alternative moist-convection scheme . . . . .	145
A.3 Results from the standard moist-convection scheme for January . . . . .	147



# List of Figures

1.1	Three mechanisms of evaporation-precipitation coupling . . . . .	16
1.2	Continental recycling ratio (Jan, Jul; REF) . . . . .	30
1.3	Surface evaporation and horizontal moisture flux density (Jan, Jul; REF) . . . . .	31
1.4	Precipitation (Jul; REF, DRY, DRY-REF) . . . . .	34
1.5	Precipitable water (Jul; REF, DRY, DRY-REF) . . . . .	35
1.6	Differences in near-surface temperature and in pressure reduced to sea-level (Jul; DRY-REF) . . . . .	41
1.7	Vertical velocity at 500 hPa and horizontal total mass flux in the lowest 13 model levels (Jul; REF, DRY, DRY-REF) . . . . .	42
1.8	Idealised responses to the suppression of land-evaporation . . . . .	45
1.9	Precipitation minus evaporation (Jul; REF, DRY, DRY-REF) . . . . .	47
1.10	Response of precipitation in relation to the imposed evaporation decrease (Jul)	49
2.1	Precipitation and evaporation (Jan, Jul) . . . . .	64
2.2	Fraction of days with strong moist convection (Jan, Jul) . . . . .	65
2.3	Horizontal winds at 925 hPa and 650 hPa and vertically integrated moisture flux (Jan, Jul) . . . . .	67
2.4	Directional shear as measured by $\Gamma$ (Jan, Jul) . . . . .	68
2.5	Prognostic precipitation versus diagnosed precipitation . . . . .	74
2.6	Degree to which moisture of continental origin is overrepresented in upper or lower levels (Jan, Jul; 3D-s) . . . . .	77
2.7	Degree to which moisture from EEU, AMA, and WAF is overrepresented in upper or lower levels (Jan, Jul; 3D-s) . . . . .	78
2.8	Continental recycling ratio (Jan, Jul; 3D-s, 3D-w, 3D-s-3D-w) . . . . .	82
2.9	Fraction of precipitation stemming from EEU, AMA, and WAF (Jan, Jul; 3D-s, 3D-w, 3D-s-3D-w) . . . . .	84

*List of Figures*

2.10	Continental recycling ratio (Jan, Jul; 2D, 2D-3D-w, 2D-3D-s) . . . . .	86
2.11	Fraction of precipitation stemming from EEU, AMA, and WAF (Jan, Jul; 2D, 2D-3D-w, 2D-3D-s) . . . . .	88
2.12	The source regions N, SW, SE, and AFR, and the western Sahel region . . .	90
2.13	Monthly precipitation in the western Sahel stemming from N, SW, SE, and AFR (3D-s, 3D-w, 2D) . . . . .	91
2.14	Spatially resolved precipitation in the western Sahel stemming from N and SW (Jul; 3D-s, 3D-w, 2D) . . . . .	92
2.15	Horizontal winds at 925 hPa and 650 hPa, ERA-Interim data (Jan, Jul) . . .	94
2.16	Fraction of days with strong moist convection, ERA-Interim data (Jan, Jul)	95
A.1	Comparison of continental recycling ratios that have been aggregated differ- ently over time . . . . .	143
A.2	Precipitation with the Tiedtke convection scheme (Jul; REF, DRY, DRY-REF)	146
A.3	Precipitation (Jan; REF, DRY, DRY-REF; standard convection) . . . . .	148
A.4	Precipitable water (Jan; REF, DRY, DRY-REF; standard convection) . . . .	149
A.5	Difference in near-surface temperature and in pressure reduced to sea-level (Jan; DRY-REF; standard convection) . . . . .	150
A.6	Vertical velocity at 500 hPa and horizontal total mass flux in the lowest 13 model levels (Jan; REF, DRY, DRY-REF; standard convection) . . . . .	151
A.7	Precipitation minus evaporation (Jan; REF, DRY, DRY-REF; standard con- vection) . . . . .	152
A.8	Response of precipitation in relation to the imposed evaporation decrease (Jan; standard convection) . . . . .	153

# List of Tables

1.1	Areal mean continental recycling ratio, evaporation, precipitation, and precipitable water (Jul; REF), and the response of precipitation and precipitable water (Jul; DRY-REF) . . . . .	38
2.1	Locations of the 1,000 km-scale rectangular source regions . . . . .	76
2.2	Annual precipitation in the western Sahel stemming from N, SW, SE, and AFR (3D-s, 3D-w, 2D) . . . . .	91



Water is the driving force in nature.

---

*(Leonardo da Vinci)*

# Introduction

## **Motivation and background**

If there is one chemical compound that contributes most to making the Earth a special planet, it is arguably water. Life formed in it and was never able to break away from it as solvent and as part of its chemical repertoire. On land life thrives in its amazing diversity only where sufficient amounts of rain soak the soils. Apart from the icy regions on Earth where abundance of life is limited because water prefers the solid state, the global distribution of biological activity on land mirrors the global distribution of precipitation. Even the one animal that sometimes seems to be beyond natural constraints is at water's mercy for drinking, food, and wealth. In particular against the background of global climate change that we are facing, to better understand the processes that determine where on Earth it rains, and how much, is a scientific endeavour whose significance can scarcely be overestimated.

### **Water's role in the atmosphere**

Water is a key ingredient not only of life—it is likewise a key ingredient of the Earth's atmosphere. Many of the processes making the atmosphere the complex system we observe are brought about by the presence of water. First, in contrast to the atmosphere's main components nitrogen and oxygen, water is a potent greenhouse gas that contributes more than half to the Earth's natural greenhouse effect (e.g. Kiehl and Trenberth, 1997). Second, water exists in the atmosphere not only as a gas but aggregates to liquid drops or solid particles where the restless air masses become (over-)saturated with water, for example as a consequence of adiabatic cooling associated with rising motion. In this state—as clouds—water strongly interacts with both shortwave (solar) and longwave (terrestrial) radiation, reflecting a substantial fraction of the incoming solar radiation back to space on the one hand and hampering the escape of terrestrial radiation to space on the other. Taken together, these two counteracting effects can result in either cooling or warming of the surface, depending critically on the cloud height. The impact of changing cloudiness on climate can be large, but the relevant processes are difficult to simulate due to their complexity. As a consequence the cloud feedback is the largest contributor to uncertainties in current climate

change projections (IPCC, 2007).

A third characteristic effect water has on the atmosphere – one that is of particular interest in the context of my dissertation – is associated with the phase transitions mentioned above. These are accompanied by the release (in case of condensation) and the absorption (in case of evaporation) of latent heat. Since evaporation takes place mainly at the surface and condensation takes place mainly within the atmosphere, heat is on average transported from the surface to the atmosphere. Moreover, the release and the absorption of latent heat are responsible for what Stevens (2005) termed the Cinderella effect: when displaced vertically, expanding or shrinking saturated air parcels follow the moist adiabat instead of the steeper dry adiabat that unsaturated air parcels follow. The transition from an unsaturated to a saturated state can have the result that a convectively stable (conditionally stable) situation suddenly becomes unstable. What follows is the conversion of convectively available potential energy (CAPE) into kinetic energy. When sufficient CAPE is released, the result is a thunderstorm that is often associated with heavy precipitation. Because most of the Earth’s surface is wet, the global mean tropospheric lapse rate ( $\sim 6.5 \text{ K km}^{-1}$ , e.g. Danielson et al., 2003) is closer to the moist adiabatic lapse rate ( $\sim 5 \text{ K km}^{-1}$ ) than to the dry adiabatic lapse rate ( $\sim 10 \text{ K km}^{-1}$ ). This reduction of the tropospheric lapse rate due to the presence of water is consistent with the transport of latent heat from the surface to the atmosphere described above.

### **What determines where it rains?**

Where on Earth it rains and how much is determined by a number of factors. First of all, the global pattern of large-scale rising and sinking motion plays a dominant role: where air masses sink, precipitation is suppressed because sinking air tends to be dry. Where in contrast air masses rise, the associated convergence of moist low-level air facilitates the formation of precipitation. In the tropics and subtropics, large-scale patterns of rising and sinking motion are mainly brought about by the thermally direct circulations known as the Hadley and Walker circulations. The meridionally oriented Hadley circulation, caused by the meridional contrast in solar heating, is associated with rising motion in the intertropical convergence zone (ITCZ) and sinking motion in the adjacent subtropics. The zonally

## *Introduction*

oriented Walker circulation, caused by asymmetric sea-surface temperatures (SSTs), is associated with rising motion in the western parts and sinking motion in the eastern parts of the ocean basins. It is interesting to note that the resulting spatial distribution of precipitation constitutes a positive feedback to the large-scale circulations that generates them in the first place. This feedback arises from the diabatic latent heating terms occurring in the regions of rising motion (e.g. Hou and Lindzen, 1992).

Such thermally direct circulations are less important in the extratropics because there the large-scale flow is, due to the more pronounced Coriolis force, approximately in geostrophic balance. In the extratropics the occurrence of precipitation is mostly associated with dynamical low-pressure areas and fronts, and the distribution of precipitation is thus to a large part determined by the position and intensity of the storm tracks. In the northern hemisphere a thermally induced surface pressure contrast develops between the two large continents on the one hand and the interjacent ocean basins on the other hand, in summer and, with opposite sign, in winter. This contrast, again associated with large-scale rising and sinking motions (which are also responsible for the monsoons), leads to reversed seasonality of precipitation over the continents and over the oceans, with precipitation rates over the continents being higher in summer than in winter, but over the ocean just the opposite. Finally, orography is globally another important factor because horizontally moving air masses are forced to rise where mountains block their way. This leads to increased precipitation rates in the upwind parts and decreased precipitation rates in the downwind parts of mountain ranges.

What is so far missing in the above list of factors is the availability of water at the Earth's surface. Water is of course permanently available for evaporation at those two thirds of the surface that are covered by ocean. By contrast, land can be anything between wet and dry. It is thus possible that air masses successively dry out as they travel over a continent because the loss of water due to precipitation is not fully compensated by evaporation. The capability to store and re-evaporate previously precipitated water varies strongly between different land-surface types. Sandy or rocky deserts for example are not able to maintain evaporation for a long time after a precipitation event; instead, large amounts of river runoff are generated. At the other extreme, forest-covered land with deep-rooted trees is able to

store large amounts of water that enables the vegetation to maintain high evaporation rates even during extensive dry seasons.

The replenishment of atmospheric water by land evaporation is known as moisture recycling or precipitation recycling. If the continental scale is considered, the mechanism is also referred to as continental moisture recycling. Because the strength of moisture recycling depends on the land-surface type, it stands to reason that land-cover conversions such as those implemented in the context of agriculture should impact precipitation patterns through enhanced or attenuated moisture recycling.

## Two categories of evaporation-precipitation coupling studies

Using an atmospheric general circulation model (AGCM), Shukla and Mintz (1982) demonstrated that the state of the land surface markedly influences the Earth’s climate. Simulating an Earth with completely wet continents and an Earth with completely dry continents, they found that “the global fields of rainfall, temperature, and motion strongly depend on the land-surface evapotranspiration<sup>1</sup>”. Since then a large number of studies has dealt with the influence of land evaporation on climate, in particular on precipitation. Interestingly, these studies can be divided in two categories.

The first category of studies dealing with the influence of evaporation on precipitation comprises sensitivity studies. In these, the authors examine directly the impact on precipitation of perturbed evaporation rates brought about by soil wetness variations. This category includes numerical studies in which AGCMs are used, as well as observational studies<sup>2</sup>. The spatial scale investigated in the numerical sensitivity studies ranges from the global scale, as in case of Shukla and Mintz (1982), down to the  $\sim 100$ – $1,000$  km scale (e.g. Hohenegger et al., 2009). Depending on the scale of the soil-wetness perturbation, either global or regional models are used, and the processes that determine the response of precipitation can be quite different. While in Shukla and Mintz (1982) the large-scale atmospheric circulation

---

<sup>1</sup>Apart from literal quotations I use the term *evaporation* instead of *evapotranspiration* also where transpiration is included, because physically transpiration is (complexly regulated) evaporation from plant tissue.

<sup>2</sup>The term *sensitivity study* is commonly used only for *model* studies in which the sensitivity of the model results to changed initial conditions, boundary conditions, model parameters, or model formulations are investigated. Here I use the term more generally in the sense of the *sensitivity of precipitation to evaporation*, which also includes observational studies.

## Introduction

played a dominant role, the focus of smaller-scale studies such as Hohenegger et al. (2009) is on the local response of the atmosphere (“local coupling”) that arises from the influence evaporation exerts on the atmosphere’s vertical thermal structure.

As mentioned above, this first category also includes observational sensitivity studies. In these, correlations between soil wetness and subsequent precipitation rates are investigated using observational data. However, apart from the problem that subsurface soil data are relatively sparse, the authors of these studies face subtle challenges when it comes to deducing causalities from correlations (e.g. Seneviratne et al., 2010). One reason for such difficulties comes from the persistence of precipitation: if it rains today, the odds are relatively high that it will also rain tomorrow, independent of the soil wetness. However, because today’s rain wets the soil one will observe correlations between soil wetness and precipitation that have not necessarily anything to do with causality in the right direction. There are nevertheless studies that have overcome these difficulties. To give a recent example, Findell et al. (2011) found that afternoon precipitation in the eastern United States and in Mexico is more probable if precedent evaporation rates are high.

The second category of evaporation-precipitation coupling studies comprises studies in which the evaporative sources of precipitation are determined. This is achieved either by means of spatio-temporally resolved numerical moisture tracing, or by means of simple (“bulk”) recycling models. The numerical studies, in which water is tagged according to its evaporative source region, can in turn be divided into two types, namely online and offline moisture tracing studies. Online tracing is performed with passive water vapour tracers (WVTs) that are incorporated directly into an AGCM. This technique has first been realised by Koster et al. (1986) and, independently, by Jousaume et al. (1986). By contrast, offline tracing methods utilise already existing atmospheric and surface data to diagnose the atmospheric transport of moisture *a posteriori*. Compared to online tracing, the offline approach typically involves additional approximations because the used data do not contain all the information necessary to perform a tracing that would be equivalent to the online approach. On the other hand, offline tracing methods offer the advantages that (I) they do not require running a complete computationally expensive AGCM, and (II) they can be applied to reanalysis data that arguably constitute the best estimate of the real

atmosphere’s evolution during recent decades.

One offline tracing method, first applied by Yoshimura et al. (2004), has become increasingly popular during recent years due to its simplicity. The method entails the vertical integration of the relevant atmospheric quantities prior to the tracing procedure. The latter is thereby reduced to the two horizontal dimensions (plus the time dimension). The assumption behind this approach is that moisture components from different evaporative source regions are well-mixed vertically. A critical assessment of this ‘well-mixed’ assumption and the associated 2D moisture tracing method is one of the core aspects of my dissertation.

Also belonging to the second category are studies in which bulk recycling models are applied. These simple models, pioneered by Budyko (1974), are mostly used to determine regional precipitation recycling ratios, i.e. the fraction of precipitation in a certain region that originates as evaporation from the same region. As in the case of numerical offline tracing, bulk recycling models are applied to already existing atmospheric and surface data. Because these models are of low dimensionality, the data are first averaged in space and time. The bulk recycling models can thus be understood as a special case of numerical offline moisture tracing with extremely coarse spatio-temporal resolution.

### **The missing link**

One – or rather *the* – key question of my dissertation is to what extent the results of studies belonging to the second category can be used to infer something about causality underlying the investigated system: if one knows which fraction of precipitation in region B stems from evaporation in region A, what can be inferred about the sensitivity of precipitation in B to evaporation in A (where B and A can also be identical)?

For a hypothetical pollutant that behaves completely passively in the atmosphere, the sought relationship is straightforward: if  $x\%$  of the pollutant arriving in region B stem from emissions in region A, then a decrease of emissions in A by  $y\%$  will reduce the amount of pollutant arriving in B by  $x\% \cdot y\%$ . But how does the situation change if the emitted substance is not at all passive, but an active component like water that strongly influences the atmosphere’s behaviour in the ways portrayed above? It is plausible that there should still be some correlation between the degree to which precipitation in B is fed by evaporation

## *Introduction*

in A and the sensitivity of precipitation in B to evaporation in A, but how strong is this link really?

The authors of studies belonging to the second category have so far been content with assuming that a strong link exists. For example, Koster et al. (1986) wrote that “the precipitation in a given region is composed of evaporative contributions from a complete set of earth divisions [...]. Knowledge of the relative magnitudes of such contributions is crucial in determining possible anthropogenic effects of certain large-scale engineering projects, such as the drainage of the White Nile swamps or the irrigation of arid lands”. More recently, van der Ent et al. (2010) stated that “the magnitude of moisture recycling can be used as an indicator for the sensitivity of climate to land-use changes”. It is astonishing that this hypothesised predictive utility of source-sink relations of atmospheric moisture has so far not been put to critical scrutiny.

At the same time the authors of sensitivity studies (i.e. those belonging to the first category) have so far barely attempted to quantify to what extent the simulated (or observed) response of precipitation to evaporation may be attributed to moisture recycling. In these studies the argumentation focuses on the active role of water in the atmosphere, as the following statement by Shukla and Mintz (1982) exemplarily reflects: “The connection between evapotranspiration and precipitation is difficult to ascertain because it depends on a large number of interacting thermodynamic and dynamical processes, which must be taken into account in a quantitative way”.

There is however a noteworthy exception where the “missing link” between the two categories of studies is not missing: Schär et al. (1999) performed sensitivity experiments with a regional AGCM and simultaneously investigated quantitatively the possibility that the simulated response of precipitation to changed evaporation rates could be attributed to moisture recycling. To this end Schär et al. (1999) applied a bulk recycling model and found that “the simulated sensitivity cannot be interpreted with the classical recycling mechanism” because the simulated reduction of precipitation was much stronger than the contribution of regional evaporation to regional precipitation could have explained. Instead, Schär et al. (1999) attributed the response to positive local coupling, where positive means that more evaporation leads locally to more precipitation, and vice-versa. That moisture recycling is

believed to play a minor role was formulated by Seneviratne et al. (2010) as follows: “The key for understanding soil moisture-precipitation interactions lies more in the impact of soil moisture anomalies on boundary-layer stability and precipitation formation than in the absolute moisture input resulting from modified evapotranspiration”.

## **Overview of and relations between the chapters**

**Chapter 1** is about the missing link between the two categories of evaporation-precipitation coupling studies. I give an account of the different mechanisms by which evaporation can in principle affect precipitation and state that a clearer distinction between these mechanisms will help to advance our understanding of evaporation-precipitation coupling. Using a global AGCM in combination with an offline 2D moisture tracing scheme I determine continental precipitation recycling ratios, i.e. the (spatio-temporally resolved) fraction of precipitation that stems from continental evaporation. I then perform a continental-scale sensitivity experiment in which continental evaporation is completely suppressed.

By investigating such an extreme perturbation, I approach the question “What do moisture recycling estimates tell us?” from the largest possible scale. But the answer may well be scale-dependent. It thus seems natural to transfer the approach to smaller spatial scales to see to what extent the answer might change. However, the 2D-approximated tracing scheme I apply in Chapter 1 is not necessarily suited for smaller scales because the smaller the spatial scale, the less appropriate the involved ‘well-mixed’ assumption appears to be. Despite this objection the 2D-approximation has recently been applied to relatively small regions by Keys et al. (2012). A critical analysis of the errors associated with the 2D-approximation that could justify its application to smaller scales is so far missing.

**Chapter 2** is about the significance of the vertical dimension in the context of atmospheric moisture tracing. I provide the critical analysis, demanded above, of the errors associated with the 2D-approximation by comparing results of 3-dimensional online moisture tracing with results obtained with the 2D-approximation. To this end I implemented passive WVTs into the AGCM ECHAM6 (Roeckner et al., 2003). Moreover, I investigate the factors that

determine whether the atmosphere is well-mixed vertically or not both from a theoretical perspective as well as by analysing the vertically resolved (i.e. 3D) moisture tracing results.

One further point I discuss in Chapter 2 is that the way passive WVTs are implemented into AGCMs is not completely determined by the model physics<sup>3</sup>. Instead, subtle degrees of freedom remain that are associated with the question how strongly precipitation on its way towards the ground exchanges water molecules with the ambient water vapour. This issue in turn makes one wonder to what extent results obtained with a “perfect” moisture tracing scheme also reveal most about the causal relations that act within the investigated system – which brings one back to the topic of Chapter 1.

**Chapter 3** is about the question how often single water molecules are recycled during their way across land masses. In contrast to Chapters 1 and 2, where analytical aspects are combined with numerical simulations, the treatment in Chapter 3 is exclusively analytical. I work out that under certain idealised conditions, including the ‘well-mixed’ assumption investigated in Chapter 2, the frequency distribution of recycling events that the water molecules contained in an air parcel have experienced attains one of two analytically derivable forms. By means of a simple scale analysis and qualitative arguments I investigate to what extent the involved limit cases and simplifications apply to the actual conditions on Earth.

## Formal remarks

Each of the three chapters constituting my dissertation corresponds to a publication either already realised or planned to appear in a peer-reviewed journal. While Chapter 1 has already been published in the journal *Hydrology and Earth System Sciences* (HESS) (Goessling and Reick, 2011), Chapter 2 is currently<sup>4</sup> under review for the journal *Atmospheric Chemistry and Physics* (ACP) but has already been pre-published in the journal’s open discussion format (ACPD) (Goessling and Reick, 2012). Chapter 3 forms the basis of

---

<sup>3</sup>In atmospheric modelling, it is customary to refer to the subgrid-scale parameterisations as the model *physics*, and to the resolved processes as the model *dynamics*. In contrast, here I use the term *physics* in its original sense, i.e. including all processes simulated by the model.

<sup>4</sup>September 2012

a third publication that will soon be submitted to an appropriate journal.

Because I conducted the studies under supervision and guidance in particular of Dr. Christian Reick, we are both co-authors of the corresponding publications. In contrast to the Introduction and the Summary, Conclusions, and Outlook, the main chapters are therefore written in the first person plural. It should also be noted that, because the chapters resemble separate publications, there is a certain degree of redundancy between them. Further, each chapter has an individual abstract. Because I decided to leave unchanged the parts already published, there are also some stylistic differences between the chapters, for example concerning the use of tenses. Finally, where I refer to Chapters 1 and 2 from Chapters 2 and 3, I decided to keep the identifiers “Goessling and Reick (2011)” and “Goessling and Reick (2012)” instead of “Chapter 1” and “Chapter 2”. I kindly ask the reader to be indulgent with these kinds of imperfections.



Shallow men believe in luck or in  
circumstance. Strong men believe in  
cause and effect.

---

*(Ralph Waldo Emerson)*

## Chapter 1

**What do moisture recycling estimates  
tell us? Exploring the extreme case of  
non-evaporating continents**

## **Abstract**

Moisture recycling estimates are diagnostic measures that could ideally be used to deduce the response of precipitation to modified land-evaporation. Recycling estimates are based on moisture-budget considerations in which water is treated as a passive tracer. But in reality water is a thermodynamically active component of the atmosphere. Accordingly, recycling estimates are applicable to deduce the response to a perturbation only if other mechanisms by which evaporation affects climate do not dominate the response—a condition that has not received sufficient attention in the literature. In our analysis of what moisture recycling estimates tell us, we discuss two such additional mechanisms that result from water’s active role. These are (I) local coupling, by which precipitation is affected locally via the thermal structure of the atmosphere, and (II) the atmospheric circulation, by which precipitation is affected on a large spatial scale.

We perform two global climate model experiments: One with and another without continental evaporation. By this extreme perturbation we test the predictive utility of a certain type of recycling measure, the “continental recycling ratio”. Moreover, by such a strong perturbation the whole spectrum of possible responses shows up simultaneously, giving us the opportunity to discuss all concurrent mechanisms jointly.

The response to this extreme perturbation largely disagrees with the hypothesis that moisture recycling is the dominant mechanism. Instead, most of the response can be attributed to changes in the atmospheric circulation, while the contributions to the response by moisture recycling as well as local coupling, though noticeable, are smaller. By our case study it is not possible to give a general answer to the question posed in the title, but it demonstrates that recycling estimates do not necessarily mirror the consequences of land-use change for precipitation.

## 1.1 Introduction

Source-target relations of passive atmospheric trace gases provide straightforward information on consequences for the target region from modified emissions at the source region. This concept is also at the bottom of a number of studies dealing with the transport of water over the continents. Realising that water is not a passive trace gas but an active constituent of the Earth's atmosphere, it appears that in this case the applicability of this concept crucially depends on the assumption that the atmospheric response following a hypothetical perturbation in evaporation is dominated by the "passive" effect evaporation exerts on the atmospheric moisture budget, i.e. by "moisture recycling". But water, existing in and transitioning between its different phases, strongly affects the atmospheric budgets of heat, momentum, and radiation. As a result, evaporation affects precipitation not only via moisture recycling (sometimes referred to as "direct coupling"), but also via local modification of the atmosphere's thermal structure ("local coupling", sometimes referred to as "indirect coupling" or "indirect recycling") and via its influence on the atmospheric large-scale circulation (Fig. 1.1). Accordingly, general statements about the predictive utility of recycling estimates that ignore possible implicit limitations should be treated with caution. One such statement is the following by van der Ent et al. (2010): "The magnitude of moisture recycling can be used as an indicator for the sensitivity of climate to land-use changes." We argue that the conditions under which such a claim is valid have not yet been examined sufficiently.

A comprehensive specification of the conditions under which moisture recycling estimates can be used reliably to indicate the sensitivity of climate to land-use change is beyond the scope of the present study. Instead we make a first step in this direction by exploring the response of climate to a well-defined extreme perturbation. From the whole suite of recycling diagnostics, we concentrate on one particular called "continental recycling ratio", that is the fraction of moisture in precipitation that stems from continental evaporation (Bosilovich et al., 2002; Yoshimura et al., 2004; van der Ent et al., 2010). For this measure the perturbation considered in our simulations is a natural choice to test its predictive utility concerning the response of precipitation to changes in surface evaporation.

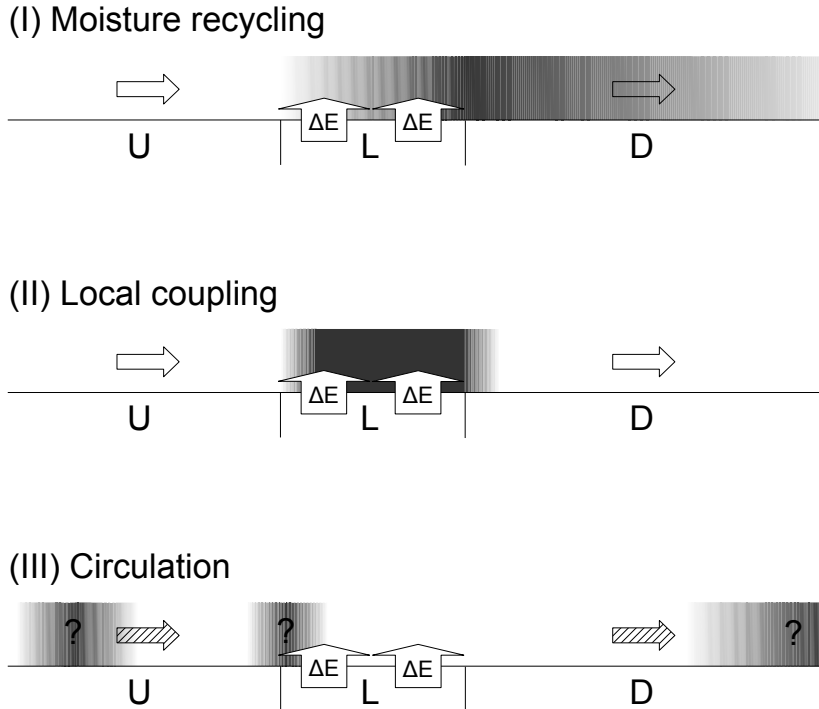


Figure 1.1: Schematic of three mechanisms via which evaporation affects precipitation. The effect of each mechanism is shown isolated from the others. The arrows pointing to the right indicate the wind direction. The colour gradients indicate the regions where precipitation responds (either positively or negatively). U = upwind region, L = local region, D = downwind region,  $\Delta E$  = imposed evaporation anomaly. (I) Moisture recycling: The precipitation response, caused by changes to the atmospheric moisture budget, grows gradually over the region of the imposed evaporation anomaly, then decays (slowly) over the downwind region. (II) Local coupling: The precipitation response, caused by changes to the thermal structure of the atmosphere, collocates with the imposed evaporation anomaly. A slight downwind shift is indicated because the structural change may need some time to develop. (III) Circulation: The precipitation response may occur anywhere, caused by changes to the 3-D large-scale atmospheric circulation (indicated by the hatching of the wind-arrows). While mechanism (I) accounts for the effect of  $\Delta E$  on the vertically integrated atmospheric moisture budget, mechanisms (II) and (III) account for modified energetics that come along with  $\Delta E$  (in particular changes in temperature).

Our investigation proceeds as follows. We first estimate continental recycling ratios from the climate data we obtain from a global model experiment that represents present-day conditions. In a second model experiment we completely suppress continental evaporation and compare the simulated response with the response that is “predicted” by the continental recycling ratios. Finally, we analyse in more detail the contributions from changes in the atmospheric circulation and from local coupling to the overall response.

As the terms “local coupling” and “large-scale circulation” imply, these mechanisms act on different spatial scales. It thus seems reasonable that the relative importance of the three processes (including moisture recycling) depends on the spatial scale of the perturbation. While local coupling acts already on comparatively small spatial scales, effects from moisture recycling and from changes in the large-scale circulation are expected to be relevant only if the spatial scale of the perturbation is sufficiently large. By suppressing continental evaporation globally, which is an extreme land-surface modification, we ensure that all mechanisms contribute to the response simultaneously – a desirable condition for a case study that is intended to demonstrate that in general several different mechanisms contribute to the response to changes in evaporation, and that a single mechanism like moisture recycling thus can only be employed to deduce the response if other mechanisms are of minor importance.

The paper is structured as follows. In Sect. 1.2 we review three mechanisms through which evaporation affects climate (Sects. 1.2.1–1.2.3) and discuss at what spatial scales they act (Sect. 1.2.4). In Sect. 1.3 we describe the climate model experiments (Sect. 1.3.1) and the method we apply to quantify continental moisture recycling in the reference experiment (Sect. 1.3.2). In Sect. 1.4 we present the resulting continental recycling ratios. In Sect. 1.5 we analyse in how far the response can be attributed to moisture recycling (Sect. 1.5.1), to the atmospheric circulation (Sect. 1.5.2), and to local coupling (Sect. 1.5.3). Finally, we critically reflect on our study in Sect. 1.6, summarise our results in Sect. 1.7, and draw conclusions in Sect. 1.8.

## 1.2 Background

We distinguish three mechanisms by which evaporation affects precipitation (Fig. 1.1). These mechanisms are commonly investigated in separate studies. In this section we provide some (non-exhaustive) background for each of the three mechanisms (Sects. 1.2.1–1.2.3) and discuss at what spatial scales they act (Sect. 1.2.4).

### 1.2.1 Moisture recycling

In most studies dealing with moisture recycling the extent to which precipitation in some location depends on moisture recycling is linked directly to the recycling ratio ( $R$ , the fraction of recycled moisture in precipitation). Since the earliest studies on moisture recycling (Benton et al., 1950) several types of measures have been introduced to quantify moisture recycling. In the following we provide a basic overview of different recycling measures.

In many studies, including most of the earlier work, moisture recycling is quantified by the regional recycling ratio ( $R_r$ ), which measures the contribution of evaporation from a particular region to precipitation inside the same region (e.g. Benton et al., 1950; Budyko, 1974; Lettau et al., 1979; Brubaker et al., 1993; Eltahir and Bras, 1994; Burde and Zangvil, 2001; Burde, 2006; Fitzmaurice, 2007). These studies are based on bulk recycling models that relate horizontal moisture influx and land-surface evaporation. For example, the bulk recycling equation applied by Brubaker et al. (1993) reads

$$R_r = \frac{E_r}{E_r + 2 F_r} \quad (1.1)$$

where  $R_r$  is the region's mean fraction of recycled moisture in precipitation,  $F_r$  is the region's horizontal moisture influx, and  $E_r$  is the region's land-surface evaporation. The individual bulk recycling models differ slightly from each other, with more recent models typically designed to relax the underlying assumptions. They are easily applicable to available data on moisture fluxes and land-surface evaporation, be it from models, observations, reanalyses, or other hybrid data. However, the bulk formulations have to employ simplifying assumptions that are hard to justify (see Fitzmaurice, 2007, for details). Also, the results depend

strongly on the size and the shape of the considered region, because  $E_r$  scales with the region's area and  $F_r$  scales with its diameter perpendicular to the prevailing wind direction. Because of this scale- and shape-dependence the regional measure  $R_r$  is of limited use for the intercomparison of estimates between different regions (see van der Ent and Savenije, 2011, for details).

Trenberth (1999) overcomes this problem by introducing a local measure, the local recycling ratio. He modifies Brubaker's formulation by replacing the spatial integrals of  $E$  and  $F$  with their local values scaled up to some length scale, which gives globally comparable values. Dirmeyer and Brubaker (2007) estimate in principle the same quantity but with a more sophisticated method. Instead of applying a bulk formulation that entails the use of temporal means, they compute a large number of back-trajectories to determine the source regions of precipitation, thereby accounting for the effect of transient fluxes. Another way to look at the local recycling ratio is to replace the (length-scale dependent) local recycling ratio by the length scale at which the local recycling ratio reaches a certain value. A natural choice for this value is  $1 - \frac{1}{e}$ , which makes the resulting length-scale correspond to the distance atmospheric air travels until the integrated surface evaporation measures up to the atmospheric moisture content (van der Ent and Savenije, 2011).

An alternative non-local measure not suffering from scale issues is the continental recycling ratio ( $R_c$ ), where the considered region is the global land-surface. In case of the continental recycling ratio "recycled moisture" equates to "moisture of continental origin" or "terrestrial moisture", and  $R_c$  equates to the fraction of continental moisture in total moisture. In principle bulk recycling models can be applied to the global land-surface, but the assumptions made in the model derivations are not appropriate given the size, shape, and heterogeneity of the continents. Also, with growing complexity of the considered region, one is interested in spatially resolved recycling ratios rather than one single mean value. Instead, continental recycling ratios can be computed numerically by tracing water that is tagged according to its origin. This approach is adopted by Numaguti (1999), Bosilovich et al. (2002), Yoshimura et al. (2004), and van der Ent et al. (2010). While Numaguti (1999) and Bosilovich et al. (2002) trace moisture 3-dimensionally within general circulation model (GCM) simulations, Yoshimura et al. (2004) and van der Ent et al. (2010) use reanalysis

data to trace moisture 2-dimensionally.

Yoshimura et al. (2004) and van der Ent et al. (2010) apply the ‘well-mixed’ assumption which reduces the problem to two spatial dimensions. This assumption implies that the atmosphere is vertically well-mixed with respect to moisture fractions of different origin, which is one of the simplifications also employed in most of the bulk recycling models (see Burde, 2006; Fitzmaurice, 2007, for details). The approach taken by Numaguti (1999) and Bosilovich et al. (2002) does not require the ‘well-mixed’ assumption, because the vertical moisture exchange is resolved explicitly. Despite this difference the authors of the four studies cited above find similar continental recycling ratios. As expected,  $R_c$  increases from upwind to downwind continental regions, for example from west to east over North America and Eurasia (in particular in northern summer), and from northeast to southwest over Amazonia.  $R_c$  maxima are around 60% in the tropics (year-round), and even 80% in the eastern part of central Eurasia (during northern summer).

The continental recycling ratio ( $R_c$ ) is the measure that we use in this case study to quantify moisture recycling (see below).

### 1.2.2 Local coupling

While moisture-recycling studies focus on the influence evaporation exerts on precipitation via the atmosphere’s moisture budget, i.e. in a spatio-temporally integrative manner (see Fig. 1.1), another class of studies focusses on the influence evaporation exerts on precipitation via the atmosphere’s thermal structure, which we refer to as local evaporation-precipitation coupling, or simply local coupling (following the nomenclature in Seneviratne et al., 2010). In contrast to moisture recycling, where *increased* evaporation can only lead to *increased* precipitation (positive coupling), local coupling can be both positive or negative.

General circulation models of the atmosphere provide a convenient way to investigate the local coupling with perturbation experiments (e.g. Rowntree and Bolton, 1983; Beljaars et al., 1996; Schär et al., 1999; Pal and Eltahir, 2001; Hohenegger et al., 2009). The perturbed variable in these studies is not evaporation directly but the initial soil wetness, and the mechanism is consistently referred to as soil moisture-precipitation coupling. The link between soil moisture and evaporation is strong as long as moisture availability rather than

energy is the evaporation-limiting factor (see Seneviratne et al., 2010, for details). Most of these studies find a positive coupling between soil moisture and precipitation, i.e. more precipitation above wetter soils. Studying convective summer precipitation over Europe with a regional climate model, Schär et al. (1999) find that the low Bowen ratio of wet soils leads to the buildup of a comparatively shallow boundary layer with high values of moist entropy, which is a source of convective instability. Further, the level of free convection is lowered, which facilitates the release of convective instability. Also, despite increased cloud cover, Schär et al. (1999) find larger net radiation into wet soils, meaning that more total moist entropy gets into the boundary layer. Findell and Eltahir (2003a) initialise a one-dimensional boundary layer model with different vertical profiles based on early-morning observations from Illinois in North America and find that, depending on the early-morning situation, the triggering of moist convection can be favoured above either wet soils or dry soils, or the triggering can be independent of the soil wetness, i.e. atmospherically controlled. Based on these results Findell and Eltahir (2003b) find that during northern summer the eastern half of the United States of America tends to show positive soil moisture-precipitation coupling, while large parts of the western half are atmospherically controlled. Only a small region in the arid southwest tends to show negative coupling.

Hohenegger et al. (2009) demonstrate that the strength and even the sign of the evaporation-precipitation coupling in atmospheric models can vary strongly with the representation of moist convection. For a situation with weak synoptic forcing in a domain around the Alps they find that two of the three investigated parameterisation schemes yield positive coupling, while negative coupling occurs with the third parameterisation scheme and when moist convection is represented explicitly through higher resolution. The different signs of the coupling relate to the presence of a stable layer sitting on top of the planetary boundary layer, which in the explicit case can be penetrated only by the more vigorous boundary-layer thermals occurring over dry soils. It remains unclear to which extent the results of Hohenegger et al. (2009) can be generalised, because they may be rather special for the synoptic situation and the mountainous terrain under investigation (C. Hohenegger, personal communication, 2011). On the other hand, there is also observational evidence that current atmospheric models do not well represent the local coupling (Dirmeyer et al., 2006).

The Global Land-Atmosphere Coupling Experiment (GLACE), to which a dozen climate-modelling groups contributed with global experiments, presents a different view on soil moisture-precipitation coupling (Koster et al., 2004). Instead of uniformly increasing or decreasing the soil wetness in a certain region, a set of model runs generated with freely developing soil wetness is compared to a set of runs generated with prescribed soil wetness. The (local) land-atmosphere coupling strength is then measured by the degree to which the variability of precipitation decreases due to the (global) prescription of soil wetness. This measure of coupling strength is considerably different from the definition used in the sensitivity studies cited above. First, the measure does not contain the sign of the coupling. Second, the measure implies that regions without naturally occurring inter-annual variability of soil wetness are diagnosed to exhibit no land-atmosphere coupling, even if imposed changes in soil wetness (e.g. due to irrigation or other land-use changes) would affect local precipitation. The latter is one of the reasons why Koster et al. (2004) find significant local coupling only in the transition zones between arid and humid climates where soil wetness naturally varies from year to year. Besides these differences, Koster et al. (2004) agree with Hohenegger et al. (2009) on the point that there is considerable disagreement between models regarding the local coupling.

The uncertainty associated with the representation of local coupling in atmospheric models highlights the need to confront models with evidence from observations. However, observational long-term soil-moisture data with sufficiently high resolution are scarce (Seneviratne et al., 2010). Another serious disadvantage of observational studies compared to modelling studies is that causal relations are much harder to establish, in particular due to the persistence of precipitation on different timescales. For this very reason Salvucci et al. (2002) question the observational evidence Findell and Eltahir (1997) provide for positive soil moisture-precipitation coupling in Illinois during northern summer. However, in a more recent study Findell et al. (2011) provide new evidence for positive local coupling in large parts of North America using observationally strongly constrained reanalysis data.

Analysing satellite-derived soil-wetness data and aircraft measurements from the Sahel, Taylor et al. (2007) find for situations where soil wetness varies spatially that meso-scale circulations act to place moist convection preferably in the circulations' updrafts, which

correspond to dry patches (see also Taylor et al., 2011). However, this finding can not be equated with a negative soil moisture-precipitation coupling. The latter would imply that (total) precipitation decreases in response to an imposed increase of soil wetness – a relation that does not follow from the negative spatial correlation. Finally, we leave the question open whether this kind of coupling, where meso-scale circulations are involved, should be classified as “local coupling”, or rather as an effect associated with changes in the atmospheric circulation (compare Fig. 1.1).

According to current knowledge positive evaporation-precipitation coupling seems to be the rule rather than the exception (Seneviratne et al., 2010). However, understanding local coupling is an ongoing effort that is a central objective of the Global Land/Atmosphere System Study (see e.g. van den Hurk and Blyth, 2008).

### 1.2.3 Circulation

Besides moisture recycling and local coupling, land-surface evaporation alters climate also via its influence on the large-scale atmospheric circulation (Fig. 1.1). The climatic response mediated through changes in the large-scale circulation is not restricted to the region of anomalous surface-evaporation itself (as in case of the local coupling) or to regions along the downwind trajectories (as in case of moisture recycling), but can occur principally anywhere. Remote effects conveyed through the large-scale circulation are also known as “teleconnections”.

The most obvious link between surface evaporation and the large-scale circulation relates to the surface-pressure distribution. When heated by solar radiation, the oceans export most of the absorbed energy as latent heat to the atmosphere (low Bowen ratio), while at the land surface a larger fraction is exported as sensible heat (high Bowen ratio) and hence warms the atmosphere. This contrast, which is the stronger the drier the continents are, results in rising motion and low-level convergence associated with low surface pressure (“thermal lows”) over the warmer continents and sinking motion and low-level divergence associated with high surface pressure over the cooler oceans. Due to geostrophy the surface-pressure distribution in turn results in cyclonic low-level circulations around the continents and anticyclonic low-level circulations around the ocean basins. Not surprisingly this effect

is strongest on the Northern Hemisphere during northern summer, the low-level westerlies over the Indian subcontinent as part of the cyclonic circulation around Eurasia being a prominent example. Note that these circulations are superimposed by other features of the large-scale circulation like the extratropical westerlies.

Shukla and Mintz (1982) demonstrate with global climate model experiments for northern summer that most of the surface-pressure contrast between land and ocean and the associated circulations vanish when the land surface is kept wet, and that the contrast and the associated circulations are amplified when the land surface is kept dry – with strong implications for the global distribution of precipitation. Saeed et al. (2009) show with a regional climate model that the present-day intensity of irrigation on the Indian subcontinent acts to attenuate the differential heating between land and ocean significantly, thereby weakening the monsoonal low-level westerlies over the region with far-reaching consequences. To give another example, Kleidon and Heimann (2000) compare global model experiments with different rooting depths in tropical South America and Africa. They find that enhanced land-surface evaporation fuels the release of latent heat in the Intertropical Convergence Zone (ITCZ). This in turn results in amplification of the Hadley circulation, with implications also for the subsiding branch in the subtropics and even beyond.

#### **1.2.4 Scale aspects**

In reality as well as in global climate models surface-evaporation affects climate through all of these mechanisms (Fig. 1.1) simultaneously. However, in some cases a (modelled) response can be attributed quite clearly to one of the mechanisms. For example, Schär et al. (1999) carry out moisture-budget calculations and conclude from these that “the simulated sensitivity (of precipitation to soil-moisture anomalies) cannot be interpreted with the classical recycling mechanism”. Seneviratne et al. (2010) put it this way: “The key for understanding soil moisture-precipitation interactions lies more in the impact of soil moisture anomalies on boundary-layer stability and precipitation formation than in the absolute moisture input resulting from modified evapotranspiration”. In Schär et al. (1999) it is also clear that the response is not caused by changes in the large-scale circulation because the integration domain, Europe, is relatively small. As a consequence the velocity

field is largely determined by the driving lateral boundary data, such that even the transit of individual low pressure systems across the domain is largely prescribed.

The larger integration domain in Saeed et al. (2009) allows for more flexibility of the velocity field in response to changes within the domain. However, the full response of the large-scale circulation can only be accounted for with global experiments, as in Shukla and Mintz (1982) and Kleidon and Heimann (2000). One may speculate whether a remake of the study of Schär et al. (1999) with a global model would reveal that changes in the large-scale circulation significantly modify the response from local coupling alone. However, it seems plausible that below some spatial scale of the perturbation the local coupling rather than the circulation dominates the response at least at the place of the perturbation.

Similarly, there should also be a spatial scale above which considerations of the atmospheric moisture budget, i.e. moisture recycling, become important. The results of Schär et al. (1999) suggest that this threshold seems to be larger than the spatial scale considered in local-coupling studies (typically 100–1000 km). The length scale of moisture recycling (Sect. 1.2.1) might be a useful indicator. van der Ent and Savenije (2011) estimate that the length scale of moisture recycling can be as small as  $\sim 1000$  km in strongly evaporating regions with moderate horizontal moisture flux densities (large  $E/F$ , in July e.g. tropical Africa, southern Europe, and eastern North America),  $\sim 2000$ – $4000$  km in regions with intermediate  $E/F$  (in July e.g. central Europe, large parts of South America, and western North America), and larger than 5000 km in regions with low  $E/F$  like deserts (see Fig. 8a in van der Ent and Savenije, 2011). Probably the scale at which moisture recycling becomes significant is already substantially below the length scale at which the integrated evaporation flux measures up to the atmospheric water content. In any case it seems that for evaporation perturbations imposed to regions larger than  $\sim 1000$  km, cumulative changes in the atmospheric moisture content can not be neglected anymore.

The key for understanding the response of precipitation to an evaporation anomaly may lie in local coupling if the scale of the perturbation is sufficiently small, but at larger scales moisture recycling and the large-scale circulation come into play. With this study we approach the issue of scale-dependence from the largest possible scale, namely the continental scale.

## 1.3 Methods

### 1.3.1 Model experiments

For our investigations we use the Earthsystem model of the Max Planck Institute for Meteorology (MPI-ESM), comprising the atmospheric general circulation model ECHAM6 (Roeckner et al., 2003), including the land-surface scheme JSBACH (Raddatz et al., 2007), at T63/L47 resolution ( $1.875^\circ \times 1.875^\circ$ , 47 levels, 10 min time step). We do not use the interactive MPI-ESM ocean component, but prescribe climatological sea-surface temperatures (SSTs) representing present-day conditions without interannual variability. Given the strong perturbation we apply (see below), the comparatively slight biases in the means of atmospheric quantities that are introduced through the use of climatological SSTs are tenable.

We run the model in two configurations. The reference experiment “REF” represents present-day conditions. In the second experiment “DRY” the continents are not allowed to exchange moisture with the atmosphere through evaporation (and, less importantly, condensation) but only through precipitation. Thereby the continents behave essentially as if they were kept completely dry. In reality a similar hydrological behaviour of the continents could in principle be provoked by transforming the continents into coarse-textured or rocky deserts with sufficiently steep slopes allowing for exhaustive runoff.

Since we focus on the direct effect of continental evaporation, or rather its absence, we prescribe continental albedo and roughness from climatologies in both experiments. This reduces the number and complexity of interactions and feedbacks that would otherwise add secondary alterations to the modelled differences in climate. The albedo and roughness climatologies stem from a 30-years model run in equilibrium (meaning that the transient phase before the model reaches a quasi-equilibrium is omitted) with dynamically modelled albedo and roughness that is otherwise identical to the REF experiment. The two equilibrium experiments REF and DRY span 30 years each (again without transient phase).

To account for the uncertainty associated with the parameterisation of moist convection, we run each of the two model experiments with two different convection schemes. One of these is the original Tiedtke mass-flux scheme. The scheme includes both deep and shallow

convection. Single-parcel ascents are used to test whether convection is triggered. The cloud-base mass-flux is determined by a moisture-convergence closure (Tiedtke, 1989). The other convection scheme, which is the standard scheme of the MPI-ESM, is still based on the Tiedtke mass-flux scheme, but the moisture-convergence closure is replaced by a closure that is based on convective available potential energy (Nordeng, 1994; Roeckner et al., 2003). Accordingly, the entrainment rates are also handled differently.

### 1.3.2 Moisture tracing

To quantify moisture recycling we compute continental recycling ratios ( $R_c$ , see Sect. 1.2.1) from climate model data in the following way. We distinguish two types of atmospheric moisture: oceanic and recycled. While oceanic moisture stems from ocean evaporation, recycled moisture stems from continental evaporation. The continental recycling ratio is the fraction of continental moisture (i.e. continentally recycled moisture, hereafter recycled moisture) in total moisture.

$$R_c = \frac{M_c}{M_c + M_o} \quad (1.2)$$

where  $M_c$  is recycled moisture and  $M_o$  is oceanic moisture. In principle this measure is defined at every point in space and time in the atmosphere for infinitesimal volumes. We, however, apply the ‘well-mixed’ assumption which implies that  $R_c$  is taken to be vertically constant. Accordingly,  $M_c$  and  $M_o$  are vertically integrated moisture densities. Ignoring temporarily that horizontal wind velocities generally vary with height, the problem reduces to two spatial dimensions. With these simplifications we can consider a Lagrangian atmospheric column travelling horizontally with the wind. The source and sink terms for  $M_c$  and  $M_o$  now read

$$\frac{dM_c}{dt} = E_c - R_c P \quad (1.3)$$

$$\frac{dM_o}{dt} = E_o - (1 - R_c) P \quad (1.4)$$

where  $t$  is time,  $P$  is precipitation from the air column, and  $E_c$  is evaporation into the air column from land, and  $E_o$  is evaporation into the air column from the ocean. Using

Eqs. (1.2)–(1.4), substituting  $M_c + M_o$  by  $W$  (precipitable water), and transforming into Eulerian formulation yields

$$\frac{\partial R_c}{\partial t} + u_{\text{eff}} \frac{\partial R_c}{\partial x} + v_{\text{eff}} \frac{\partial R_c}{\partial y} = \frac{E_c}{W} (1 - R_c) - \frac{E_o}{W} R_c \quad (1.5)$$

where  $u_{\text{eff}}$  is the effective wind component along the zonal coordinate  $x$ , and  $v_{\text{eff}}$  is the effective wind component along the meridional coordinate  $y$ . Since the air column can not be over land and over the ocean at the same time, only one of the right-hand-side terms can be nonzero at a time, depending on the location. The effective wind components in this 2-dimensional formulation are vertical mean values weighted by the local water vapour partial pressure, such that

$$\begin{aligned} Q_u &= u_{\text{eff}} W = u_{\text{eff}} \left( g^{-1} \int_0^{p_0} q(p) \, dp \right) \\ &= g^{-1} \int_0^{p_0} u(p) q(p) \, dp \end{aligned} \quad (1.6)$$

where  $Q_u$  is the zonal component of the vertically integrated horizontal moisture flux,  $g$  is gravitational acceleration,  $p$  is pressure,  $p_0$  is surface pressure, and  $q$  is specific moisture (all phases). Equation (1.6) analogously applies to the meridional component of the vertically integrated horizontal moisture flux,  $Q_v$ . Equations (1.5) and (1.6) can also be derived from vertical integration of the full 3-dimensional equations (not shown)<sup>1</sup>.

Equation (1.5) reveals that precipitation, although occurring in Eqs. (1.3) and (1.4), does not influence  $R_c$  directly. The reason is that, with the ‘well-mixed’ assumption, precipitation removes recycled moisture and oceanic moisture from the atmospheric column in proportion to their respective abundance. Precipitation affects  $R_c$  only indirectly through its effect on  $W$ .

We discretise Eq. (1.5) with upwind differencing (e.g. Press et al., 2007) on the spatio-temporal grid of the model data ( $1.875^\circ \times 1.875^\circ$ , 10 min time step) and run the algorithm over all model years of the REF experiment. Again we incorporate only the results from the last 30 years of equilibrium climate into our analysis. Since there is no continental moisture

---

<sup>1</sup>see Chapter 2, Sect. 2.2 for the derivation that we omitted here

in the DRY experiment, there is no need to apply the tracing to it.

## 1.4 Recycling in the reference experiment

The distribution of the continental recycling ratio (Fig. 1.2) is determined by the rate of surface evaporation, the horizontal moisture flux density (Fig. 1.3), and the land-sea geometry. As a result the continental recycling ratio increases from continental upwind coasts to downwind coasts with respect to the prevailing winds. Steep  $R_c$ -gradients occur where strong evaporation combines with moderate horizontal moisture-flux density (e.g. tropical Africa), or where the air flows perpendicular to a steep evaporation gradient (e.g. Sahel in January), or a combination thereof (e.g. China in July). Since  $R_c$  is bound between zero and one (as follows from Eq. 1.5) and, hence, saturates when approaching these bounds, the  $R_c$ -gradient also depends on the value of  $R_c$  itself.

Please note that the monthly averaged continental recycling ratios shown in Fig. 1.2 are precipitation-weighted values rather than uniformly weighted time-averages (see the last paragraph in this section and Fig. A.1 in the appendix for a discussion of the consequences of this choice).

In the REF experiment continental moisture contributes up to 80 % (on monthly average) to the atmosphere's total water content. This peak value is reached in central Asia, Siberia, and the north-eastern parts of North America in July. At this time of the year  $R_c$  exceeds 60 % in the whole Arctic region, meaning that the main sources of moisture are the large land masses enclosing the pole. In January  $R_c$  in the northern extratropics hardly reaches 20 % because of strongly reduced land-surface evaporation. In the southern extratropics  $R_c$  is low even during the Southern-Hemisphere summer (January) because of the absence of comparatively large land masses.

In the tropics  $R_c$  peaks at about 50 % in the downwind regions of Africa and South America with weak seasonality. Despite strong land-surface evaporation continental moisture does not accumulate in the tropics as much as it does in the northern extratropics during summer, because air travelling between the tropical continents encounters large, strongly evaporating ocean basins. In consequence, air reaching South America or Africa contains almost no

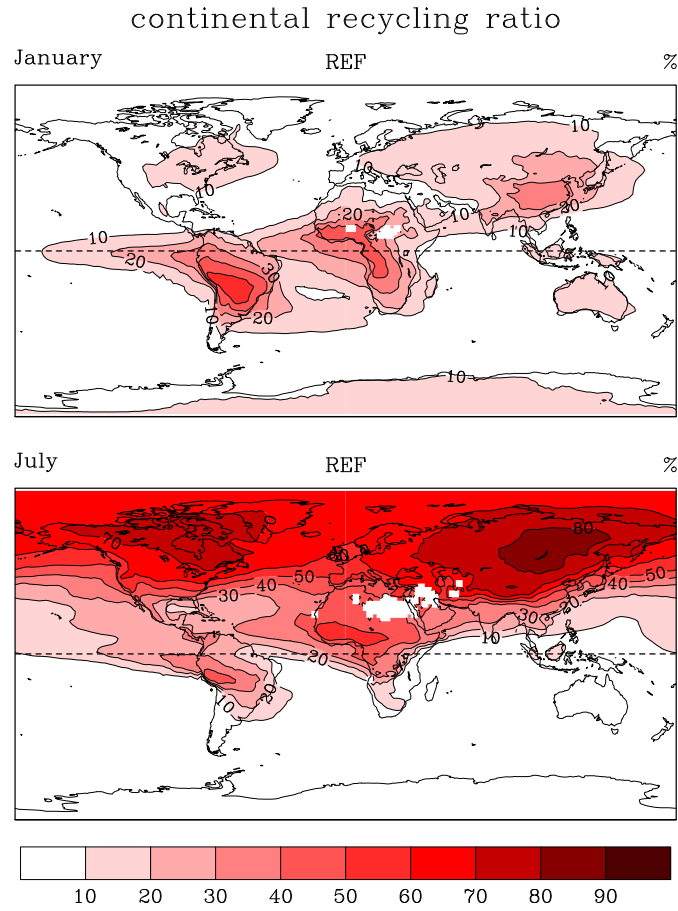


Figure 1.2: Continental recycling ratio  $R_c$  (% continental moisture in precipitation) in the REF experiment.

recycled moisture. This is different in the northern extratropics, where  $R_c$  is still relatively high after an ocean crossing. Additionally, horizontal moisture flux densities are usually higher in the tropics because the warmer atmosphere contains more moisture (Fig. 1.3, see also Fig. 1.5, top panel).

Comparing estimates averaged over the same period of time, our results agree well with the estimates published by Numaguti (1999), Bosilovich et al. (2002), Yoshimura et al. (2004), and van der Ent et al. (2010). (In the latter study the continental recycling ratio is termed “continental precipitation recycling ratio” and is different from the also discussed “continental evaporation recycling ratio”.) The similarity of the estimates obtained with 2-dimensional tracing, which our study has in common with Yoshimura et al. (2004) and van der Ent et al. (2010), compared to the estimates obtained with 3-dimensional tracing

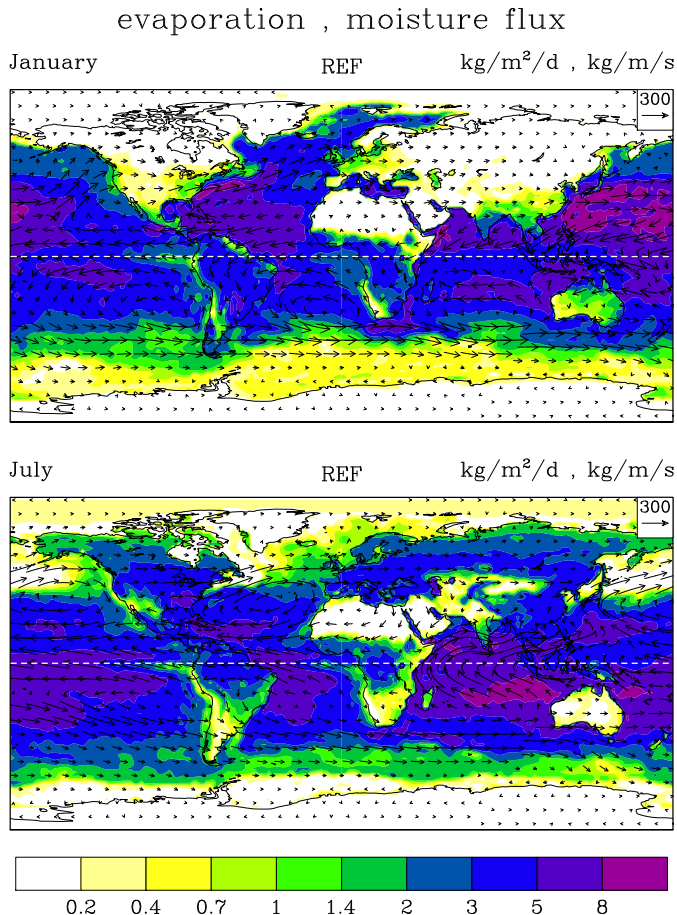


Figure 1.3: Surface evaporation  $E$  (colours,  $\text{kg m}^{-2} \text{d}^{-1}$ ) and horizontal moisture flux density  $Q$  (arrows,  $\text{kg m}^{-1} \text{s}^{-1}$ ) in the REF experiment.

(Numaguti, 1999; Bosilovich et al., 2002), suggests that the error introduced by the vertical integration is acceptably small for our large-scale considerations.

Regarding the comparability of the results there are two more technical differences to mention. First, Yoshimura et al. (2004) and van der Ent et al. (2010) do not trace moisture near the poles but treat moisture entering from the polar regions as oceanic moisture. In northern summer, when we obtain almost 70% continental moisture in the Arctic, Yoshimura et al. (2004) and van der Ent et al. (2010) obtain significantly lower values adjacent to the Arctic. Due to the prevailing zonal direction of the moisture transport, this seems to have minor influence on the continental recycling ratios below  $\sim 70^\circ$  north. Second, in contrast to the other four studies including ours, Numaguti (1999) shows uniformly weighted time-averages instead of precipitation-weighted values. The resulting differences are small for monthly

means, but not negligible for annual means because on the annual time scale continental recycling ratios and precipitation covary significantly (see Fig. A.1 in app. A).

Please note that in all studies, including Bosilovich et al. (2002) and van der Ent et al. (2010) who show values only on the continents, continentally recycled moisture (i.e. moisture of continental origin) is also tracked in the atmosphere over the ocean. One can argue that moisture of continental origin that rains into the ocean should not be called *continentally recycled*. However, although we show values also over the ocean, we use this term to emphasise that our continental recycling ratio is the same quantity as the one discussed in van der Ent et al. (2010).

## 1.5 Response to suppressed continental evaporation

To keep this paper concise, in the following we focus on the results for July only, when continental evaporation and, hence, moisture recycling are most pronounced (compare Figs. 1.2 and 1.3). The main conclusions we draw from the analysis of the situation in July are consistent with the situation in January. We provide all corresponding figures for January in the appendix.

The use of the original Tiedtke convection scheme in place of the standard scheme yields a significantly different precipitation distribution in some places, particularly in the tropics. However, the response to the suppression of continental evaporation is very similar with both schemes (see Fig. A.2 in the appendix), indicating that our results are to some extent robust to the choice of the convection scheme. Due to the similarity of the responses, in the following we discuss only the results obtained with the standard convection scheme.

We argue that, without local coupling and changes in the large-scale circulation, the hydrological response to the suppression of continental evaporation would closely resemble the pattern of continental recycling ratios in the REF experiment. Building on this argument we suggest that the significance of continental moisture recycling compared to other mechanisms can be judged by the similarity between the pattern of continental recycling ratios and the pattern of the hydrological response. In the following we thus first try to interpret the response to the suppression of continental evaporation from a moisture-recycling per-

spective by comparing these patterns (Sect. 1.5.1), and then analyse in how far changes of the atmospheric circulation (Sect. 1.5.2) and local coupling (Sect. 1.5.3) contribute to the response.

### 1.5.1 The moisture-recycling perspective

If moisture recycling were the dominant factor controlling the response to the suppression of continental evaporation, the response of precipitation (Fig. 1.4) and precipitable water (Fig. 1.5) would mirror the pattern of continental recycling ratios in the REF experiment (Fig. 1.2, bottom). To underline the moisture-recycling perspective, the difference plots of precipitation and precipitable water show relative differences with the red part of the colour scale kept identical to the colour scale of the continental recycling ratios.

For the moment ignoring the sign of the response, the changes in precipitation and precipitable water in July (Figs. 1.4 and 1.5) conform to the continental recycling ratios in two large-scale aspects (Table 1.1). First the response is stronger on the Northern Hemisphere ( $\Delta P = -21\%$ ,  $\Delta W = -3\%$ ) than on the Southern Hemisphere ( $\Delta P = -8\%$ ,  $\Delta W = -0.8\%$ ). This is in line with the continental recycling ratio (NH:  $R_c = 31\%$ , SH:  $R_c = 3\%$ ). However, this tendency would be expected also for effects due to local coupling or effects due to changes in the large-scale circulation, because the perturbation is much stronger on the Northern Hemisphere (see continental evaporation rates in Fig. 1.3, bottom panel). Second the response is much stronger over the continents ( $\Delta P = -54\%$ ,  $\Delta W = -7\%$ ) than over the ocean ( $\Delta P = -7\%$ ,  $\Delta W = -0.4\%$ ). This is also in line with the response one would expect if moisture recycling were the dominant mechanism (land:  $R_c = 50\%$ , ocean:  $R_c = 14\%$ ). However, a stronger response on the continents compared to the ocean would also be expected if local coupling were the dominant factor. Regarding effects from the large-scale circulation one expects a response not only over the continents but also over the ocean, although it is less clear to what extent changes in the circulation should affect the continents more than the ocean (compare Sect. 1.2.3). In summary, these two large-scale aspects (the stronger response (I) in the Northern Hemisphere and (II) over the continents) conform to the moisture-recycling perspective but, because they could also be due to non-recycling mechanisms, they do not suffice to attribute the response to moisture recycling.

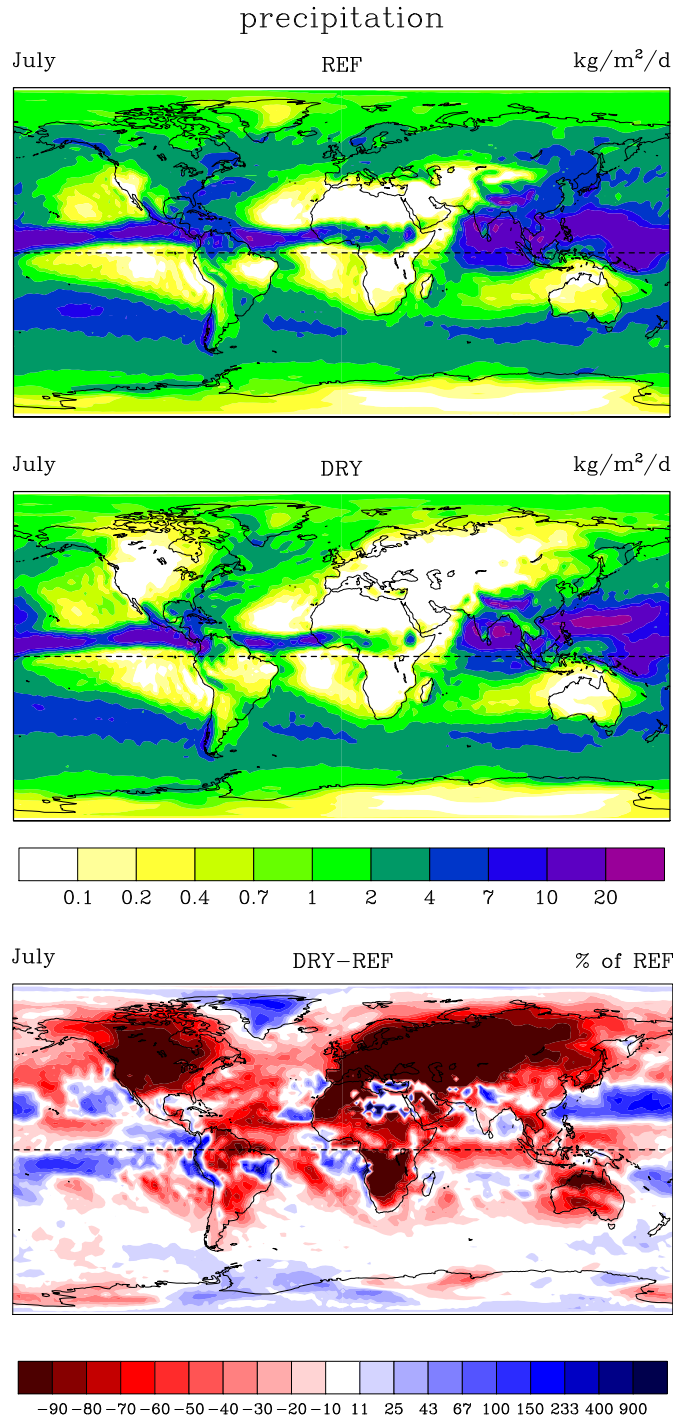


Figure 1.4: Precipitation ( $\text{kg m}^{-2} \text{d}^{-1}$ ) in July in the REF experiment (top panel), in the DRY experiment (middle panel), and the difference between the two (bottom panel, %). Note that the red part of the colour scale of the difference plot is kept identical to the one used in Fig. 1.2 to allow for direct comparison. The values of the blue part of the colour scale of the difference plot equate to (10%, 20%, ..., 90%) in relation to the DRY experiment. See Fig. A.3 in the app. A for January.

## 1.5 Response to suppressed continental evaporation

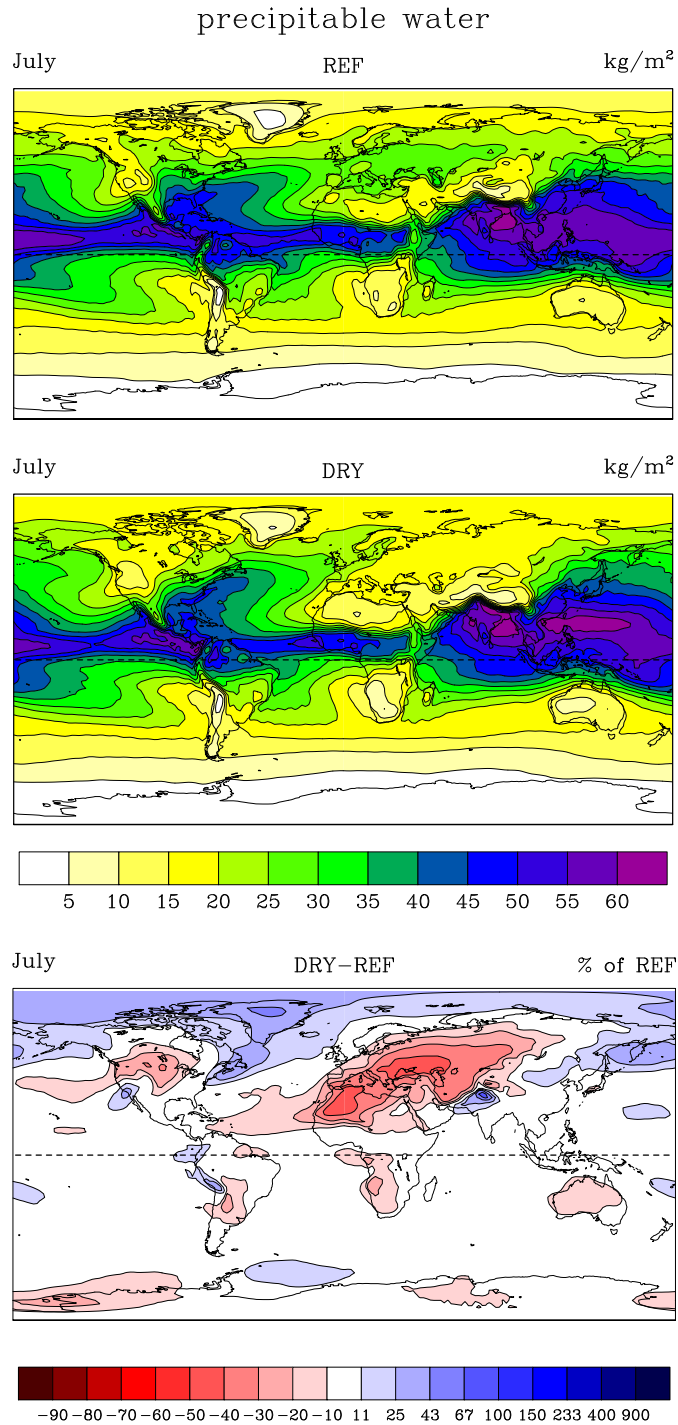


Figure 1.5: Precipitable water ( $\text{kg m}^{-2}$ , vapour + liquid + ice) in July in the REF experiment (top panel), in the DRY experiment (middle panel), and the difference between the two (bottom panel, %). Note that the colour scale of the difference plot is kept identical to the ones used in Figs. 1.2 and 1.4, bottom, to allow for direct comparison. The values of the blue part of the colour scale of the difference plot equate to (10 %, 20 %, ..., 90 %) in relation to the DRY experiment. See Fig. A.4 in the appendix for January.

Now also accounting for the sign of the response, the probably strongest evidence from large-scale aspects supporting that moisture recycling contributes at least to some extent to the response is the globally prevailing decrease of precipitable water, in particular over the continents (Table 1.1). The much stronger decrease of precipitation is also in line with the continental recycling ratios, but in contrast to precipitable water a strong decrease of precipitation over the continents could also be due to positive local coupling.

A clear indication that other mechanisms than moisture recycling contribute substantially to the signal is the occurrence of *increased* precipitation and *increased* precipitable water in many regions (Figs. 1.4 and 1.5). The atmosphere in the Arctic carries about 30 % more water in the DRY experiment, although almost 70 % of the atmospheric water in the REF experiment stem from continental evaporation. Greenland receives 40 % more precipitation in the DRY experiment. Other regions with increased precipitation include the Himalayas, eastern Brazil, the Andes, and the edges of the Pacific ITCZ. While moisture recycling can not explain any increase in precipitation or precipitable water in response to decreased evaporation, negative local coupling is a possible explanation for a precipitation increase only over land. The latter might be the case in eastern Brazil, where evaporation rates in the REF experiment are high, but negative local coupling as an explanation is implausible in Greenland, where (I) evaporation rates from the icy land-surface are low already in the REF experiment and (II) precipitable water is simultaneously increased in the whole region including the upwind located eastern coast of North America. It therefore seems that large parts of the response are not attributable to moisture recycling, but rather to differences in the large-scale circulation (see Sect. 1.5.2 for details).

Even without differences in the large-scale circulation it seems implausible that moisture recycling can “act” across an ocean basin as large as for example the Atlantic. First, in contrast to land, the ocean is an inexhaustible water reservoir for atmospheric considerations. Second the boundary layer, which contains most of the atmospheric moisture, is mostly well-mixed. This suggests that the hydrological state of the atmosphere has a short memory over the ocean, meaning that the moisture content returns to a quasi-equilibrium faster than it takes the air to cross a sufficiently large ocean basin. This implies that, for example, Eurasia is not affected by North America’s evaporation and vice versa, at least not through

moisture recycling – despite the substantial fraction of moisture they receive from each other as continental recycling ratios reveal (Fig. 1.2). Over land the situation is different: Since evaporation is constrained by moisture availability, an atmospheric dry-anomaly can persist and intensify. These considerations conform to the finding that the atmosphere over the ocean is not systematically drier in response to the suppression of continental evaporation (Fig. 1.5). To take into account that the continental recycling ratio of an air mass is irrelevant for its hydrological state after having crossed a large ocean basin, in the following we only consider intra-continental gradients of the continental recycling ratio when trying to attribute aspects of the hydrological response to moisture recycling. Note that the consideration of recycled (continental) moisture over the ocean is not specific to our study because in all earlier studies estimating continental recycling ratios the recycled moisture is tracked also over the ocean (compare Sect. 1.4, last paragraph).

Continental recycling ratios increase from continental upwind regions to downwind regions (Fig. 1.2). This conforms to the expectation that dry-anomalies should intensify along atmospheric trajectories over the continents in response to suppressed land-evaporation. Hence, from the moisture-recycling perspective, changes in precipitable water and, consequently, precipitation are expected to be smaller in upwind regions and progressively larger (negative) towards downwind regions (compare Fig. 1.3). But our experiments show a different response. Over Eurasia the hydrological response is opposite to what would be expected from the recycling ratios: In the upwind (western) parts of Eurasia the atmosphere carries up to 40 % less moisture in the DRY experiment compared to the REF experiment. The drying declines in eastward direction until at the eastern coast of Asia the atmosphere carries even 20 % more moisture in the DRY experiment (Fig. 1.5). The precipitation response is similar, though stronger in magnitude: The largest part of western Eurasia receives less than 10% of the precipitation in the REF experiment. Only in the easternmost part of extratropical Eurasia the precipitation decrease declines (Fig. 1.4). These tendencies recur very similarly in North America. Apparently the extratropical response is dominated by non-recycling mechanisms.

In the Tropics the hydrological response is strongly influenced by non-recycling mechanisms as well. In tropical Africa the continental recycling ratio peaks north of the equator,

Table 1.1: Areal mean (July) continental recycling ratio ( $R_c$ ), evaporation ( $E$ ), precipitation ( $P$ ), and precipitable water ( $W$ ) in the REF experiment, and the response  $\Delta P$  and  $\Delta W$  to the suppression of land-evaporation (DRY-REF).

Region	Location °N/°E	$R_c$ %	$E_{\text{REF}}$ kg m <sup>-2</sup> d <sup>-1</sup>	$P_{\text{REF}}$ kg m <sup>-2</sup> d <sup>-1</sup>	$\Delta P$ % of REF	$W_{\text{REF}}$ kg m <sup>-2</sup>	$\Delta W$ % of REF
Europe*	37..71/-10..59	66	3.0	2.2	-95	25	-29
Africa*	-34..37/-18..59	52	1.0	0.9	-66	27	-12
Northern Asia*	37..76/59..179	77	2.4	2.5	-79	23	-5
Southern Asia*	7..37/59..140	41	2.4	5.4	-29	39	-3
Oceania*	-47..7/97..177	8	1.0	1.1	-46	21	-7
North America* (excl. Gr.)	11..78/-166..-53	59	2.9	2.8	-69	25	-3
Greenland*	60..84/-70..-14	69	0.14	1.2	+40	8	+34
South America*	-54..11/-82..-35	23	2.4	2.2	-38	30	-4
Global land		50	1.8	2.1	-54	24	-7
Global ocean		14	3.7	3.6	-7	29	-0.4
Northern Hemisphere		31	2.8	3.9	-21	35	-3
Southern Hemisphere		3	3.5	2.4	-8	20	-0.8
Global land & ocean		20	3.2	3.2	-16	28	-2

\* land only

in particular in tropical West Africa (Fig. 1.2, bottom panel). In contrast, precipitable water is almost unchanged in tropical West Africa, but considerably decreased south of the equator along Africa's western coast (Fig. 1.5). The response of precipitation approximately resembles the response of precipitable water (Fig. 1.4). However, focussing only on those parts of Africa located south of the equator with prevailing easterlies in July, the response to some extent conforms to the moisture-recycling perspective: Continental recycling ratios increase from approximately 0% at the upwind (eastern) coast to 10–40% at the downwind (western) coast, while precipitable water and precipitation are more or less unchanged at the upwind coast, but decreased by 20% and almost 100%, respectively, at the downwind coast. Note, however, that the absolute amounts of precipitation and precipitable water in this region are already low in the REF experiment, with strong meridional gradients (Figs. 1.4 and 1.5, upper panels).

Similar to Africa, in tropical South America we find on the one hand that mechanisms other than moisture recycling substantially contribute to the signal, while on the other hand the response to some extent conforms to the moisture-recycling perspective. The increase of precipitable water and precipitation along the downwind located tropical part of the Andes (Figs. 1.4 and 1.5) stands in contrast with the coinciding maximum of the continental recycling ratio (Fig. 1.2, bottom panel). At the upwind located eastern coast neither the precipitation increase south of the equator, nor the decrease of precipitable water as well as precipitation from the equator northward can be explained by moisture recycling. However, the drying around the Tropic of Capricorn seems to be at least partly attributable to moisture recycling. When the air is advected from the Atlantic to eastern Brazil it is still as moist in the DRY experiment as in the REF experiment, but along the south-bending trajectory (compare Fig. 1.3, bottom panel) a dry-anomaly intensifies until around Paraguay the atmosphere is 20% drier in the DRY experiment, accompanied by 70% less precipitation. Compared to southern tropical Africa the absolute amounts of precipitable water and precipitation are considerably larger and, hence, the response more meaningful.

## 1.5.2 Response of the atmospheric circulation

As elaborated in the last section the response of precipitable water and precipitation seems to be largely dominated by other mechanisms than moisture recycling (compare Fig. 1.1). In this section we show how the large-scale circulation reacts to the suppression of continental evaporation (compare also Sect. 1.2.3).

Due to the absence of latent cooling at the land surface, the continents are substantially warmer without continental evaporation (Fig. 1.6, top panel). Not surprisingly the spatial distribution of the warming conforms rather closely to the evaporation rate in the REF experiment (Fig. 1.3, bottom panel), though the response is amplified in the northern extratropics in summer because of reduced cloud cover in the DRY experiment (not shown). While tropical Africa and tropical South America are about 7 K warmer in the DRY experiment, the continental northern midlatitudes, which exhibit comparable evaporation rates in summer in the REF experiment, are 10–15 K warmer in the DRY experiment. Deviations of the warming from the evaporation rates in the REF experiment are also due to the fact that the surface temperatures are not only locally determined, but also by advection. For example the record warming (more than 15 K) around Lake Baikal, located in the downwind parts of Eurasia, is supported by the intensification of heat-anomalies along the air's path over the largest of all continents.

The direction of the response of the large-scale circulation is basically in agreement with Shukla and Mintz (1982), although Shukla and Mintz (1982)'s wet-soil case is much wetter than our REF experiment. As in Shukla and Mintz (1982) the warming of the continents (Fig. 1.6, top panel) is accompanied by a decrease of surface pressure over the continents and a compensating increase of surface pressure over the ocean basins (Fig. 1.6, bottom panel). In particular the summerly heat lows over Eurasia and North America and the corresponding highs over the North Atlantic and the North Pacific are strongly enhanced, such that the pressure difference between the ocean basins and the continents (15–25 hPa in the REF experiment) almost doubles. In consequence the anticyclonic low-level circulations over the North Atlantic and the North Pacific as well as the cyclonic low-level circulations over Eurasia (together with northern Africa) and North America are strongly amplified (Fig. 1.7, arrows). The associated amplification of low-level convergence (and high-level divergence)

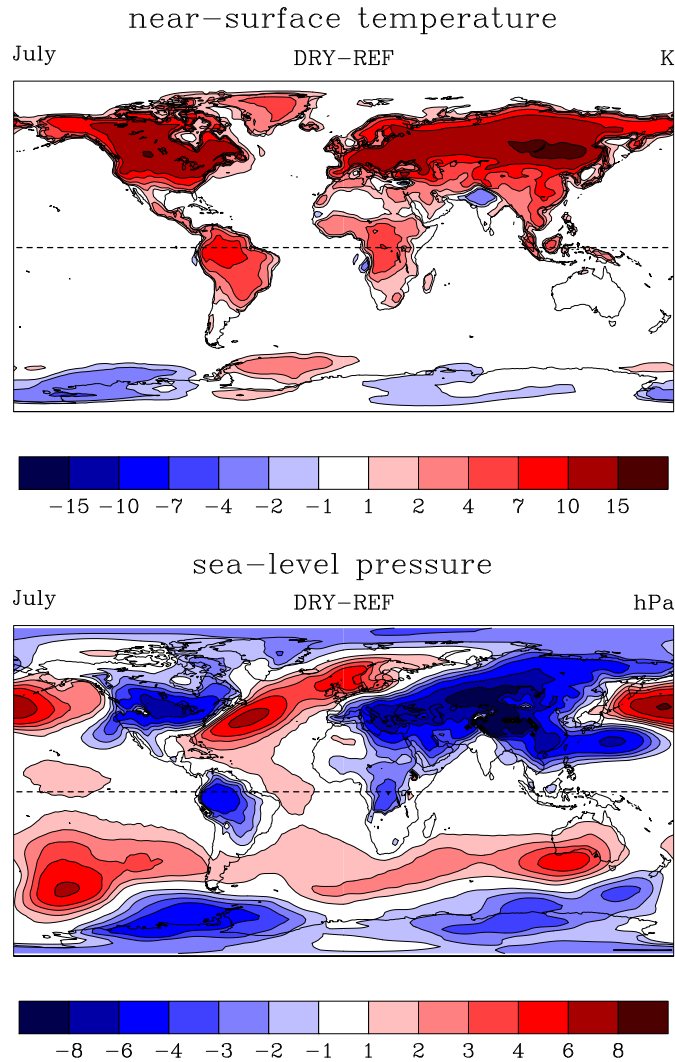


Figure 1.6: Top: Difference in near-surface (2 m) temperature in July (K, DRY-REF). Bottom: Difference in pressure reduced to sea-level in July (hPa, DRY-REF). See Fig. A.5 in the appendix for January.

over the continents, measured by the mean vertical velocity at 500 hPa, is inhomogeneously distributed (Fig. 1.7).

Owing to the modified surface-pressure field the mid-latitude westerlies over Eurasia and North America are considerably weaker in the DRY experiment (Fig. 1.7). This results in more continental and, hence, drier conditions in particular in the western parts of the continents (Figs. 1.5 and 1.4). Precipitable water is most affected in a large region spanning from the western coast of northern Africa over the Mediterranean to the Caspian Sea because the westerlies over Europe are not only weaker, but partly even turn into northerlies, such

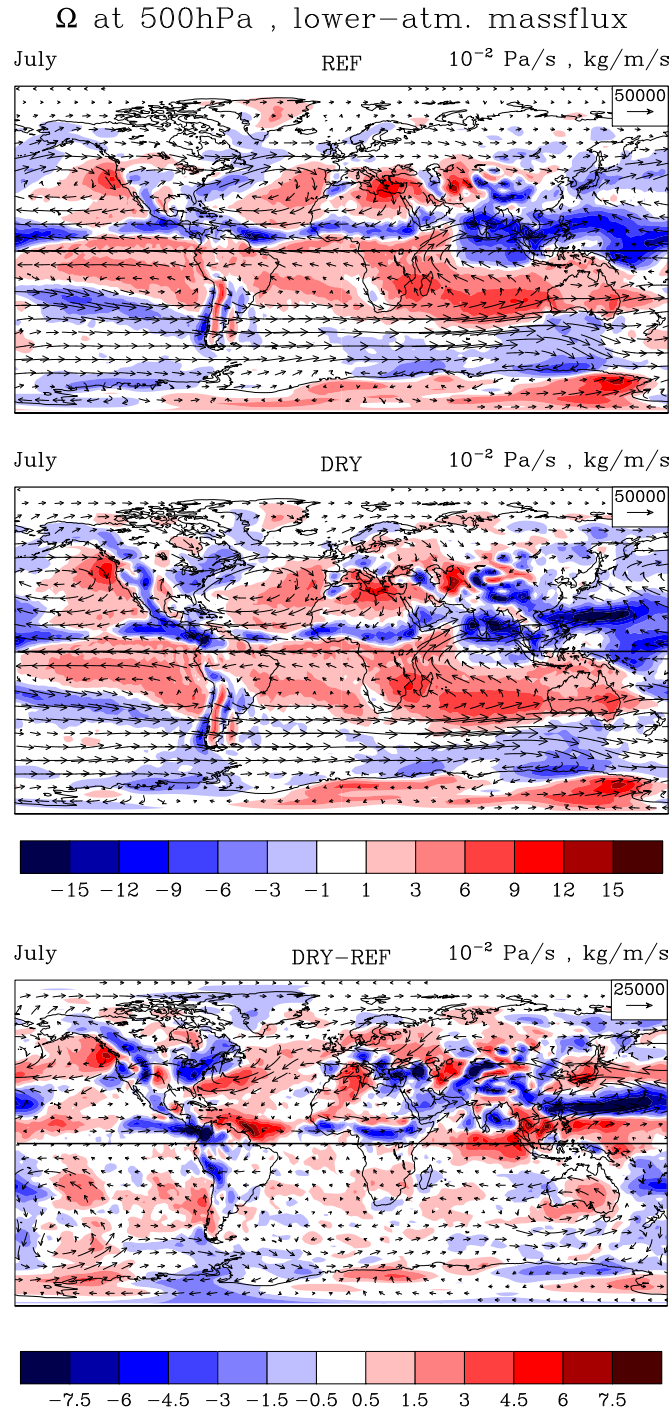


Figure 1.7: Vertical velocity ( $\Omega$ ) at 500 hPa (colours,  $\text{Pa s}^{-1}$ ) and horizontal total mass flux in the lowest 13 model levels (arrows,  $\text{kg m}^{-1} \text{s}^{-1}$ ) in July in the REF experiment (top panel), in the DRY experiment (middle panel), and the difference between the two (bottom panel). The lowest 13 model levels correspond approximately to the lower half of the atmosphere. Hence, the vertical velocity at 500 hPa approximately corresponds to the divergence of the shown mass flux. Note that the scale for both  $\Omega$  and the mass flux are changed by a factor 2 in the bottom panel to make the differences better visible. See Fig. A.6 in the appendix for January.

that drier air masses from the north are advected into the region.

The strengthening of the cyclonical low-level circulation around Eurasia and northern Africa is also apparent in its southern branch, which includes the monsoonal low-level westerlies over the Indian subcontinent (Fig. 1.7). In consequence more moisture is advected from the Arabian Sea and precipitates when encountering the high mountain ranges of the Himalayas (Fig. 1.4). As a side remark, the strengthening of the westerlies over the Indian subcontinent also explains the salient cooling in northern India and Pakistan (Fig. 1.6, top panel).

The differences in surface pressure (Fig. 1.6, bottom panel) result in stronger low-level southwesterlies along the eastern coast of North America and the eastern coast of Eurasia north of Japan (Fig. 1.7) in the DRY experiment. Consequently, more moisture is transported into the Arctic, where precipitable water is increased by about 30 % and precipitation is also considerably enhanced, particularly in Greenland.

Because of the absence of the Coriolis force at the equator, the decreased surface pressure in tropical South America and tropical Africa (Fig. 1.6, bottom panel) does not cause continental-scale changes of low-level vorticity (Fig. 1.7). But the low-level convergence patterns (in particular the ITCZ, measured by the vertical velocity at 500 hPa, Fig. 1.7) are strongly altered in response to the suppression of continental evaporation. While in the REF experiment in July the ITCZ is similarly strong to the west and to the east of Central America, the western part over the Pacific is much stronger than the eastern part over the Atlantic in the DRY experiment, associated with increased and decreased precipitation, respectively (Fig. 1.4). In Africa the ITCZ is shifted southward in the DRY experiment. While most of tropical Africa experiences much drier conditions, the precipitation rates around  $5^{\circ}$  N, now located within the ITCZ, are not as much decreased as to the north and to the south. Over the tropical warm pool areas in the Indic and the western Pacific the ITCZ is considerably shifted to the north, while over the central Pacific the double-ITCZ is more pronounced in the DRY experiment than in the REF experiment. Again, these changes are reflected in the precipitation rates (Fig. 1.4). The strong modifications of the low-level convergence patterns and precipitation over the ocean are particularly remarkable given that the two experiments are driven with identical SSTs.

### 1.5.3 Effects from local coupling

From the comparison of continental recycling ratios with the actual hydrological response (Sect. 1.5.1) and the elucidation of changes in the large-scale circulation (Sect. 1.5.2) it becomes apparent that effects associated with the large-scale circulation rather than moisture recycling dominate the overall response. However, it still seems astonishing that (I) the precipitation response is so extreme, whereby the most extreme decrease of almost 100% is comparatively sharply delimited to the continents, and (II) that, apart from some tropical exceptions, the upwind to downwind drying-gradients one would expect from moisture-budget considerations are completely absent. Admittedly the latter is to a large part due to changes in the large-scale circulation, but one has to note that for example the westerlies over Eurasia and North America, although significantly attenuated, are still westerlies in the DRY experiment. These arguments suggest that another factor contributes to the overall response, namely (positive) local evaporation-precipitation coupling (compare Fig. 1.1).

The comparison of local vertical profiles of the thermal structure of the atmosphere between our two experiments is not as instructive as in the typical local-coupling studies (compare Sect. 1.2.2) because the advected profiles at any location are already different between the experiments due to the strong response of the large-scale circulation. However, it is reasonable that the substantially drier and warmer continental surfaces (Fig. 1.6, top panel) strongly influence the local generation of precipitation.

In eastern Brazil, where neither moisture recycling nor changes in the large-scale circulation seem to be responsible for the precipitation increase (Fig. 1.4), the response may be caused by negative local coupling. Otherwise the strong precipitation decrease over most continental regions correlates to the evaporation rates in the REF experiment (Fig. 1.3, bottom panel), which points at positive local coupling. Schär et al. (1999) find with regional simulations for summerly Europe that the decrease of precipitation amounts to approximately half of the imposed decrease of evaporation (see also next section). This makes it also quantitatively plausible that a significant fraction of the precipitation decrease we find in response to the suppression of continental evaporation may actually be attributable to positive local coupling, although this is hard to prove from our results.

In principle it seems possible that under certain circumstances the response of precipita-

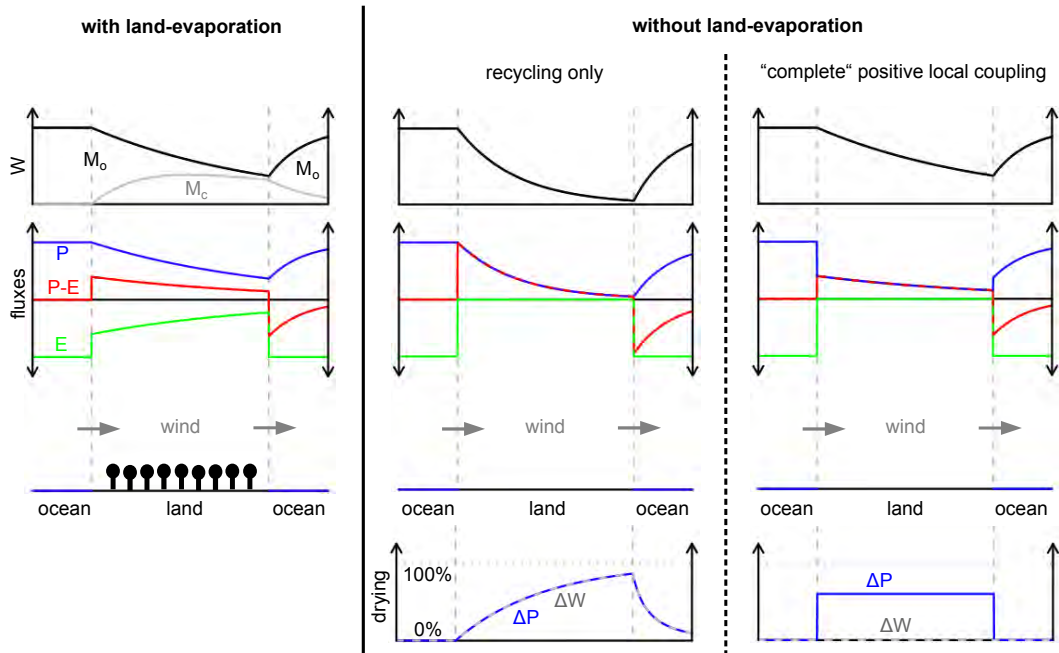


Figure 1.8: Illustration of two principally possible idealised responses to the suppression of land-evaporation as 1-D-transects through a continent. Left panel: reference situation with continental evaporation. Middle panel: response to the suppression of continental evaporation dominated by moisture-recycling. Right: response to the suppression of continental evaporation in a special case: The decrease in precipitation completely compensates for the missing evaporation, such that  $P - E$  is unaffected.  $W$  = precipitable water,  $M_o$  = oceanic moisture,  $M_c$  = continentally recycled moisture,  $P$  = precipitation,  $E$  = evaporation. The graphs at the bottom show the relative reduction ( $\frac{\text{REF}-\text{DRY}}{\text{REF}}$ ) of  $P$  (blue, solid) and  $W$  (grey, dashed). Units are arbitrary.

tion due to positive local coupling completely compensates for changes in evaporation, such that the net water loss from the atmosphere to the land (precipitation minus evaporation,  $P - E$ ) remains unaltered despite the suppression of evaporation. This possibility suggests a simplistic but yet instructive picture that is illustrated in Fig. 1.8.

The figure contrasts two possible idealised responses to the suppression of land-evaporation, one with moisture recycling dominating the response (middle panel), and one with non-recycling mechanisms acting to cancel out the effect from moisture recycling (right panel). The figure shows profiles of precipitable water and surface fluxes as 1-D-transects through an idealised continent along the prevailing wind direction, with oceans situated upwind and downwind. Before landfall the air is in a quasi-equilibrium humidity state over the ocean,

meaning that precipitation and evaporation are in balance ( $P - E = 0$ ). In the reference situation (Fig. 1.8, left panel), the evaporative fraction over the continent is assumed to be constant at 60%, meaning that 40% of the precipitation are removed from the system as runoff. With precipitation assumed to be a function of precipitable water ( $W$ ) only, here exemplarily as  $P \propto W$  (compare Savenije, 1995), precipitable water and the surface fluxes decrease continuously (exponentially) from the upwind coast to the downwind coast. In parallel the continental recycling ratio ( $M_c/W$ ) increases. When the air leaves the continent it returns to its initial equilibrium, with the ocean providing the moisture needed to remove the deficit ( $P - E < 0$ ).

Like in the reference situation, in the moisture-recycling case (Fig. 1.8, middle panel) precipitation is assumed to be a function of precipitable water only ( $P \propto W$ ) and, hence, evolves continuously with precipitable water. Without continental evaporation the progressive atmospheric moisture loss is stronger than in the reference situation. The relative reduction of both precipitable water and precipitation compared to the reference situation (bottom graph) increases from upwind to downwind, conforming to the increase of the continental recycling ratio in the reference situation.

Instead we now assume the special case that, due to strong positive local coupling, the decrease in precipitation results in unchanged  $P - E$  (Fig. 1.8, right panel). In consequence, precipitable water evolves as in the reference situation, and the relative precipitation decrease is 60% on the whole continent – the upwind to downwind drying-gradient vanishes (bottom graph). In other words, the upwind response due to “complete” positive local coupling annihilates the effect one would expect from moisture recycling.

Before coming to the major conclusion we draw from this simplistic picture, we analyse in how far the response of precipitation compensates for the missing moisture input by evaporation in our model experiments. Figure 1.9 (bottom panel) reveals that in July  $P - E$  over land tends to increase in response to the suppression of continental evaporation. This means that, in contrast to the simplistic case of “complete” positive local coupling illustrated in Fig. 1.8, the response of precipitation does not completely compensate for the missing evaporation in most continental regions.

Relating the local response of precipitation to the local land-surface evaporation in the

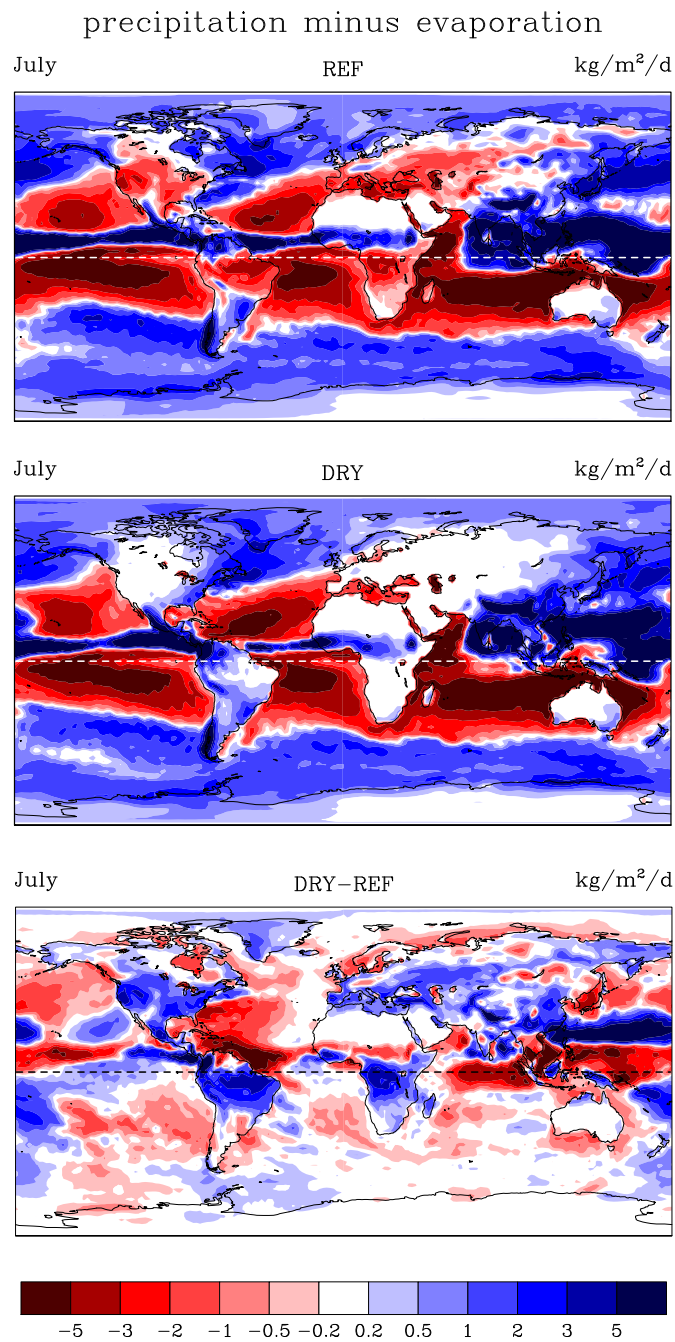


Figure 1.9: Precipitation minus evaporation ( $\text{kg m}^{-2} \text{d}^{-1}$ ) in July in the REF experiment (top panel), in the DRY experiment (middle panel), and the difference between the two (bottom panel). See Fig. A.7 in the appendix for January.

REF experiment (Fig. 1.10) however shows that in large parts of the continents the decrease of precipitation compensates for a substantial fraction of the missing evaporation. Closer inspection of the patterns in Figs. 1.9 and 1.10 further reveals that regions where the response of precipitation compensates for much less than 100 % of the missing evaporation are almost exclusively located where in the REF experiment the land is a source of moisture in July. Such places include the tropical wet-dry climates that have their dry season in July when the ITCZ is located further to the north, but also the mid-latitude summer-dry climates of Eurasia and North America. Where the land is a moisture source in the REF experiment (a situation that is not captured by the simplistic picture in Fig. 1.8), not even the total loss of precipitation could completely compensate for the missing evaporation. In these regions moisture recycling must contribute to the response that follows the suppression of evaporation *a priori*.

It is probably no coincidence that the South American region around the Tropic of Capricorn and the western coast of southern Africa – the regions where the drying in July seems to be partly attributable to moisture recycling (Sect. 1.5.1) – are located downwind of strong continental moisture-source regions. On the other hand, for Eurasia and North America the simplistic picture illustrated in Fig. 1.8 may partly explain why there are no upwind to downwind drying-gradients in response to the suppression of continental evaporation in July, even though we know that a large part of the response is caused by changes in the atmospheric circulation (Sect. 1.5.2).

Although largely unrealistic for several reasons, the simplistic picture illustrated in Fig. 1.8 demonstrates in a striking manner that moisture recycling estimates could in principle be completely useless to predict the consequences of land-use change, even without changes in the atmospheric circulation. While we do not at all claim that the case of “complete” positive local coupling is a prevalent situation in reality, the simplistic picture strongly supports our key argument: moisture recycling estimates have first to be shown to actually tell us something before they can be used to deduce the response of precipitation to land-use change.

Finally, it seems worth to mention that, ignoring the high latitudes, regions with particular high compensation in July (Fig. 1.10) are to some extent spatially correlated with the

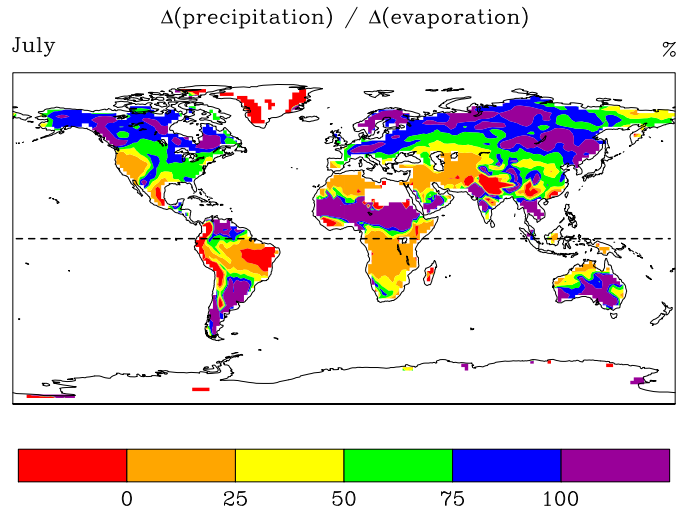


Figure 1.10: The response of precipitation in relation to the imposed evaporation decrease ( $\frac{P_{\text{DRY}} - P_{\text{REF}}}{-E_{\text{REF}}}$ , %) in July. Note that  $\Delta E = -E_{\text{REF}}$  and  $(P - E)_{\text{DRY}} = P_{\text{DRY}}$  because  $E_{\text{DRY}} = 0$ . Violet indicates overcompensation (the land becomes a weaker moisture sink;  $P_{\text{DRY}} < (P - E)_{\text{REF}}$ ), blue, green, yellow and orange indicate incomplete compensation (precipitation still decreases, but the land becomes a stronger moisture sink or weaker moisture source;  $(P - E)_{\text{REF}} < P_{\text{DRY}} < P_{\text{REF}}$ ), and red indicates an amplification of the effect from the evaporation decrease (precipitation increases and thus adds to the evaporation decrease;  $P_{\text{DRY}} > P_{\text{REF}}$ ). Continental regions with negative evaporation (=dew) in the REF experiment are left white. See Fig. A.8 in the appendix for January.

northern-summer “hot spot” regions in Koster et al. (2004). This supports the idea that some of the precipitation response may be due to local coupling. The obvious mismatch in high latitudes is not surprising given that the “hot spots” in Koster et al. (2004) include the precondition that evaporation is subject to interannual variability.

## 1.6 Discussion

The MPI-ESM is capable of reproducing the most important aspects of present-day climate (e.g. Hagemann et al., 2006). This does not guarantee that the model behaves realistic under strongly perturbed conditions, as it is the case in our DRY experiment. In particular the part of the response due to local coupling is subject to considerable inter-model variation that probably is largely attributable to the parameterisation of moist convection (see Sect. 1.2.2). On the other hand we find a very similar response with an alternative moist convection

scheme. Since the large-scale circulation is less susceptible to questionable parameterisation schemes it stands to reason that general circulation models are more reliable in this aspect than for local coupling. And indeed, with a comparable setup Shukla and Mintz (1982) find a similar large-scale response. Note however that in the wet-soil case of Shukla and Mintz (1982) the continents are much wetter than in our REF experiment, so that the response they find is even more pronounced. Anyway, our results claim for validation by similar studies using other models.

However, we argue that for the purpose of this case study—to demonstrate that recycling estimates do not *necessarily* mirror the consequences of changes in evaporation—the realism of the perturbation and the accuracy of the simulated response are not of great relevance. More important is that the perturbation we apply to test the predictive utility of the recycling measure considered in this study, namely the continental recycling ratio, is immediately suggested by its definition. By subjecting the continental recycling ratio to critical scrutiny instead of recycling measures that quantify moisture recycling on a smaller spatial scale (e.g. the local recycling ratio), we approach the question posed in the title from the largest possible scale.

The computed recycling patterns are based on a vertically integrating tracing scheme (Sect. 1.3.2). It is evident that this simplification introduces some error into the estimates, in particular where the usually stably stratified free atmosphere is seldomly mixed in the vertical through high convection and/or where horizontal winds are substantially sheared in the vertical. The latter is typically not so much the case in the extratropics, where the flow is dominated by cyclones and anticyclones, but may be more relevant closer to the equator. For example in tropical western Africa during northern summer a north-east directed moisture flux in the monsoon layer below 750 hPa is essentially compensated by a reverse flow above 750 hPa. The weak horizontal moisture flux remaining after vertical integration presumably results in an overestimation of moisture recycling. However, the errors are acceptably small given the similarity of recycling estimates obtained with (Yoshimura et al., 2004; van der Ent et al., 2010, and this study) and without (Numaguti, 1999; Bosilovich et al., 2002) vertical integration. Furthermore, the focus of our study is on continental-scale patterns, in particular intra-continental upwind to downwind gradients, rather than on accurate regional

estimates.<sup>2</sup>

To keep the interpretability of our results as clear as possible, we use identical climatologies of surface albedo, surface roughness, and SSTs in both experiments. The climatic response of the fully dynamical atmosphere-ocean-land system to the suppression of continental evaporation could be considerably different from the response we obtain with our more tightly controlled setup. Important missing feedbacks involve for example albedo changes associated with the extent of snow and sea-ice covered areas. However, our setup is not designed to give a most realistic full-dynamics response, but to make a first step in assessing the informativeness of moisture recycling estimates. We have no reason to assume that one or more of the missing feedbacks would change the response in such a way that our conclusions would have to be revised significantly.

Throughout the paper we distinguish three mechanisms by which evaporation affects precipitation (Fig. 1.1). However, the sharp separation of the mechanisms, in particular of moisture recycling and local coupling, is not beyond question. We argue that moisture recycling acts slowly, i.e. spatio-temporally integrative, by its influence on the (vertically integrated) atmospheric moisture budget. In contrast, local coupling acts fast, i.e. locally, by its influence on the vertical thermal structure of the atmosphere. This point of view seems to conform to Schär et al. (1999) and Seneviratne et al. (2010) (see Sect. 1.2.4). However, this distinction is not always made so clearly. For example, in Dirmeyer et al. (2009) and in van den Hurk and van Meijgaard (2010) local recycling ratios (more precisely the temporal correlations of local recycling ratios and soil moisture) are used together with other indicators to decide which locations might be susceptible to local land-atmosphere coupling. We think that the conceptual separation of local coupling and moisture recycling might help to better understand the complex interactions between the land and the atmosphere. However, we concede that in reality the two mechanisms may not be as clearly distinguishable as we think.

---

<sup>2</sup>The results of Chapter 2 confirm the validity of the speculations given in this paragraph.

## 1.7 Summary

The idea that moisture recycling estimates can be used to indicate the sensitivity of climate to land-use change relies on the condition that the atmospheric response following a perturbation in evaporation is dominated by the “passive” effect of evaporation on the atmospheric moisture budget, i.e. by moisture recycling. We argue that this implicit condition has not sufficiently been examined yet. Besides moisture recycling, changes in evaporation influence climate also through local coupling and changes in the atmospheric circulation (Fig. 1.1), where the latter two mechanisms are due to the active role water plays in the atmosphere. Since the three mechanisms act on different scales, it stands to reason that their relative importance depends on the spatial scale of the perturbation. In the present study we approach this issue from the largest possible scale by exploring the relation between continental recycling ratios and the response that follows the complete suppression of continental evaporation.

Focussing on July we find that the largest part of the response can be attributed to the atmospheric circulation, which changes largely due to the intensification of the continental thermal lows. A major consequence in the extratropics is that the westerlies over Eurasia and North America are weakened, which in turn results in drier (more continental) conditions in the western parts of these two continents. The fact that the most severe decrease in precipitation is rather sharply restricted to the continents suggests that positive local coupling adds to the continental drying. The continental recycling ratios obtained from the reference experiment reveal that effects due to moisture recycling should affect the eastern (downwind) parts of Eurasia and North America rather than the western (upwind) parts. That the actual (simulated) response does not conform to this expectation suggests that the non-recycling mechanisms dominate the response. However, the magnitude of the overall drying, although occurring in the “wrong” parts of the continents, is probably also due to moisture recycling (or, more precisely, its absence).

Also in the tropics the response to the suppression of continental evaporation is to a large part due to changes in the atmospheric circulation. In contrast to the extratropics, where the surface-pressure distribution alters mainly the strength and the pattern of horizontal

atmospheric motions, the tropical response is dominated by changes in the strength and the position of the regions of low-level convergence (the ITCZ). However, in tropical wet-dry climates during the dry season, when these regions are strong moisture sources ( $P - E < 0$ ), we find that the atmosphere in response to the missing surface evaporation becomes progressively drier along the prevailing wind direction. Here it seems that moisture recycling is at least as important as the other mechanisms. Our results thus indicate that, for continental-scale perturbations, in some (tropical) regions moisture recycling estimates may be more useful than in other (extratropical) regions.

## 1.8 Conclusions

Our case study demonstrates that moisture recycling estimates can not consistently be used as reliable indicators for the sensitivity of precipitation to modified land-evaporation. More specifically our results indicate that the predictive utility of continental recycling ratios is rather limited because other mechanisms than moisture recycling, induced by water's active role in the atmosphere, dominate the response to the suppression of continental evaporation. It may still be that smaller perturbations yield higher correlations between the response one expects from correspondingly defined recycling estimates and the actual (simulated) response – but this hope must be supported by scientific evidence that is currently missing. Specific analyses that build on the principles of our case study while focussing on smaller spatial scales could help to advance our understanding of moisture recycling and its interplay with local coupling and the atmospheric circulation.

It seems that the range of spatial scales at which the predictive utility of moisture recycling estimates might be high is narrowed not only from the large scale, as our case study demonstrates, but also from the small scale: Studies on local coupling suggest that below 100–1000 km effects from local coupling dominate the response to land-surface perturbations (see Sect. 1.2.4). Without further investigations one can only speculate whether at intermediate spatial scales moisture recycling estimates might be informative indicators. Therefore, further modelling studies (and, ultimately, observational studies) are needed to replace speculations by evidence. Our case study does not suffice to answer the question

*Chapter 1 What do moisture recycling estimates tell us?*

what moisture recycling estimates tell us, but we think that it is a first step towards an answer. Moreover, we hope that our study stimulates a wider discussion on the predictive utility of moisture recycling estimates for the response of precipitation to land-use change.

*The appendix contains supplementary material related to this chapter including a discussion on different averaging methods to obtain recycling ratios (A.1), results obtained with the original Tiedtke convection scheme (A.2), and results for January (A.3).*

I can foretell the way of celestial bodies, but can say little about the movement of a small drop of water.

---

*(Galileo Galilei)*

## Chapter 2

# Atmospheric water vapour tracers and the significance of the vertical dimension

## Abstract

Atmospheric water vapour tracers (WVTs) are an elegant tool to determine source-sink relations of moisture “online” in atmospheric general circulation models (AGCMs). However, it is sometimes desirable to establish such relations “offline” based on already existing atmospheric data (e.g. reanalysis data). One simple and frequently applied offline method is 2D moisture tracing. It makes use of the ‘well-mixed’ assumption, which allows to treat the vertical dimension integratively.

Here we scrutinise the ‘well-mixed’ assumption and 2D moisture tracing by means of analytical considerations in combination with AGCM-WVT simulations. We find that vertically well-mixed conditions are seldomly met. Due to the presence of vertical inhomogeneities, 2D moisture tracing (I) neglects a significant degree of fast-recycling, and (II) results in erroneous advection where the direction of the horizontal winds varies vertically. The latter is not so much the case in the extratropics, but in the tropics this can lead to large errors. For example, computed by 2D moisture tracing, the fraction of precipitation in the western Sahel that originates from beyond the Sahara is  $\sim 40\%$ , whereas the fraction that originates from the tropical and southern Atlantic is only  $\sim 4\%$ . Full (i.e. 3D) moisture tracing however shows that both regions contribute roughly equally, which reveals the results of an earlier study as spurious.

Moreover, we point out that there are subtle degrees of freedom associated with the implementation of WVTs into AGCMs because the strength of mixing between precipitation and the ambient water vapour is not completely provided by such models. We compute an upper bound for the resulting uncertainty and show that this uncertainty is smaller than the errors associated with 2D moisture tracing.

## 2.1 Introduction

Source-sink relations of atmospheric moisture characterise the Earth's hydrological cycle. They have been used for example to investigate the cause of extreme precipitation events (e.g. Sodemann et al., 2009) and to estimate to what extent precipitation is sustained by continental moisture recycling (e.g. van der Ent et al., 2010). Source-sink relations of atmospheric moisture are considered to contain information on how strongly precipitation somewhere is causally linked to evaporation elsewhere, though the conclusiveness of source-sink relations to establish causalities is not beyond controversy (Goessling and Reick, 2011). Nevertheless, knowledge about the paths moisture takes in the atmosphere is believed to be associated with at least some predictive skill, for example regarding the impact potential land-use changes may have on precipitation patterns.

By measuring the ratios of stable water isotopes in precipitation (e.g. Dansgaard, 1964; Salati et al., 1979), one can retrieve only vague information on where the water has evaporated; the few degrees of freedom that are associated with the stable-isotope composition do not allow for the determination of a reasonably resolved spatial pattern of the evaporative sources. To determine the latter one has to recur to numerical tracing of moisture, which can be realised either offline, i.e. *a posteriori*, using suitable data on evaporation, precipitation, and atmospheric transport, or online within an atmospheric general circulation model (AGCM).

Online moisture tracing was first applied by Koster et al. (1986) and Joussaume et al. (1986). In this context, Bosilovich (2002) coined the term *passive water vapour tracers* (WVTs), where passive means that the AGCM's prognostic variables are not affected by the WVTs (see also Bosilovich and Schubert, 2002; Bosilovich et al., 2002). Online tracing offers the advantage that any variables characterising the atmospheric state are available at the AGCM's temporal and spatial resolution, including the vertical dimension. Disadvantages of online tracing are that (I) AGCMs not constrained by data assimilation can not reproduce particular real-world situations but only reflect the Earth's long-term climate, including inevitable biases, and that (II) to determine the fate of the moisture evaporated from each predefined set of source regions one has to run the whole computationally expensive AGCM.

By contrast, offline moisture tracing is computationally less expensive and can be applied to different kinds of data including reanalyses that arguably constitute the best guess of the evolution of the global atmospheric state during recent decades. While the generation of reanalyses involves AGCMs, the stored output data typically do neither contain all atmospheric state variables that are needed to perform a full 3D tracing comparable to the online tracing, nor is their spatio-temporal resolution as high as in case of the online tracing. While the large-scale flow field is usually sufficiently characterised by reanalysis data, the processes that cause vertical redistribution of moisture – turbulent diffusion and precipitation – are usually not sufficiently characterised.

Several offline moisture tracing techniques have been developed that cope with the limitations of reanalysis-like data. Among these are sophisticated approaches like the Lagrangian particle dispersion method (e.g. Stohl and James, 2004) and the quasi-isentropic back-trajectory method (e.g. Dirmeyer and Brubaker, 1999), but also the conceptually simpler approach of 2D moisture tracing (Yoshimura et al., 2004; van der Ent et al., 2010; van der Ent and Savenije, 2011; Goessling and Reick, 2011; Keys et al., 2012). In the latter case the atmospheric fields are integrated vertically before the tracing is then performed only in the horizontal dimensions.

2D moisture tracing has been applied to estimate continental precipitation recycling ratios (i.e. the (spatially resolved) fraction of precipitation that stems from continental evaporation; Yoshimura et al. (2004); van der Ent et al. (2010); Goessling and Reick (2011)) and continental evaporation recycling ratios (i.e. the (spatially resolved) fraction of evaporation that precipitates on land; van der Ent et al. (2010)), but has also been used to determine source-sink relations at geographically smaller scales. Recently, Keys et al. (2012) used 2D moisture tracing to determine what they call the precipitationsheds of certain regions supposed to be particularly vulnerable to changes in precipitation. For the western Sahel, Keys et al. (2012) found that the Mediterranean and adjacent regions contribute substantially to the region’s growing-season precipitation, while relatively small amounts of moisture are advected from the tropical Atlantic ocean (Fig. 3 in Keys et al. (2012)).

However, we have argued earlier (Goessling and Reick, 2011) that 2D moisture tracing may produce large errors particularly in tropical and subtropical western Africa because of

the meteorological situation prevailing there in summer: while in the monsoonal layer below 750 hPa moisture is advected from the tropical Atlantic, the African Easterly Jet above 750 hPa carries moisture from the east and the north. In this study we therefore put one focus on the western Sahel.

The theoretical basis of 2D moisture tracing is the so-called ‘well-mixed’ assumption: The fractions of moisture stemming from different evaporative source regions in total atmospheric moisture are assumed to be independent of height. The ‘well-mixed’ assumption has a long history and was first used in the context of simple, regionally applied recycling models (e.g. Budyko, 1974; Brubaker et al., 1993; Eltahir and Bras, 1994). These recycling models included further simplifications that were associated with averaging over other dimensions. Put in context to these simpler recycling models, 2D moisture tracing is the least simplifying method that still invokes the ‘well-mixed’ assumption for the vertical dimension – all other dimensions (the horizontal space dimensions and the time dimension) are explicitly resolved. It seems worth to mention that there are also attempts to relax the ‘well-mixed’ assumption while keeping simplifications regarding the other dimensions (e.g. Burde, 2006; Fitzmaurice, 2007).

To investigate the validity of the ‘well-mixed’ assumption, Bosilovich (2002) traced moisture from different source regions located in North America using an AGCM equipped with WVTs. Bosilovich (2002) found that the moisture stemming from these regions tends to be inhomogeneously distributed vertically, with moisture of local origin being enriched in low levels. In one part of our study we further investigate the validity of the ‘well-mixed’ assumption using basically the same methodology as Bosilovich (2002). However, we also quantify the errors that arise from the 2D approximation by comparing source-sink relations of atmospheric moisture as determined by 2D and 3D moisture tracing.

It turns out, however, that the online 3D moisture tracing itself, which we use as reference, bears some uncertainty in the way it is implemented: While the net exchange of water molecules between falling rain drops and the ambient air is part of an AGCM’s implementation, assumptions have to be made regarding the degree to which gross evaporation and gross condensation act to mix the precipitation with the ambient water vapour. Instead of trying to come up with one single implementation that is as close as possible to reality – which

is a non-trivial task (see Sect. 2.8)–, we implemented two different 3D moisture tracing variants that span the range of possible behaviour: In one case precipitation is assumed to mix instantaneously with the ambient water vapour (strong mixing), and in another case it is assumed that only the net exchange of water between precipitation and air takes place (weak mixing). This allows us to estimate the maximum uncertainty associated with this issue.

The paper is structured as follows. In Sect. 2.2 we set forth the theoretical basis of the 2D approximation and show that 2D tracing is exact under vertically well-mixed conditions. In Sect. 2.3 we present characteristics of the atmosphere that determine whether the atmosphere is well-mixed or not. These characteristics hence strongly influence the accuracy of the 2D approximation. We then describe the implementation of WVTs into the AGCM ECHAM6 in Sect. 2.4.1, followed by a short validation of the WVT scheme in Sect. 2.4.2. In Sect. 2.5 we investigate to what extent the ‘well-mixed’ assumption holds according to our simulations. Subsequently, we quantify in Sect. 2.6 the maximum uncertainty of 3D moisture tracing that is related to the question of how strongly precipitation mixes with the ambient water vapour. In Sect. 2.7 we compare results obtained by 2D moisture tracing with results obtained by 3D moisture tracing. Finally, we discuss limitations and further aspects in Sect. 2.8 and draw conclusions in Sect. 2.9.

## 2.2 The theoretical basis of 2D moisture tracing

In this section we discuss the theoretical basis of the 2D approximation and demonstrate that 2D moisture tracing is exact – where we mean “identical to 3D moisture tracing” – if the ‘well-mixed’ assumption is valid. We demonstrate that well-mixed conditions are necessary for 2D moisture tracing to be exact for two reasons. The first concerns the question from which height precipitation is drawn, and the second relates to the impact of wind shear on horizontal moisture advection.

The ‘well-mixed’ assumption implies that water molecules of different origin are perfectly mixed in the vertical dimension, i.e. that the fraction  $f_i$  of any WVT species  $i$  in total

moisture is independent of height  $z$  [m]:

$$f_i(z) = \frac{q_i(z)}{q(z)} \stackrel{!}{=} \hat{f}_i \quad \forall z \quad (2.1)$$

where  $q_i$  [kg/kg] is the specific concentration of moisture stemming from the source region  $i$ ,  $q$  [kg/kg] is the total specific moisture for which it holds that  $q = \sum_i q_i$ , and

$$\hat{f}_i = \frac{\hat{q}_i}{\hat{q}} \quad (2.2)$$

with

$$\hat{q}_i = \int_0^\infty \rho q_i dz \quad (2.3)$$

and

$$\hat{q} = \int_0^\infty \rho q dz \quad (2.4)$$

where  $\rho$  [kg/m<sup>3</sup>] is the air density. Here and in the following we simplify the notation inside integrals by dropping the argument that indicates the dependency of the variables on  $z$  (a notation that we adopt also for the other spatio-temporal dimensions).

If the ‘well-mixed’ assumption (Eq. 3.4) does not hold, the composition of precipitation  $P$  arriving at the surface depends on the height from which the moisture originates:

$$\frac{P_i}{P} = \frac{\int_0^\infty f_i p^* dz}{\int_0^\infty p^* dz} \quad (2.5)$$

where  $P_i$  [kg/m<sup>2</sup>] is the amount of precipitation that stems from the source region  $i$  and  $p^*(z) dz$  [kg/m<sup>2</sup>] is the amount of precipitation drawn from the height  $z$ . It is obvious that  $p^*$  can be interpreted as a vertical weight function. Note, however, that  $p^*$  is not simply the (vertically resolved) difference of condensation and re-evaporation, but the result of a downward propagating integrative process that involves additional assumptions regarding the gross terms of condensation and evaporation, see below. Only if the ‘well-mixed’ assumption (Eq. 3.4) holds, Eq. (2.5) becomes  $P_i/P = \hat{f}_i$ , i.e. the vertical dimension does not need to be resolved to correctly determine the composition of precipitation.

We now turn to the second reason why 2D moisture tracing requires well-mixed conditions

to be exact, which concerns horizontal advection. To this end we start from the full 3D transport (advection) equation, and derive the 2D formulation by vertical integration. For the sake of simplicity we omit one of the two horizontal dimensions. The full transport equation for a WVT species  $i$  without sources and sinks reads

$$\frac{\partial(\rho q_i)}{\partial t} + \frac{\partial(\rho q_i u)}{\partial x} + \frac{\partial(\rho q_i w)}{\partial z} = 0 \quad (2.6)$$

where  $u$  [m/s] is the wind speed along the horizontal dimension  $x$  [m], and  $w$  [m/s] is the wind speed along the vertical dimension. As a side remark, in large-scale AGCMs the vertical term can only partly be handled explicitly because subgrid-scale processes (“turbulent diffusion”) typically dominate the vertical transport. Turbulent (convective) processes are therefore handled by additional parameterisations.

Vertical integration of Eq. (3.1) gives

$$\int_0^\infty \frac{\partial(\rho q_i)}{\partial t} dz + \int_0^\infty \frac{\partial(\rho q_i u)}{\partial x} dz = 0. \quad (2.7)$$

The integral of the vertical term in Eq. (3.1) is zero because  $w = 0$  for  $z = 0$  and  $\rho \rightarrow 0$  for  $z \rightarrow \infty$ . Equation (2.7) can be rewritten as

$$\frac{\partial \hat{q}_i}{\partial t} + \frac{\partial \hat{q}_i \hat{u}_i}{\partial x} = 0 \quad (2.8)$$

with

$$\hat{q}_i = \int_0^\infty \rho q_i dz \quad (2.9)$$

and

$$\hat{u}_i = \frac{\int_0^\infty \rho q f_i u dz}{\int_0^\infty \rho q f_i dz}. \quad (2.10)$$

Here,  $\hat{u}_i$  is a tracer-density-weighted vertical average of the horizontal wind speed, and multiplication of  $\hat{u}_i$  with the vertically integrated tracer mass  $\hat{q}_i$  gives the vertically integrated horizontal flux of the WVT species  $i$ .  $\hat{u}_i$  can thus be interpreted as an effective wind speed at which the WVT species  $i$  is horizontally advected.

If  $f_i$  varies with height,  $\hat{u}_i$  is generally different for different tracer species  $i$ . If, however,

the ‘well-mixed’ assumption holds,  $f_i$  drops out of Eq. 2.10 and, hence,  $\hat{u}_i$  becomes the WVT-species independent effective wind speed  $\hat{u}$ :

$$\hat{u}_i = \hat{u} = \frac{\int_0^\infty \rho q u \, dz}{\int_0^\infty \rho q \, dz} \quad \forall i \quad (2.11)$$

which leads to the horizontal advection equation of the 2D approximation:

$$\frac{\partial \hat{q}_i}{\partial t} + \frac{\partial \hat{q}_i \hat{u}}{\partial x} = 0. \quad (2.12)$$

This relation is exact if  $f_i$  is independent of height, i.e. if the ‘well-mixed’ assumption holds (Eq. 3.4).

Equation (2.10) further reveals that  $\hat{u}_i = \hat{u} \quad \forall i$  also if the horizontal winds are not sheared vertically, meaning that in this case the 2D-approximated horizontal advection term is exact irrespective of the validity of the ‘well-mixed’ assumption. However, without well-mixed conditions the determination of the composition of precipitation would still require vertically resolved tracer fields (see above).

In summary, the results of the above considerations are:

- If the atmospheric moisture is perfectly well-mixed vertically, the 2D approximation is exact. This is true even if the horizontal winds are sheared vertically.
- If the atmospheric moisture is not well-mixed but the horizontal winds are vertically uniform, the 2D advection term is exact. However, in this case the composition of precipitation can not be determined exactly without resolving the vertical dimension.

Of course in reality the atmosphere is not perfectly well-mixed vertically, and the horizontal winds are not uniform vertically. However, the above analysis reveals that the size of errors introduced by 2D moisture tracing must depend on the degree to which atmospheric conditions deviate from these limit cases. Therefore, we investigate in the next section key characteristics of the atmosphere that largely influence the above mentioned factors, and analyse in Sect. 2.5 to what extent 3-dimensionally simulated atmospheric conditions deviate from well-mixed conditions.

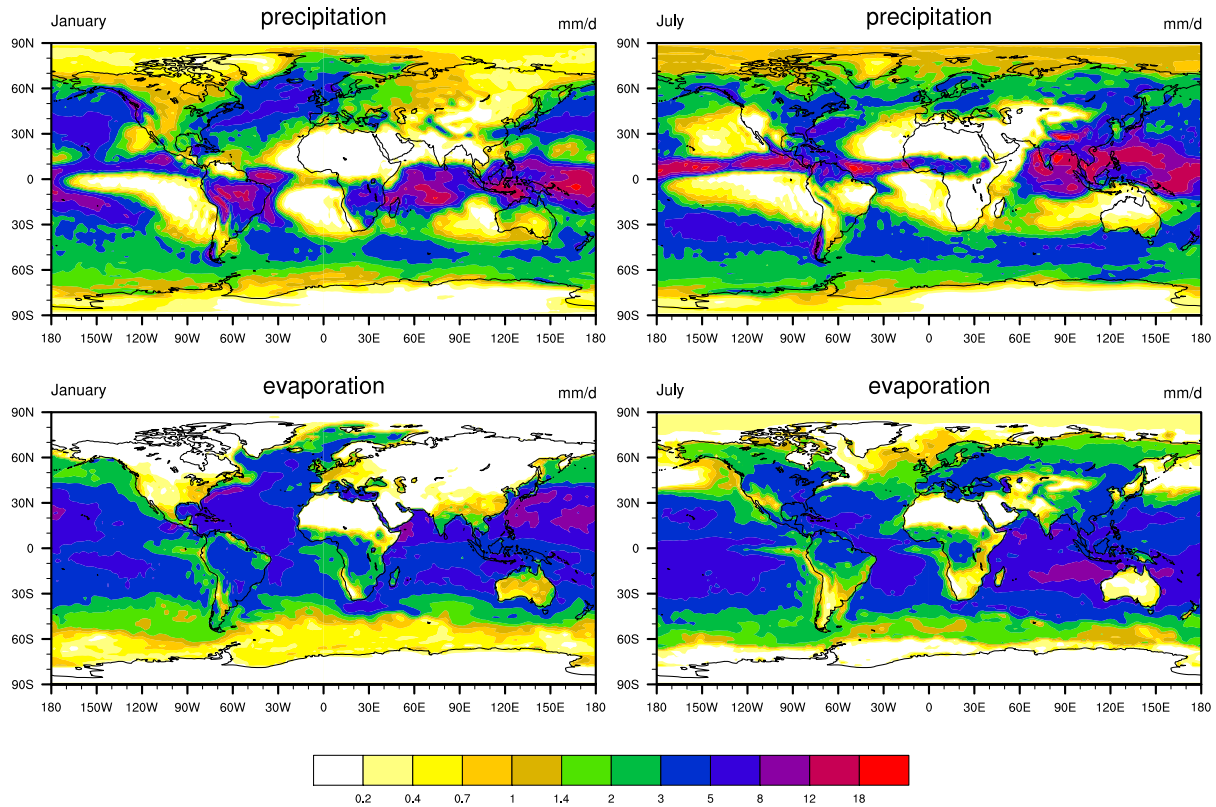


Figure 2.1: Simulated precipitation (top, mm/d) and evaporation (bottom, mm/d) for January (left) and July (right).

## 2.3 Relevant characteristics of the atmosphere

The numerical simulations we investigate in this paper are generated with ECHAM6 (Roeckner et al., 2003), the atmosphere-land component of the Max Planck Institute for Meteorology’s Earth system model (MPI-ESM), at T63/L47 resolution ( $1.875^\circ \times 1.875^\circ$ , 47 levels, 10 minutes time-step) with prescribed climatological sea-surface temperatures (SSTs) representing present-day conditions without interannual variability. In physical terms, all model experiments are binary identical (see the last paragraph of Sect. 2.4.1) and only the passive tracers behave differently between the experiments. The simulated patterns of precipitation and evaporation, averaged over 10 years of equilibrated climate as all results shown in the following, are depicted in Fig. 2.1.

The basic assumption behind 2D moisture tracing is the ‘well-mixed’ assumption: Atmospheric moisture is assumed to mix rapidly in the vertical dimension, resulting in a vertically



Strong moist convection occurs frequently in the tropical rain belt, which shifts its position during the course of the year, and in the extratropical stormtrack regions (Fig. 2.2). In the latter the signal is strongly seasonal: Over the ocean, the frequency of strong moist convection is much higher during the respective hemisphere's winter, i.e. when the stormtracks are more pronounced. In contrast, over the northern extratropical continents strong moist convection is more frequent in northern summer. These patterns indicate qualitatively when and where vertical inhomogeneities with respect to moisture composition can be expected to relax quickly towards well-mixed conditions. Of course it is not only the strength of vertical mixing, but also the degree to which inhomogeneities are generated in the first place that determines whether the atmosphere attains an approximately well-mixed state. In the following we consider two factors that are responsible for the generation of vertical inhomogeneities.

First, vertical inhomogeneities with respect to moisture composition are generated by surface evaporation (Fig. 2.1, bottom) which acts to enrich moisture of local origin in the lower part of the atmosphere. One may consider surface evaporation as the primary cause of vertical inhomogeneities. Second, vertical inhomogeneities can be generated by advection if the horizontal winds are sheared vertically. This mechanism may be considered as a secondary cause of vertical inhomogeneities because it generates vertical inhomogeneities out of horizontal inhomogeneities. If the horizontal winds are sheared vertically, the composition of different layers in the atmosphere can be very different, in particular if vertical mixing is weak.

An idea to what extent the winds are sheared vertically can be obtained by comparing monthly means of the near-surface (925 hPa) winds and the mid-tropospheric (650 hPa) winds (Fig. 2.3, top and middle). For a more quantitative assessment one also has to take into account that the specific humidity of the air decreases steeply with height due to the temperature gradient, meaning that the same windspeed is associated with stronger moisture transport in lower levels than in higher levels.

It stands to reason that directional shear of the horizontal wind is more effective in generating vertical inhomogeneities than speed shear of the horizontal wind; in case of vertically uniform wind directions but varying wind speeds, a relatively low degree of vertical

### 2.3 Relevant characteristics of the atmosphere

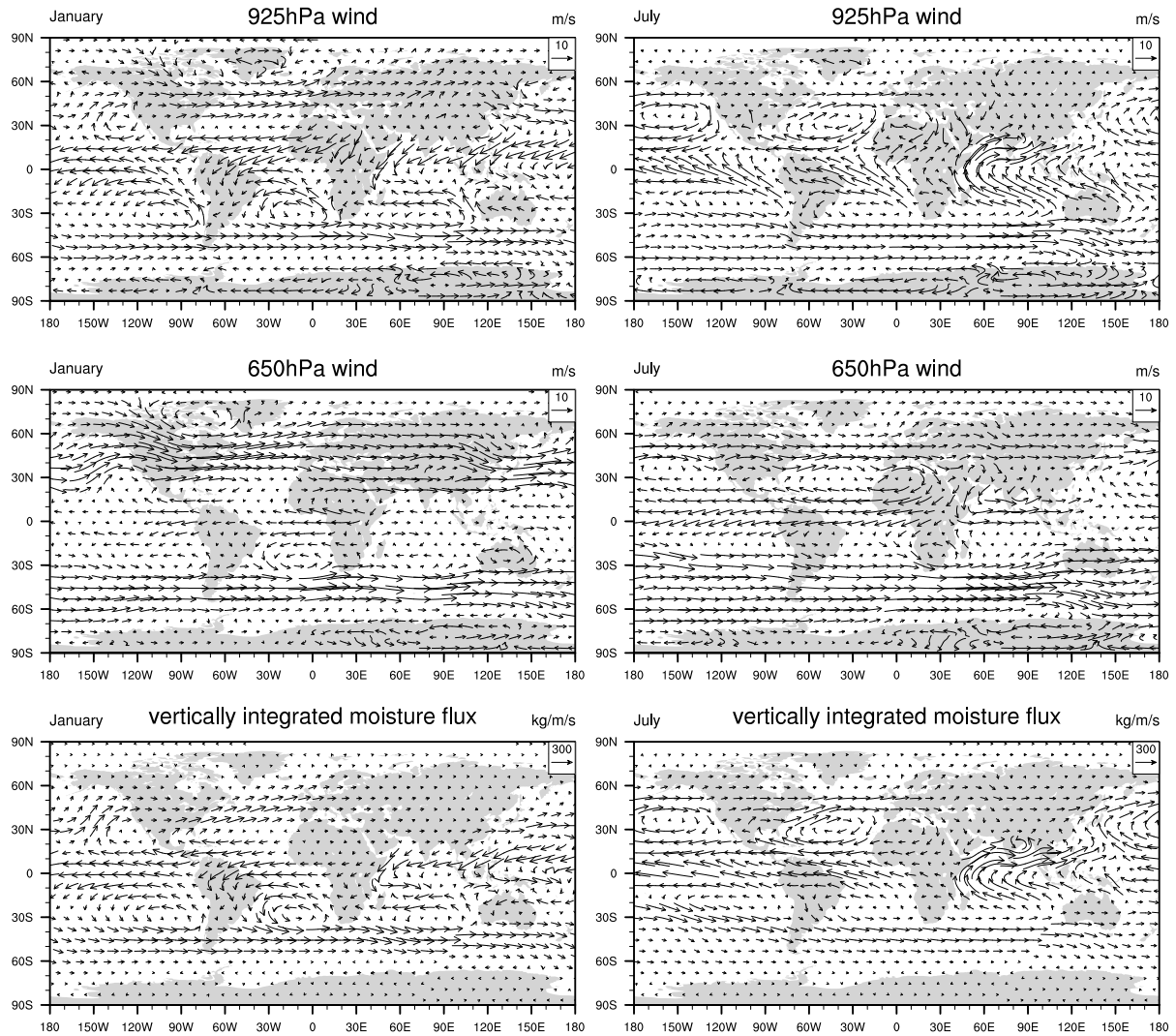


Figure 2.3: Horizontal winds at 925 hPa (top, m/s) and 650 hPa (middle, m/s), and vertically integrated moisture flux (bottom, kg/m/s) for January (left) and July (right).

mixing may suffice to maintain close to well-mixed conditions. We therefore introduce a measure  $\Gamma$  that quantifies the degree to which shear generates vertical inhomogeneities as follows:

$$\Gamma := \frac{\left\| \int_0^\infty \rho q \begin{pmatrix} u \\ v \end{pmatrix} dz \right\|}{\int_0^\infty \left\| \rho q \begin{pmatrix} u \\ v \end{pmatrix} \right\| dz} \quad (2.13)$$

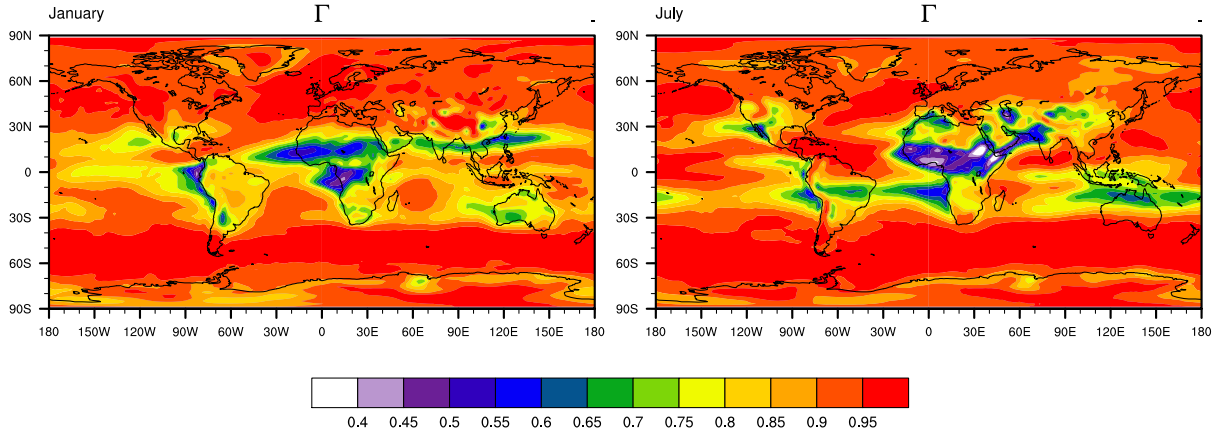


Figure 2.4: Directional shear as measured by  $\Gamma$  (Eq. 2.13) for January (left) and July (right). Please note that the numerator and the denominator in Eq. (2.13) are averaged separately over time.

where  $z$  is geometrical height,  $\rho$  is air density,  $q$  is specific humidity,  $u$  and  $v$  are the zonal and the meridional component of the horizontal wind, and  $\|\cdot\|$  is the Euclidean norm. While the numerator is proportional to the absolute value of the vertically integrated horizontal moisture flux (Fig. 2.3, bottom), the denominator is proportional to what this flux would be if the winds at all heights pointed in the same direction (with the same orientation). Obviously,  $\Gamma \in [0, 1]$ , with low values indicating strong directional shear of the horizontal moisture flux and high values indicating weak directional shear of the horizontal moisture flux. In the following we refer to  $\Gamma$  simply as directional shear.

$\Gamma$  (computed for 6-hourly data) reveals that strong directional shear is mostly confined to the tropics (Fig. 2.4). This is due to the fact that the weak Coriolis force near the equator allows the development of thermally direct circulations, while in the extratropics the Coriolis force acts to establish flow in approximate geostrophic balance, leading to vertically more uniform wind directions. Another striking feature is that strong directional shear often occurs at continental coasts, for example at the South American and African western coasts both in January and in July, and in a band ranging from the Gulf of Oman over India and Indochina to the Philippine Sea in January. This feature supports the supposition that directional shear is mainly caused by thermally direct circulations, because the latter are typically strongest in the vicinity of continental coasts.

Considered together, the frequency of strong moist convection (Fig. 2.2) and the magnitude of directional shear (Fig. 2.4) provide a qualitative idea of when and where the atmosphere may attain close to vertically well-mixed conditions, meaning that 2D moisture tracing may be an appropriate approximation. However, a precise quantification of the errors that are introduced by vertical integration can only be obtained by direct comparison of results from 2D and 3D moisture tracing. We provide such a comparison in Sect. 2.7, where we come back to the quantities discussed in this section to explain the simulated differences.

## 2.4 Atmospheric water vapour tracers in ECHAM6

### 2.4.1 Implementation

Passive tracers in ECHAM6 (Roeckner et al., 2003) are horizontally advected with a flux-form semi-Lagrangian scheme introduced by Lin and Rood (1996). Vertical diffusion of tracers is implemented with the eddy diffusion method where the diffusivity is parameterised in terms of the turbulent kinetic energy (e.g. Garratt, 1992). Vertical redistribution of tracers is also caused by moist convection which is implemented in ECHAM6 with a Tiedtke-Nordeng scheme (Tiedtke, 1989; Nordeng, 1994). No horizontal diffusion is applied to tracers.

In addition to being transported as a passive tracer, atmospheric moisture is redistributed vertically by precipitation, which acts to keep water concentrations in higher levels low. Within an AGCM the vertically resolved precipitation fluxes can in principle be taken directly from the AGCM’s internal (prognostic) variables. However, due to numerical issues related to the implementation of the flux-form advection scheme (Jöckel et al., 2001) and also due the moist convective parameterisation, ECHAM6 is not completely conserving water mass. We therefore decided to use an alternative method to diagnose the vertically resolved precipitation fluxes. This method ensures that the model’s prognostic moisture is permanently equal to the sum over all WVTs.

In this approach the vertically resolved precipitation flux is diagnosed every time-step by comparing the model’s internal (prognostic) moisture  $q_{\text{prog}}$  with the not yet precipitation-

corrected sum over all WVT species

$$q_{\text{wvt}}(z) = \sum_{i=1}^N q_i(z) \quad (2.14)$$

where  $N$  is the number of WVTs and  $q_i$  is the specific concentration (kg/kg) of tracer  $i$ . For the method to be valid, any sources of atmospheric moisture as well as the atmosphere's initial moisture must be covered by one of the WVT species.

To avert obscurities, it seems advisable to give a comment on the terms gross and net that we use in the following. Gross re-evaporation and gross condensation account for all water molecules that cross the interface between the liquid (or solid) phase and the gaseous phase (i.e. the air). Considering for example air that is in contact with liquid water, and assuming that the air is saturated with respect to water vapour, gross re-evaporation and gross condensation take place at the same rate  $R = C$ . In consequence, net condensation  $C - R$  (which is always equal to -1 times net re-evaporation) is zero. In fact, gross evaporation is generally not a function of the air's humidity, but only of the interface temperature because the latter determines the frequency at which water molecules heading towards the air are fast enough to overcome the attractive force exerted by the adjacent water molecules. Given a fixed interface temperature, the dependence of net evaporation/condensation on the air's humidity results only from the dependence of the gross condensation term on the air's humidity (for a detailed discussion see Silberberg et al., 1996).

The procedure described in the following is applied at the end of every model time-step and adjusts the sum over all WVTs  $q_{\text{wvt}}$  to the model's prognostic moisture  $q_{\text{prog}}$  ( $= q$ ). Having thus started identically, after one model time-step without provision for vertical transport by precipitation,  $q_{\text{wvt}}$  is larger than  $q_{\text{prog}}$  if the local balance of gross condensation minus gross evaporation ( $C - R$ , [(kg/kg)/s]) is positive. This is the case if net moisture is removed from the air at cost of an increasing downward precipitation flux. On the other hand,  $q_{\text{wvt}}$  is smaller than  $q_{\text{prog}}$  if  $C - R$  is negative. This is the case if moisture is added to the air by net re-evaporation of precipitation. It is

$$(C - R)(z) = \frac{q_{\text{wvt}}(z) - q_{\text{prog}}(z)}{\Delta t} \quad (2.15)$$

where  $\Delta t$  [s] is the time-step length. One obtains the vertically resolved precipitation flux  $P(z)$  [kg/(m<sup>2</sup> s)] for the considered time-step at any height by integrating  $C - R$  from the respective height to the top of the atmosphere:

$$P(z) = \int_z^\infty (C - R)(z') \rho(z') dz'. \quad (2.16)$$

Analogously to Eqs. (2.15) and (2.16), it holds for single WVT species that the change due to precipitation within the considered time-step is

$$\frac{\Delta q_i(z)}{\Delta t} = (C_i - R_i)(z) \quad (2.17)$$

and that

$$P_i(z) = \int_z^\infty (C_i - R_i)(z') \rho(z') dz'. \quad (2.18)$$

However, while  $(C - R)$  is known (Eq. 2.15),  $(C_i - R_i)$  is unknown. For the gross terms  $C_i$  and  $R_i$  we know that

$$C_i(z) = \frac{q_i(z)}{q_{\text{wvt}}(z)} C(z) \quad (2.19)$$

and

$$R_i(z) = \frac{P_i(z)}{P(z)} R(z). \quad (2.20)$$

If  $C$  and  $R$  are known individually, Eqs. (2.18)–(2.20) constitute a closed system of equations and can be solved proceeding from the top of the atmosphere downward, allowing to derive the change of each individual tracer species (Eq. 2.17). Adding these changes to the tracer concentrations  $q_i$  gives the precipitation corrected values  $q_i^{\text{corr}} = q_i + \Delta q_i$ , so that by Eqs. (2.14) and (2.15)  $q_{\text{wvt}}^{\text{corr}} = q_{\text{prog}}$ . Setting  $q_i := q_i^{\text{corr}}$  at the end of the procedure hence ensures that  $q_{\text{wvt}}$  and  $q_{\text{prog}}$  start identically into the next time-step, which is necessary for the validity of our method.

However,  $C$  and  $R$  are not known individually, but only  $C - R$  (Eq. 2.15), leaving Eqs. (2.18)–(2.20) underdetermined. Notably, this problem is not specific to our approach in which  $C - R$  is diagnosed from the differences between  $q_{\text{wvt}}$  and  $q_{\text{prog}}$  (Eq. 2.15). AGCMs themselves operate only with the net term  $C - R$  because the gross terms are not relevant

for the physical system, i.e. the total water mass and energy balance. Hence, additional assumptions have to be made regarding the gross terms  $C$  and  $R$  in order to close the above system of equations.

One possible way to proceed would be to estimate realistic values of the gross condensation and re-evaporation terms from thermodynamical considerations that make use of the AGCMs' internal variables. Relevant quantities would include not only central physical ones like temperature, but also highly parameterised quantities such as those associated with moist convection. In particular the complex nature of moist convection entails that the derivation of realistic gross terms is not a trivial task. This has motivated us to implement two different variants of the tracing with simple assumptions regarding the gross terms instead of developing a complex submodel. The two variants reflect the two extremes regarding the question of how large the gross terms  $C$  and  $R$  are.

In the first case (variant 3D-s, "strong mixing") we assume that  $C$  and  $R$  are very large, meaning that the precipitation mixes rapidly (in case of the discrete layers of the AGCM instantaneously) with the ambient water vapour. The instantaneous equilibration leads to

$$\text{variant 3D-s:} \quad \frac{P_i(z)}{P(z)} = \frac{q_i(z)}{q_{\text{wvt}}(z)} \quad (2.21)$$

which closes the system of equations defined by Eqs. (2.18)–(2.20). For a discrete model layer this case means that all precipitation entering at the layer's top mixes with the layer's water vapour, and that the composition of the precipitation leaving the layer at its bottom equals the composition of the resulting mixture.

In the second case (variant 3D-w, "weak mixing") we assume that only the net exchange between the precipitation and the ambient air takes place:

$$\text{variant 3D-w:} \quad C(z) = \max((C - R)(z), 0) \quad (2.22)$$

which implies that  $R(z) = \max(-(C - R)(z), 0)$ . This is an alternative to Eq. (2.21) to close the system of equations defined by Eqs. (2.18)–(2.20). For a discrete model layer this case means the following: If net condensation occurs, the composition of the layer's water vapour remains unchanged while only the composition of the precipitation is modified by

the condensing water molecules. If however net re-evaporation occurs, the composition of the precipitation remains unchanged while only the composition of the layer’s water vapour is modified by the re-evaporating water molecules.

The main difference resulting from the two variants is that in case of the 3D-s variant the surface precipitation is composed like the near-surface water vapour, whereas in case of the 3D-w variant the surface precipitation is composed like the water vapour that resides in those higher atmospheric layers where the precipitation originally formed. In Sect. 2.8 we argue that, roughly speaking, the 3D-s variant resembles stratiform precipitation and the 3D-w variant resembles convective precipitation. Nevertheless we do not treat stratiform precipitation and convective precipitation, which are handled separately within ECHAM6, differently. Instead, we apply in separate simulations either always the 3D-s variant or always the 3D-w variant. This allows us to estimate the maximum uncertainty associated with the question of how strongly precipitation mixes on its way towards the surface with the ambient water vapour.

But the main motivation of this work is not to quantify uncertainties associated with full (3D) moisture tracing, but to investigate the errors that are introduced by vertical integration prior to the tracing, i.e. errors that are associated with 2D moisture tracing. In Sect. 2.2 we showed analytically that the 2D approximation is exact if the ‘well-mixed’ assumption is valid – in this case 2D and 3D moisture tracing are identical. Hence one can convert the full 3D tracing to a scheme that is equivalent to 2D moisture tracing by imposing artificially well-mixed conditions. This can be achieved by mixing completely the WVTs in each atmospheric column after every model time-step while preserving the vertical profile of the total moisture, leading to the third variant that we implemented:

$$\text{variant 2D:} \quad q_i(z) = \hat{f}_i \cdot q(z). \quad (2.23)$$

Please note that it does not matter which of the 3D variants is taken as a basis for the reduction to the 2D variant because vertical differences in the WVT tendencies that exist between the two 3D variants are immediately nullified by the application of Eq. (2.23).

The fact that the tracing schemes are completely passive, meaning that they do not affect

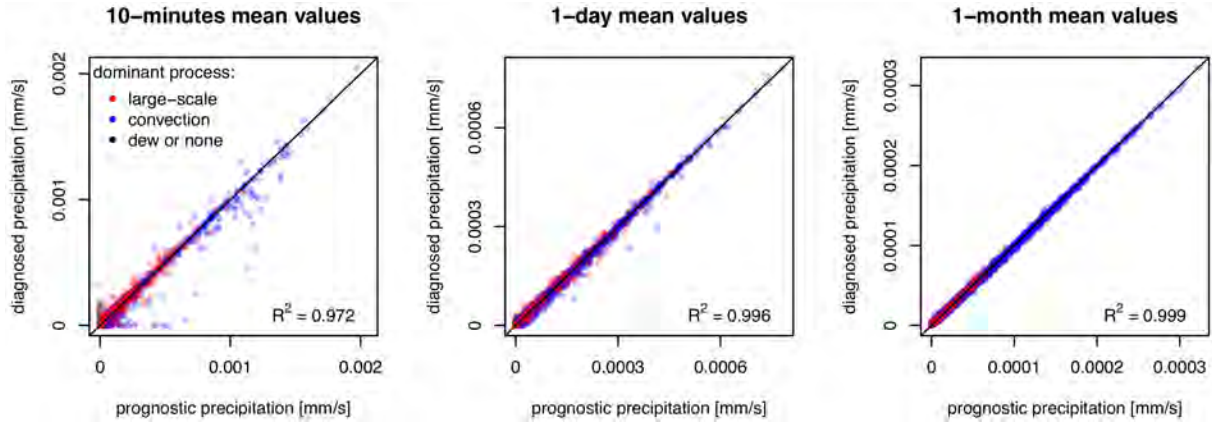


Figure 2.5: Prognostic precipitation (including dew) versus diagnosed precipitation (see Eq. 2.16) at the surface. Left: Values of a single (i.e. 10 minutes) time-step. Middle: Values averaged over one day. Right: Mean values averaged over one month. Each of the 18,432 points represents one grid cell of the AGCM. The black line denotes identity. The colours indicate which process contributes most to the prognostic precipitation, either stratiform (large-scale) precipitation (red), convective precipitation (blue), or dew or none (black).  $R^2$  is the fraction of variance explained by the identity function.

the evolution of the physical model state, allows us to simulate the moisture tracing with different tracing variants on top of binary identical model runs (see the first paragraph of Sect. 2.3) by using identical initial conditions. We can thus attribute any differences between the results of the tracing variants exclusively to the above described differences between their implementation.

## 2.4.2 Technical validation

As described in Sect. 2.4.1 we do not use ECHAM6’s internal (prognostic) precipitation fluxes for the downward transport of WVTs, but diagnose vertically resolved precipitation fluxes after every time-step. To demonstrate consistency between our diagnosed precipitation rates and the ones computed by ECHAM6, we now compare them with each other.

At the surface, for a proper comparison between the model’s internal downward moisture flux and the diagnosed flux it is necessary to add dew to the model’s precipitation, because the computation of  $C - R$  (Eq. 2.15) in the lowest atmospheric layer captures not only the net flux between the precipitation and the ambient air, but also the condensation to the

surface (though not the evaporation from the surface, because the latter is already treated explicitly). The model’s “prognostic precipitation” discussed in the following thus includes dew.

Comparison of the model’s prognostic precipitation and the diagnosed precipitation for a single (10-minutes) time-step reveals that the diagnosed precipitation largely agrees with the prognostic precipitation (Fig. 2.5, left). For a single time-step the variance explained by the identity function amounts to  $\sim 97.2\%$ . At some locations the diagnosed precipitation is considerably different from the prognostic precipitation, revealing that the mass of the WVTs and/or the prognostic water are not completely conserved in ECHAM6. The fact that in case of most outliers the dominating process is convective precipitation suggests that a large part of the error is due to the parameterisation of moist convection, though some of the error is probably due to numerical issues (Jöckel et al., 2001). However, averaging precipitation rates over longer periods of time shows that the errors are not systematic (Fig. 2.5, middle and right): Averaged over one month, the diagnosed precipitation is everywhere virtually identical to the prognostic precipitation (variance explained by the identity function:  $\sim 99.9\%$ ). This supports the validity of our implementation.

## 2.5 On the validity of the ‘well-mixed’ assumption

In Sect. 2.2 we showed analytically that the 2D approximation is exact if the fractions of all WVT species are perfectly well-mixed vertically. Therefore, before comparing results of the different tracing variants 3D-s, 3D-w, and 2D in Sects. 2.6 and 2.7, we investigate in this section to what extent the WVT species from different evaporative source regions are actually well-mixed vertically. To this end we analyse results obtained for two sets of source regions using only the 3D-s moisture tracing variant. Those aspects of the results that we discuss in this section are virtually identical for the 3D-w variant, which we therefore do not consider here.

The first set of source regions is defined by the model’s land-sea mask, meaning that only oceanic and continental moisture are distinguished. In the second set we distinguish four evaporative source regions, of which three are defined by 1,000 km x 1,000 km-rectangles

Table 2.1: Locations of the 1,000 km-scale rectangular source regions

Name	abbrev.	meridional range (°N)	zonal range (°E)
Eastern Europe	EEU	50.4 - 59.7	30.9 - 47.8
Amazonia	AMA	-9.3 - 0.0	295.3 - 304.7
Western Africa	WAF	7.5 - 16.8	0.0 - 9.3

located on different continents (Tab. 2.1, marked by black boxes in Figs. 2.7, 2.9, and 2.11) while the fourth comprises the remainder of the Earth’s surface.

To quantify to what extent a WVT species  $i$  is well-mixed vertically we define the measure  $\Psi_i$  as follows:

$$\Psi_i := 2 \frac{\int_{z^*}^{\infty} \rho q_i dz}{\int_0^{\infty} \rho q_i dz} - 1 \quad (2.24)$$

where  $z^*$  is determined by

$$\frac{\int_{z^*}^{\infty} \rho q dz}{\int_0^{\infty} \rho q dz} = 0.5 \quad (2.25)$$

which means that half of the total atmospheric moisture resides above  $z^*$  and the other half resides below  $z^*$ . Obviously,  $\Psi_i \in [-1, 1]$ , with  $\Psi_i = 0$  indicating well-mixed conditions and negative (positive) values indicating higher concentrations in the lower (upper) half of the atmospheric moisture column. Computing  $\Psi$  for the moisture of continental origin (Fig. 2.6) and for the moisture stemming from the three rectangular source regions (Fig. 2.7) reveals that well-mixed conditions are overall rather scarce.

In Sect. 2.3 we argued qualitatively that whether the atmosphere is close to well-mixed vertically or not results from the interplay between the generation of vertical inhomogeneities on the one hand and the strength of vertical mixing on the other hand. While vertical inhomogeneities are generated by surface evaporation (Fig. 2.1, bottom) and by directional shear (Fig. 2.4), vertical mixing that involves not just the boundary layer but also the free troposphere occurs mainly through the action of deep moist convection (Fig. 2.2). The fact that well-mixed conditions are relatively rare (Figs. 2.6 and 2.7) means that vertical mixing is mostly not strong enough to nullify the generation of inhomogeneities by surface evaporation and directional shear.

The influence of surface evaporation on  $\Psi$  is straight forward: While within the respective

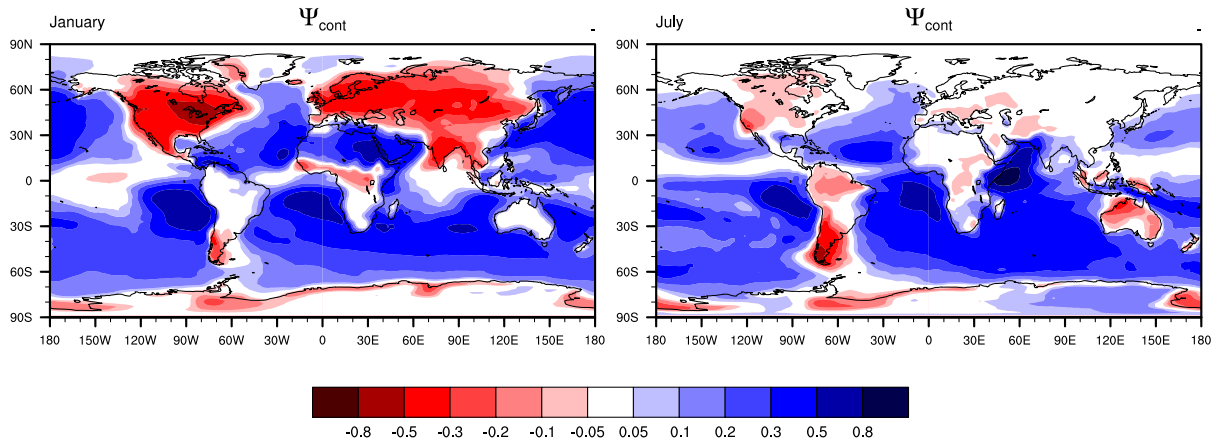


Figure 2.6: The degree to which moisture of continental origin is overrepresented in the upper half (positive values) or the lower half (negative values) of the atmospheric moisture column ( $\Psi_{\text{cont}}$ , Eq. 2.24), for January (left) and July (right). The results shown here are calculated for the 3D-s variant; those for the 3D-w variant are very similar (not shown).

source region surface evaporation acts to enrich moisture originating from the region in the lower levels of the atmosphere (decreasing  $\Psi$ ) directly, outside the respective source region surface evaporation acts to enrich moisture originating from the region in the upper levels indirectly by enriching moisture of different origin in the lower levels (increasing  $\Psi_i$ ). This effect is clearly visible in the patterns of  $\Psi$  (Figs. 2.6 and 2.7):  $\Psi_{\text{cont}}$  is mostly negative over land and positive over the ocean, and  $\Psi_{\text{EEU}}$ ,  $\Psi_{\text{AMA}}$ , and  $\Psi_{\text{WAF}}$  are mostly negative within the respective regions and positive outside.

Strongly negative values of  $\Psi$  inside the source regions only occur where strong moist convection is rare (Fig. 2.2). Otherwise, a substantial enrichment of local moisture in the lower levels is prevented by vertical mixing. For  $\Psi_{\text{cont}}$  this is the case for example in large parts of South America in January and in large parts of Eurasia in July. In case of the smaller-scale regions, close to well-mixed conditions inside the region itself occur only in AMA in January due to the vigorous daily mixing by deep convection. At the other extreme are the conditions in EEU in January: Here, almost all moisture stemming from the region is concentrated in the lower half of the atmospheric moisture—not only inside the region itself but in large parts of the northern hemisphere. This reflects the stable atmospheric stratification that prevails during the northern-hemispheric winter over the northern land

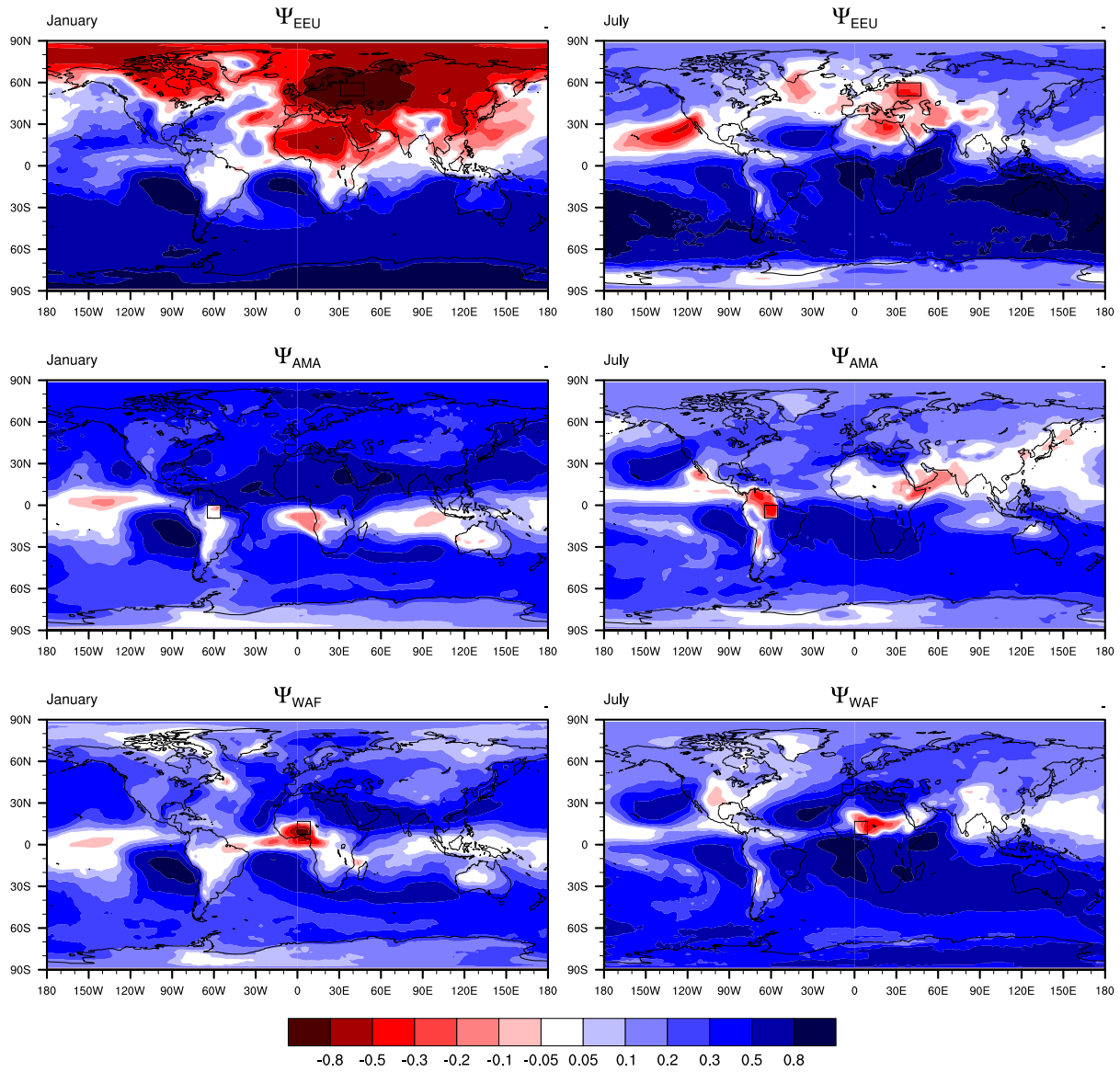


Figure 2.7: The degree to which moisture originating from the regions EEU ( $\Psi_{\text{EEU}}$ , top), AMA ( $\Psi_{\text{AMA}}$ , middle), and WAF ( $\Psi_{\text{WAF}}$ , bottom) is overrepresented in the upper half (positive values) or the lower half (negative values) of the atmospheric moisture column (Eq. 2.24), for January (left) and July (right). The results shown here are calculated for the 3D-s variant; those for the 3D-w variant are very similar (not shown).

and sea-ice areas, effectively suppressing deep convection (Fig. 2.2).

It is generally an interesting question at which distance from the source regions well-mixed conditions are attained by vertical mixing. Apart from the just mentioned case of EEU in January, negative values of  $\Psi$  directly associated with the regions’ surface evaporation are mostly constrained to the close proximity of the respective source regions (Figs. 2.6 and 2.7). This means that vertical inhomogeneities generated inside the regions typically do not persist for more than a couple of hundred kilometers until vertical mixing has largely nullified the inhomogeneities. Besides the special case of EEU in January, it seems that also in most of the other cases negative values of  $\Psi$  generated inside the source regions are preserved for considerably more than a few hundred kilometers at least in one direction, for example in July to the south of EEU, to the north-west of AMA, and to the east of WAF.

Inspection of the vertical structure of the winds (Fig. 2.3, top and middle, and Fig. 2.4) however reveals that it is rather directional shear that is responsible for these negative- $\Psi$ -tails, meaning that they are not simply due to the preservation of the low-level enrichment generated inside the source regions. For example, the tail to the north-west of AMA and the tail to the east of WAF, both in July, are due to a situation where low-level winds advect air masses directly from the respective source region while mid-tropospheric winds blow from a different direction. An analogous situation leads to negative values of  $\Psi_{\text{EEU}}$  to the south of EEU in July where the westerlies have a significant southward component that is absent in the mid-troposphere. However, in the latter case the “tail” with negative values of  $\Psi_{\text{EEU}}$  covers a much larger area because the subsiding branch of the Hadley cell south of  $\sim 35^\circ\text{N}$  is associated with virtual absence of deep convection (Fig. 2.2), meaning that vertical inhomogeneities are preserved once air masses have entered the subtropics from the north.

Beyond the primary regions of low-level enrichment (negative  $\Psi$ ) in the vicinity of the respective source regions,  $\Psi$  not only attains values around zero, corresponding to well-mixed conditions, but is mostly positive. As mentioned above, this is primarily due to the action of surface evaporation (Fig. 2.7). However, apart from the narrow transition zones, i.e. where  $\Psi$  switches its sign, close to well-mixed conditions also occur in some more distant locations. Most striking is a band of close to well-mixed conditions for all considered source

regions (Figs. 2.6 and 2.7) near the equator, which is obviously due to strong mixing caused by frequently occurring deep convection within the Intertropical Convergence Zone (ITCZ) (Fig. 2.2).

Well-mixed conditions—and even low-level enrichment—at locations far away from the respective source regions can also be generated by a suitable vertical structure of the winds, where suitable means that the low-level winds advect air from regions containing higher fractions of moisture stemming from the considered source region than the higher-level winds do. This is for example the reason for the negative values of  $\Psi_{\text{AMA}}$  and  $\Psi_{\text{WAF}}$  above the tropical eastern Pacific in January, but also for the negative values of  $\Psi_{\text{EEU}}$  between Hawaii and California in July (Fig. 2.7). In the latter case, near-surface winds advect extratropical air masses from the north while mid-tropospheric easterlies advect tropical air masses from the east (Fig. 2.3, top right and middle right). Because the overall prevailing zonal winds act to mix air masses faster zonally than meridionally, air masses located within the same zonal band as the source region under consideration contain tendentially more moisture stemming from the source region than air masses in other zonal bands. This explains not only why  $\Psi_{\text{EEU}}$  is strongly negative between Hawaii and California in July, but also why  $\Psi_{\text{AMA}}$  and  $\Psi_{\text{WAF}}$  are strongly positive at the same time and place. Moreover, the fact that mixing occurs faster in zonal than in meridional direction also explains why, apart from the direct vicinity of the tropical source regions, the patterns of  $\Psi_{\text{AMA}}$  and  $\Psi_{\text{WAF}}$  are generally similar.

Well-mixed conditions for atmospheric moisture of different origin are apparently not the rule. As set out in Sect. 2.2, this implies that in most places 2D moisture tracing is necessarily associated with errors. We showed that two types of errors can be distinguished: Given the ‘well-mixed’ assumption is not valid, (I) it matters from which level precipitation originates, and (II) the 2D horizontal advection term (Eq. 2.12) is not exact. As we show in Sect. 2.7, both factors are responsible for differences between 2D and 3D moisture tracing. But basically only the first of the two factors is responsible for differences between the two 3D moisture tracing variants 3D-s and 3D-w, which is the subject of the following section.

## 2.6 Uncertainties associated with 3D moisture tracing

Before coming to the main subject of this study, namely the relation between 2D and 3D moisture tracing, we first discuss the uncertainties in 3D tracing arising from the different assumptions on how precipitation mixes with the ambient water vapour. As described in Sect. 2.4.1 we apply two variants of 3D moisture tracing: In case of the variant 3D-s precipitation mixes instantaneously with the ambient water vapour (strong mixing), and in case of the variant 3D-w no mixing apart from that associated with net condensation/re-evaporation occurs (weak mixing). Since these variants are at the two extremes of the range of possible assumptions, they allow us to estimate the maximum uncertainty associated with the question of how strongly precipitation mixes with the ambient water vapour. In the following we compare tracing results obtained with the two 3D moisture tracing variants, focussing on the simulated composition of precipitation. We use the same two sets of evaporative source regions considered in the previous section, beginning with the experiments in which a distinction is made between continental and oceanic moisture.

Using the land-sea mask to determine the continents and the ocean as evaporative source regions implies that the results with respect to the composition of precipitation are continental recycling ratios (following Goessling and Reick (2011), here and in the following we denote continental *precipitation* recycling ratios simply as continental recycling ratios, or  $R_c$ ).  $R_c$  is defined as the (spatially resolved) fraction of precipitation that stems from continental evaporation. Overall, both 3D moisture tracing variants give very similar patterns of  $R_c$  (Fig. 2.8). In agreement with earlier studies (Numaguti, 1999; Bosilovich et al., 2002; Yoshimura et al., 2004; van der Ent et al., 2010; Goessling and Reick, 2011) we find that  $R_c$  increases from continental upwind coasts to downwind coasts with weak seasonality in the tropics and strong seasonality in the extratropics, where the latter is mainly due to the seasonality of evaporation (Fig. 2.1, bottom). While the highest values of  $R_c$  occur in eastern Eurasia in July with more than 80%, peak values in the continental tropics are around 60% throughout the year.

Regarding the computed continental recycling ratios, the most striking difference between 3D-s and 3D-w is that 3D-s almost exclusively gives higher values on the continents and

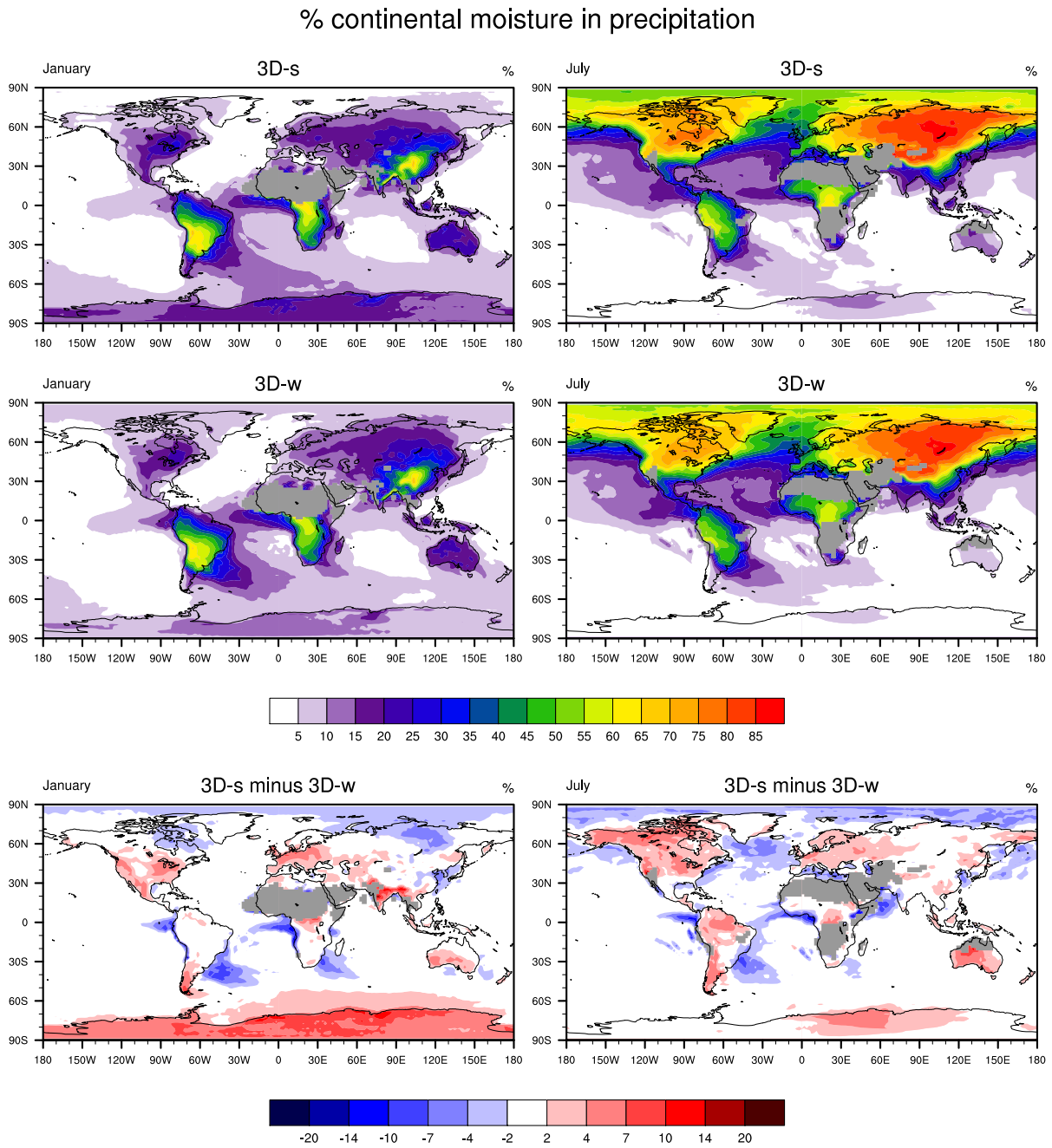


Figure 2.8: The continental recycling ratio ( $R_c$ , % continental moisture in precipitation) as simulated with 3D-s (top) and 3D-w (middle), and the difference between the two (bottom), for January (left) and July (right). Grey areas are masked because less than five out of the ten years used for computing the averages have non-zero precipitation in the considered month, leading to statistically non-robust estimates.

lower values over the ocean (Fig. 2.8, bottom). To explain this land-ocean contrast one has to recall that, in contrast to the 3D-w variant, in the 3D-s variant the precipitation arriving at the surface reflects the composition of the near-surface atmospheric moisture rather than that of the higher-level moisture (compare Sect. 2.4.1). The land-ocean contrast in the difference pattern can hence be explained by  $\Phi_{\text{cont}}$  (Fig. 2.6): On the continents (over the ocean) the fraction of continental (oceanic) moisture in total moisture is larger near the surface than in higher levels. Using a term coined by Lettau et al. (1979), 3D-s features stronger fast-recycling than 3D-w, implying that moisture of local origin is overrepresented in precipitation.

There are of course deviations from the correlation between  $\Psi_{\text{cont}}$  and the differences between 3D-s and 3D-w. For example, north of lake Baikal in January 3D-s gives lower continental recycling ratios albeit  $\Psi_{\text{cont}}$  is negative. Such discrepancies exist for two reasons: First the definition of  $\Psi$  (Eq. 2.24) implies that  $\Psi_{\text{cont}}$  only captures differences between the compositions of the lower and the upper half of the atmospheric moisture, although the composition generally also varies within the two halves. Second the average composition of the atmospheric moisture column, although very similar, is not identical between the WVT variants 3D-s and 3D-w (not shown) – a secondary consequence of the different implementations. Despite of these two reasons for deviations the patterns are closely correlated, revealing that  $\Psi_{\text{cont}}$  explains most of the differences in  $R_c$  between 3D-s and 3D-w.

We now turn to the second set of evaporative source regions (Tab. 2.1). Analogously to what we find in the difference patterns of continental recycling ratios, 3D-s gives higher fractions of locally evaporated moisture in precipitation than 3D-w within the source regions and lower fractions outside (Fig. 2.9). The reason is again that locally evaporated water is overrepresented near the surface within the source regions and mostly underrepresented near the surface in the relevant locations outside the source regions (Fig. 2.7), confirming that the 3D-s variant features stronger fast-recycling.

At first glance it may surprise that there seem to be no differences between 3D-s and 3D-w at some distance from the three source regions (Fig. 2.9, bottom) although strong vertical inhomogeneities exist globally (Fig. 2.7). Indeed such differences exist. However, they are noticeable only in relative terms (not shown), not in absolute terms which are shown in

% moisture from EEU+AMA+WAF in precipitation

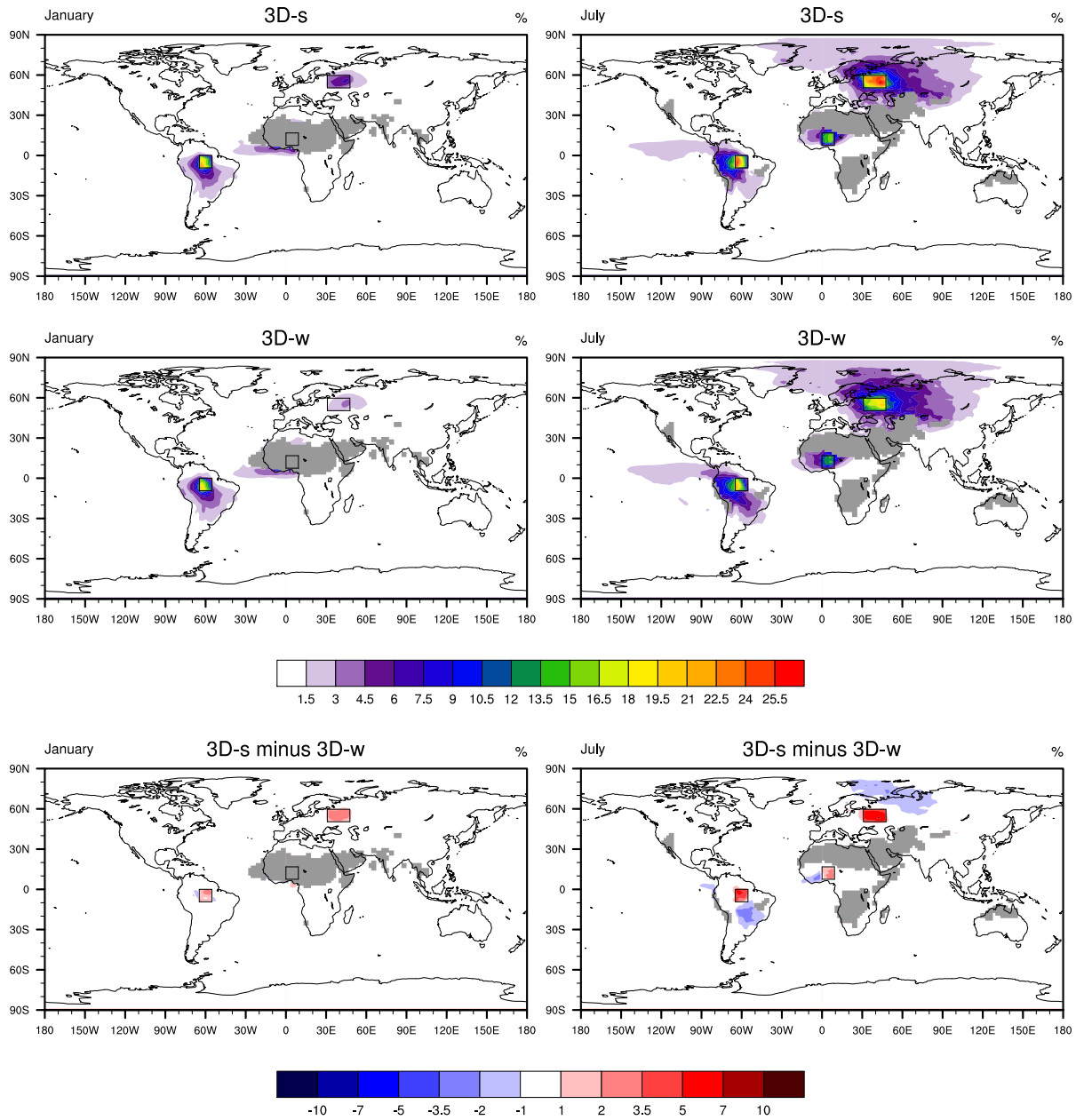


Figure 2.9: The fraction of precipitation that originates from the rectangular source regions EEU, AMA, and WAF (black boxes) as simulated with 3D-s (top) and 3D-w (middle), and the difference between the two (bottom), for January (left) and July (right). Grey areas are masked because less than five out of the ten years used for computing the averages have non-zero precipitation in the considered month, leading to statistically non-robust estimates. Because the regions receiving significant amounts of precipitation from the three source regions are well separated, we took the liberty to show only the sum instead of three individual plots.

Fig. 2.9, bottom: far away from the relatively small source regions the fraction of moisture stemming from these regions is just very small.

## 2.7 Errors introduced by the 2D approximation

To quantify the errors that are introduced by the 2D approximation we now compare the results obtained with variant 2D (which is equivalent to conventional offline 2D moisture tracing) to the results obtained with the 3D moisture tracing variants (see Sect. 2.4.1). In addition to the two sets of evaporative source regions considered in Sects. 2.5 and 2.6, here we also consider a third set of source regions that serves to determine the evaporative sources of precipitation in the western Sahel region—a case investigated by Keys et al. (2012). It has already been hypothesised that the 2D approximation may lead to large errors in this region (Goessling and Reick, 2011; Dirmeyer, 2011).

First we consider again continental recycling ratios ( $R_c$ ). Regarding continental-scale features the continental recycling ratios derived with 2D moisture tracing are not too different from those derived with 3D moisture tracing (Fig. 2.10, compare also with Fig. 2.8). However, the errors introduced by the 2D approximation are generally larger than the uncertainty associated with 3D tracing. Further, while results obtained with the two 3D variants are very similar regarding the shapes of the patterns, the 2D tracing leads to conspicuously modified shapes. Differences between 2D and 3D tracing tend to be largest in the tropics where strong directional shear occurs (Fig. 2.4). Here, differences in  $R_c$  between 2D and 3D in some places amount to more than 20% in either direction.

Compared with 3D moisture tracing, 2D moisture tracing gives mostly lower values of  $R_c$  on the continents and higher values over the ocean (Fig. 2.10, middle and bottom). This land-ocean contrast, which is clearer in the extratropics than in the tropics, has the same cause as the land-ocean contrast in the differences between the two 3D variants (Fig. 2.8, bottom), namely the fact that moisture of local origin is overrepresented in low levels (Fig. 2.6). In this respect 3D-w can be considered an intermediate variant between 3D-s and 2D: In the 3D-s variant the surface precipitation is composed like the near-surface water vapour, in the 3D-w variant the surface precipitation is composed like the water vapour in those levels

% continental moisture in precipitation

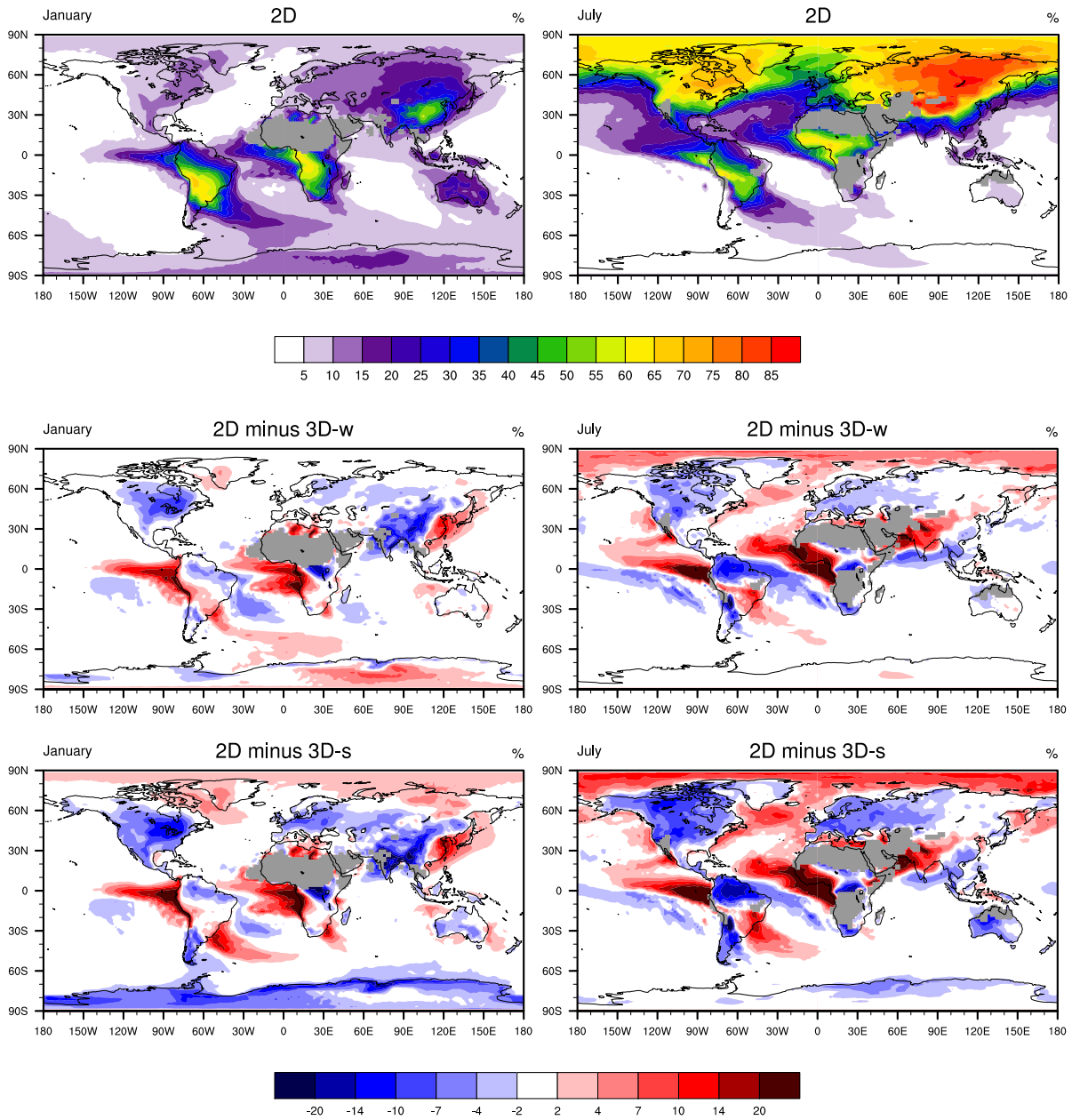


Figure 2.10: Continental recycling ratios ( $R_c$ , % continental moisture in precipitation) as simulated with 2D (top), and the difference between 2D and 3D-w (middle) and between 2D and 3D-s (bottom), for January (left) and July (right). Grey areas are masked because less than five out of the ten years used for computing the averages have non-zero precipitation in the considered month, leading to statistically non-robust estimates. Compare Fig. 2.8 for the absolute values of 3D-s and 3D-w.

where the precipitation is originally formed, and in the 2D variant the surface precipitation is composed like the vertically averaged atmospheric column.

In Sect. 2.6 we argued that the 3D-w variant gives lower continental recycling ratios on the continents than the 3D-s variant because of weaker fast-recycling. The fact that the 2D variant, which does not account for fast-recycling at all, gives even lower continental recycling ratios on the continents than the 3D-w variant suggests that the 3D-w variant still features some fast-recycling. As an aside, this implies that, at least in ECHAM6, precipitation on average forms at those relatively low levels where there is still a noticeable enrichment of locally evaporated moisture.

For the extratropics the difference patterns of  $R_c$  (Fig. 2.10, middle and bottom) and  $\Psi_{\text{cont}}$  (Fig. 2.6) suggest that the neglect of fast-recycling is the main reason for errors associated with the 2D approximation. In the tropics, however, another factor comes into play. The spatial patterns of  $R_c$  derived with 2D and 3D moisture tracing exhibit a characteristic structural difference: The continental recycling ratios derived with 2D tracing tend to have steeper gradients, most strikingly to the west of both Africa and South America in the vicinity of the equator. Also, while in the extratropics errors introduced by the 2D approximation are rather shape preserving, the errors in the tropics are associated with changes in the shape of the patterns of  $R_c$ . The reason for these structural differences (the steeper gradients and the modified pattern shapes obtained with 2D tracing) is that in the tropics directional shear (Fig. 2.4) causes basically horizontal dispersion of atmospheric moisture components, resulting in smoothed horizontal gradients. This effect is missing in the vertically integrative 2D approach. It is hence in these tropical regions where the largest differences, not only in magnitude but also in shape, between continental recycling ratios obtained with 2D and 3D moisture tracing occur.

The already described difference between the tropics and the extratropics is also evident in the results for the three smaller evaporative source regions (Fig. 2.11, middle and bottom). Within EEU the 2D approximation substantially underestimates the fraction of local moisture in precipitation, and outside EEU the fraction of moisture from EEU in precipitation is overestimated. The main explanation for this is, again, the neglect of fast-recycling. For the tropical regions AMA and WAF there is apparently also an element of this, causing mostly

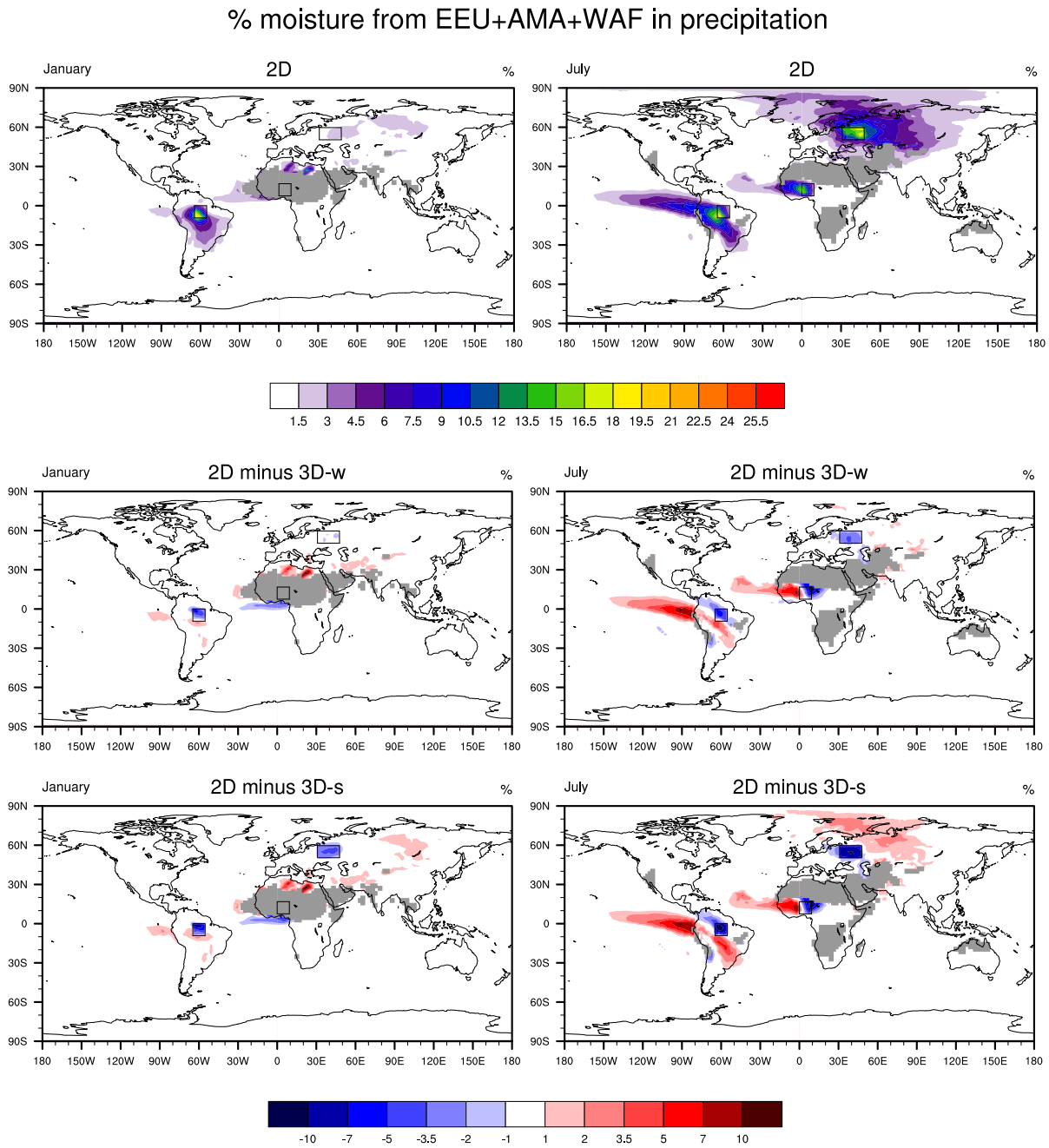


Figure 2.11: The fraction of precipitation that originates from the rectangular source regions EEU, AMA, and WAF (black boxes) as simulated with 2D (top), and the difference between 2D and 3D-w (middle) and between 2D and 3D-s (bottom), for January (left) and July (right). Grey areas are masked because less than five out of the ten years used for computing the averages have non-zero precipitation in the considered month, leading to statistically non-robust estimates. Because the regions receiving significant amounts of precipitation from the three source regions are well separated, we took the liberty to show only the sum instead of three individual plots.

an underestimation of recycling within the source regions and an overestimation outside. However, the shape of the resulting patterns is considerably altered by the 2D approximation only in the tropics. This is most obvious in July: While 3D moisture tracing reveals that moisture evaporated from WAF is preferentially advected northeastward (Fig. 2.9, top right and middle right), the results of the 2D approximation suggest that the moisture is mainly advected westward (Fig. 2.11, top right). For moisture evaporated from AMA in July, 3D moisture tracing gives highest fractions in precipitation along the western boundary of the source region, whereas the 2D approximation gives peak values in the southwestern corner. An even more salient difference in this case is that the 2D approximation diagnoses that substantial amounts of moisture stemming from AMA precipitate over the tropical eastern Pacific—a feature that the full tracing reveals as an artefact.

These errors in the tropics are obviously due to the layered structure of the atmosphere. In AMA in July, the monsoonal layer below  $\sim 750$  hPa carries air masses northeastward while the African easterly jet above  $\sim 750$  hPa blows westward (Fig. 2.3, top right and middle right). Due to the high wind speeds, the horizontal moisture flux associated with the African easterly jet outweighs the flux associated with the moister but slower moving monsoonal layer, explaining why the 2D variant diagnoses a westward advection of moisture (Fig. 2.3, bottom right). This leads to erroneous results because most of the moisture stemming from WAF is concentrated in the northwestward flowing monsoonal layer (Fig. 2.7, bottom right). An analogous explanation can be given for the differences seen in AMA in July described above, where the prevailing easterlies have a northward component near the surface but a southward component in the mid-troposphere (Fig. 2.3, top right and middle right), combined with considerably non-zero values of  $\Psi_{\text{AMA}}$  (Fig. 2.7, middle right).

The meteorological conditions in these regions are different in January. At this time of the year WAF is subject to subtropical large-scale subsidence, the ITCZ being located further to the south (Fig. 2.1, top left). Because of the associated absence of precipitation this region is not very interesting in the context of our study at that time of the year. By contrast, AMA, located south of the equator, receives considerably more precipitation in January than in July. The higher frequency of strong moist convection in January (Fig. 2.2) is associated with stronger vertical mixing. This in combination with a relatively low degree

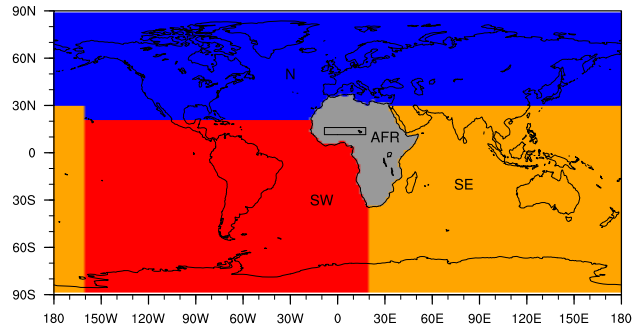


Figure 2.12: The four evaporative source regions N (north), SW (southwest), SE (southeast), and AFR (Africa) that we use to determine the sources for precipitation in the western Sahel region (black rectangle).

of directional shear (Fig. 2.4) acts to prevent significant enrichment of local moisture near the surface (Fig. 2.7, middle left). Consequently, in AMA in January the 2D approximation gives reasonable results, the only deficit seeming to be the neglect of a moderate degree of fast-recycling (Fig. 2.11, left).

As discussed above, the transport of moisture evaporated from WAF in July can be determined only poorly using the 2D approximation. The reason for this is that, given the strong generation of vertical inhomogeneities by surface evaporation and by directional shear, the counteracting degree of vertical mixing does not suffice to establish well-mixed conditions. This already indicates that, likewise, the evaporative source regions for precipitation in the nearby located western Sahel can probably not be diagnosed adequately using the 2D approximation.

Keys et al. (2012) diagnosed the evaporative sources for precipitation in the western Sahel (and other regions) applying 2D moisture tracing to ERA-Interim reanalysis data (Dee et al., 2011). In the following we investigate how much error in this specific case must be expected to arise from the use of the 2D approximation. To this end we apply all three moisture tracing variants to a third set of evaporative source regions comprising Africa (AFR), those regions located to the southwest of Africa (SW), those regions located to the southeast of Africa (SE), and the remainder, i.e. those regions located to the north of Africa (N) (Fig. 2.12). When we refer to the western Sahel, we mean the rectangular region ranging from  $8.4^{\circ}\text{W}$  to  $17.8^{\circ}\text{E}$  and from  $11.2^{\circ}\text{N}$  to  $16.8^{\circ}\text{N}$  (see the black rectangles in Figs. 2.12

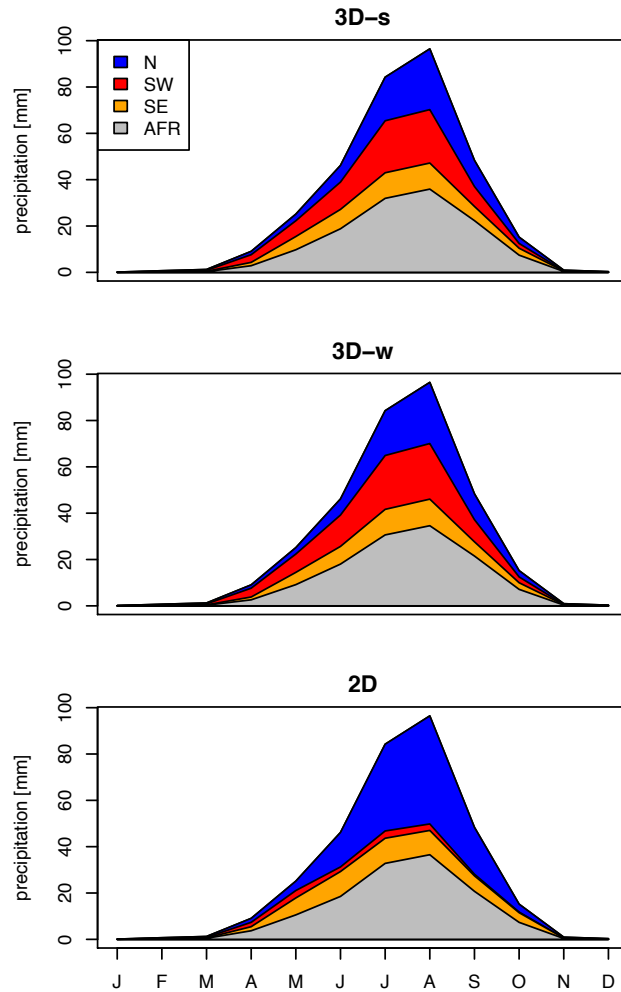


Figure 2.13: Monthly absolute contribution to precipitation (mm) in the western Sahel from the four evaporative source regions (compare Fig. 2.12) as determined by the moisture tracing variants 3D-s (top), 3D-w (middle), and 2D (bottom).

Table 2.2: Contribution to annual precipitation in the western Sahel from the four evaporative source regions N, SW, SE, and AFR (compare Fig. 2.12) as determined by the moisture tracing variants 3D-s, 3D-w, and 2D

source region	3D-s	3D-w	2D
N	22 %	22 %	40 %
SW	24 %	26 %	4 %
SE	14 %	14 %	16 %
AFR	40 %	38 %	40 %

and 2.14), which is approximately the same region as the one investigated by Keys et al. (2012).

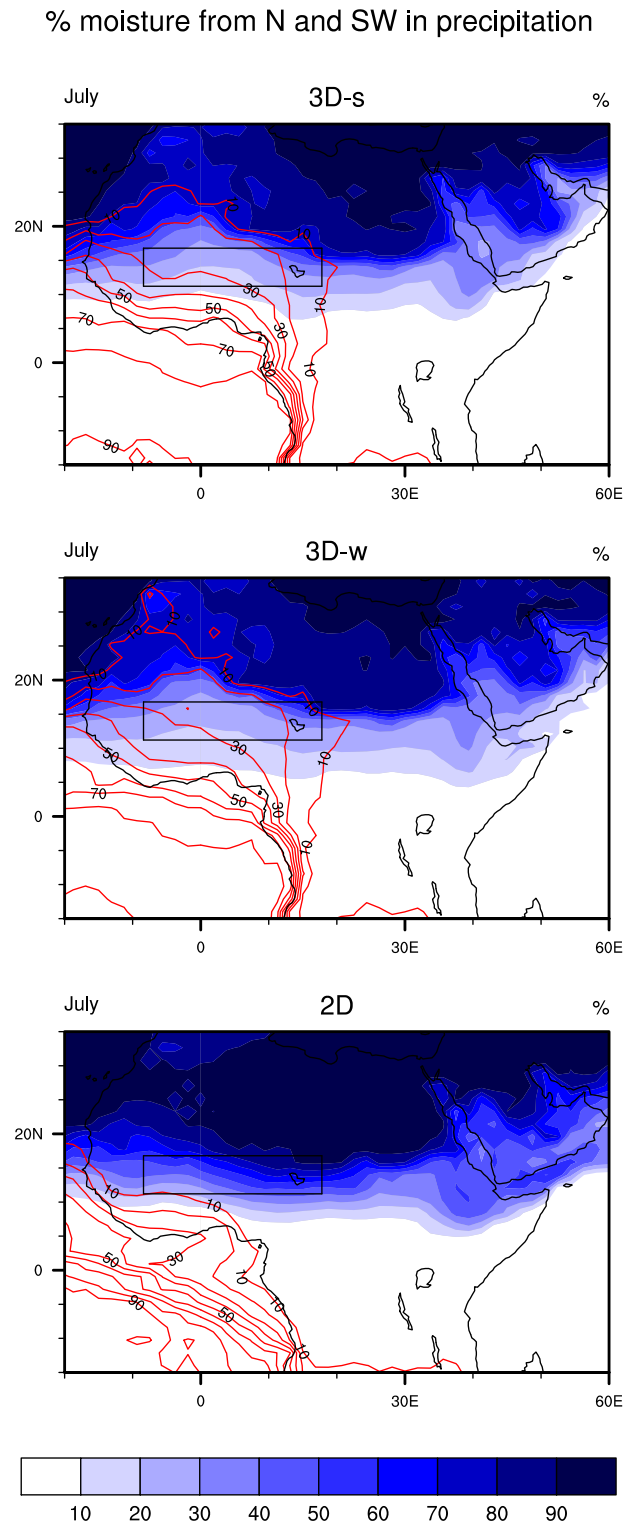


Figure 2.14: Relative contribution to precipitation (%) in the western Sahel (black rectangle) in July from the regions N (blue shading) and SW (red lines) (compare Fig. 2.12) as determined by the moisture tracing variants 3D-s (top), 3D-w (middle), and 2D (bottom).

The contributions to western Sahelian precipitation from AFR and SE are reasonably well reproduced by the 2D approximation, but the contributions from N and SW are not (Tab. 2.2, Figs. 2.13 and 2.14); while the well-agreeing 3D variants reveal that approximately equal amounts stem from N and SW, the 2D variant almost completely misses the contribution from SW, compensated by an increased contribution from N. The reason for this deficit is, as already discussed for the moisture stemming from WAF, the layered structure of the atmosphere: the low-level monsoonal layer advects air masses from the southwest while the African Easterly Jet above advects air masses from the northeast (Fig. 2.3), whereby vertical mixing is not strong enough to maintain well-mixed conditions.

In accordance with the results from our 2D variant, Keys et al. (2012) found much less moisture stemming from the tropical Atlantic than from the Mediterranean and the adjacent regions. Our results obtained with a resolved vertical dimension however indicate that the contributions are approximately equal. It thus seems that the precipitation shed of the western Sahel as determined by Keys et al. (2012) (see Fig. 3 therein) is strongly biased towards the northeast.

## 2.8 Discussion

In the following we first discuss potential model deficits and compare important atmospheric characteristics as simulated with ECHAM6 to ERA-Interim data (Dee et al., 2011). Thereafter follows a comment on a (further) methodological difference between Keys et al. (2012) and our study. We then discuss further aspects that are associated with the distinction between net and gross rates of evaporation and condensation, leading finally to the question of what should be the guiding principle for the development of a “best” way to trace moisture in the atmosphere.

Of course ECHAM6’s climate contains unavoidable biases, and the usage of climatological SSTs in this study adds to these. One may therefore wonder if our results can be transferred to the real world. First, our theoretical considerations are of course not affected. Second, we relate the simulated differences between 2D and 3D moisture tracing to atmospheric characteristics that can likewise be evaluated for other atmospheric data sets like reanalysis

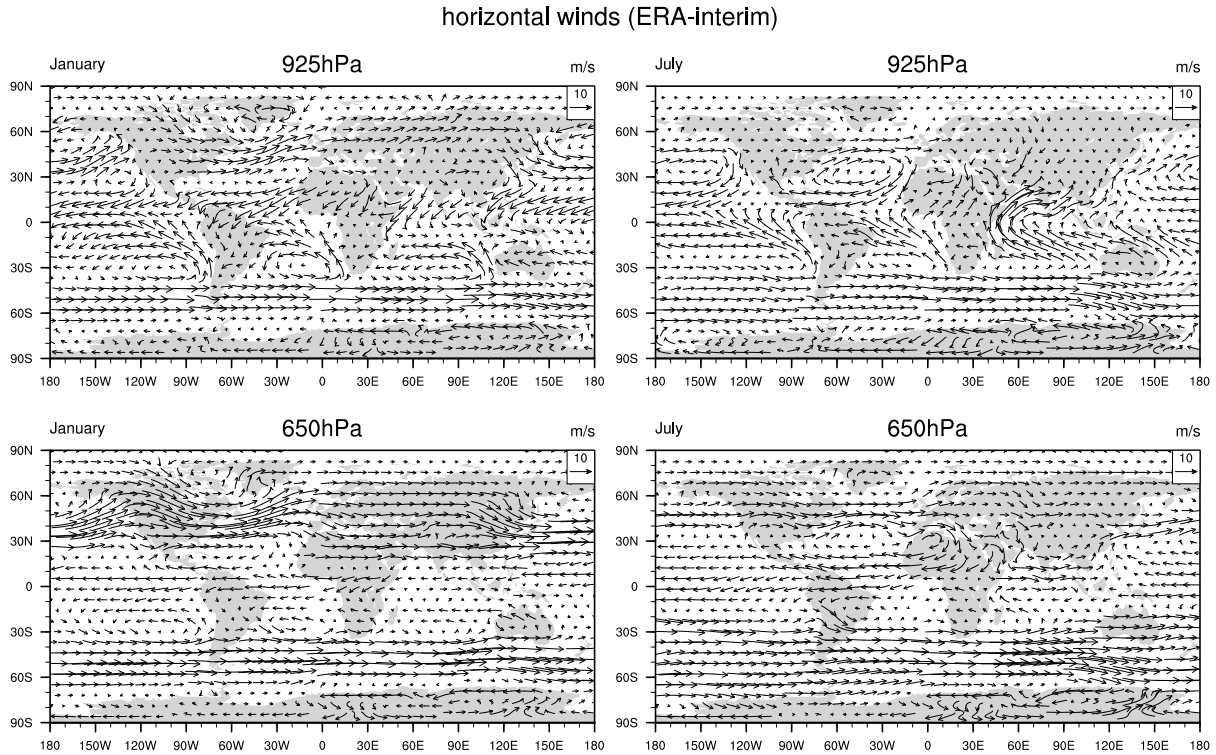


Figure 2.15: Horizontal winds at 925 hPa (top, m/s) and 650 hPa (middle, m/s) from ERA-Interim reanalysis data (Dee et al., 2011) for January (left) and July (right), averaged over the years 2001–2010. Compare Fig. 2.3, top and middle.

data. This way potential differences between our findings and the real world (approximated by reanalysis data) can be assessed. In fact, the key atmospheric characteristics seem to be, at least qualitatively, reasonably well reproduced by ECHAM6, as the following comparison with ERA-Interim data (Dee et al., 2011) shows.

One strength of AGCMs clearly lies in their ability to reproduce large-scale circulation patterns relatively well, because these are to a large extent determined by the physically well-founded primitive equations at resolved scales, and to a lesser extent by uncertain parameterisations such as those needed for moist convective processes. The comparison of the horizontal winds as simulated by ECHAM6 (Fig. 2.3, top and middle) with ERA-Interim data (Fig. 2.15) supports this notion. Features of the vertical wind structure that we referred to in the previous sections are confirmed to exist also in the real world, including for example the layered structure in tropical western Africa.

Somewhat less well reproduced by ECHAM6, at least when driven with climatological

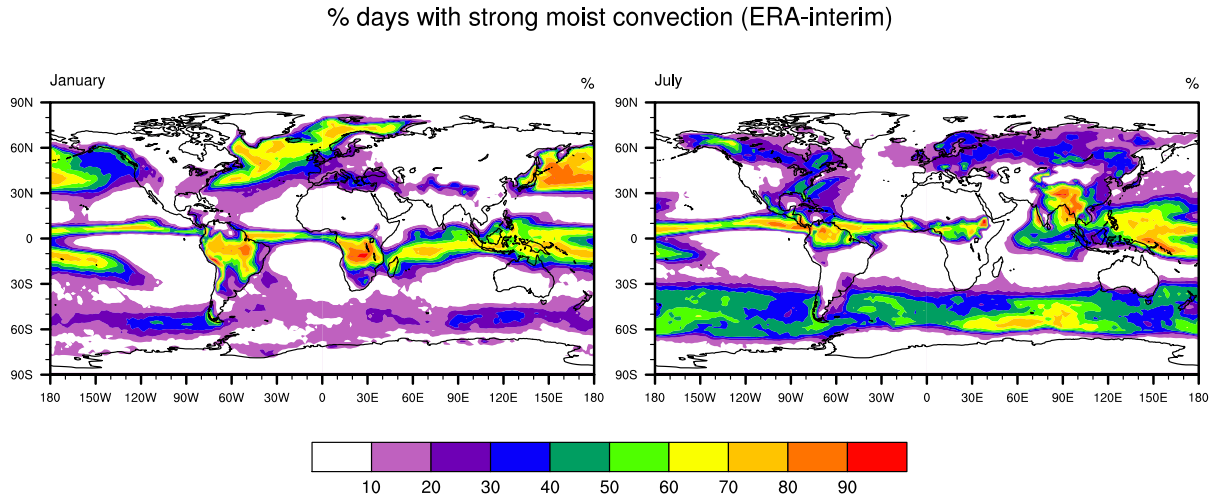


Figure 2.16: Fraction of days with strong moist convection from ERA-Interim reanalysis data (Dee et al., 2011) for January (left) and July (right), remapped to a T63 grid and averaged over the years 2001–2010, where we consider events as strong if the generated daily amount of convective precipitation exceeds 10% of the total column water content. Compare Fig. 2.2.

SSTs as in this study, appears to be the frequency of strong moist convection (Fig. 2.16, compare Fig. 2.2). While the overall spatial pattern is clearly captured, ECHAM6 tends to underestimate the frequency of days with convective precipitation exceeding 10% of the atmosphere’s vertically integrated moisture content. This suggests that ECHAM6 tends to underestimate the degree of vertical mixing in the free troposphere, though this potential deficit should be of quantitative rather than qualitative nature. Regarding the extensively discussed region of tropical western Africa, it seems worth to mention that in this region ECHAM6 apparently reproduces the frequency of strong moist convection reasonably well.

It should be mentioned that Keys et al. (2012) applied their diagnostic 2D moisture tracing scheme not forward in time, but backward. This allowed them to determine the evaporative source regions for precipitation in the western Sahel (and in other regions) at grid-point spatial resolution, whereas we, keeping to forward tracing, distinguished only four large predetermined source regions. However, the differences between 2D and 3D tracing should not depend on the temporal direction in which the tracing is carried out.

In Sect. 2.6 we pointed out that 3D, i.e. “full”, moisture tracing itself bears some uncertainties, even if the underlying atmospheric model is assumed to be perfect. These

uncertainties arise from the fact that the evolution of the atmosphere's physical state does not depend on gross but only on net rates of condensation and re-evaporation, i.e. their difference  $C - R$ , making it unnecessary to work with gross rates in atmospheric models. However, a precise tracing of moisture requires knowledge of the gross rates, because these are needed to determine to what extent precipitation mixes with the ambient water vapour. The two 3D moisture tracing variants we applied are at the two extremes of the possible range of assumptions. This means that it could well be possible to narrow down the uncertainty associated with this issue by incorporating existing knowledge about the degree of mixing between precipitation and the ambient water vapour. Such knowledge could be derived from measurements of stable water isotopes, from targeted smaller-scale modelling studies, or even from simple thermodynamical considerations. It could also make sense to distinguish different precipitation generating mechanisms, foremost convective and large-scale processes, as the following considerations suggest.

During deep convective events precipitation occurs in the relatively narrow convective updrafts only. The precipitation exchanges water molecules only with the ambient water vapour inside the updrafts and, accounting for entrainment and detrainment, with the immediate surroundings of the updrafts. This means that equilibration with respect to composition between precipitation and ambient water vapour happens only within the updrafts, while the air in the much larger downdrafts is not in contact with the precipitation. This suggests that the composition of the precipitation arriving at the surface is to a relatively large degree determined by the composition of the upper-level atmospheric moisture from which the precipitation originally formed.

By contrast, stratiform (large-scale) precipitation is characterised by rather uniform horizontal conditions, meaning that precipitation exchanges water molecules with the large water vapour reservoir of all the air. This suggests that in stratiform situations the composition of the precipitation arriving at the surface is not so much determined by the composition of the upper-level atmospheric moisture from which the precipitation originally formed, but rather resembles the composition of the lower-level atmospheric moisture. The latter seems particularly reasonable if the rain drops are relatively small, which is more common for stratiform precipitation than for convective precipitation. These differences between stratiform

and convective precipitation suggest that the 3D-s variant may rather resemble stratiform precipitation, whereas the 3D-w variant may rather resemble convective precipitation. However, we leave such prospects regarding the optimisation of 3D moisture tracing open for future research.

A final thought shall carry the issue associated with the distinction of gross and net rates of condensation and re-evaporation even further. We point out that the lack of necessity to determine the gross rates within AGCMs curtails the possibility to perform “perfect” 3D moisture tracing with passive water vapour tracers, where “perfect” means that the origin and fate of water is correctly determined at the molecular level. Instead, subtle degrees of freedom exist in the system that can only be accounted for with additional assumptions. Strictly speaking, this problem exists not only at the interfaces between condensed and gaseous water compartments in the atmosphere, but also at the Earth’s surface. Consider for example an air mass that is saturated with respect to the ocean’s surface temperature residing over the ocean. In this case net evaporation/condensation is zero, yet gross evaporation and gross condensation take place and cause an exchange of water molecules.

A “perfect” moisture tracing would have to account for these additional gross exchange fluxes as well. This admittedly peculiar conclusion brings to mind the question what the benefit of a truly perfect moisture tracing would be, apart from the mere satisfaction of intellectual curiosity. We think that the ultimate purpose of moisture tracing is to learn something about causality within the atmospheric branch of the hydrological cycle, to help finding answers to questions of the kind “How does precipitation in B depend on evaporation in A?”. This ultimate purpose of moisture tracing should be the guiding principle for the development of a “best” way to trace moisture in the atmosphere. But is a moisture tracing that is perfect on the molecular level also the best way to determine causalities? Or is it possible that a tracing procedure that omits gross rates and accounts only for net rates is more suitable to determine causal connections between evaporation and precipitation? This issue seems to have escaped the attention of the scientific community and, to our opinion, deserves future exploration.

## 2.9 Summary and conclusions

The primary focus of this study is the assessment of errors that are introduced by the application of 2D moisture tracing as opposed to the “exact” method of 3D moisture tracing. To this end we analysed the theoretical basis of the 2D approximation – the ‘well-mixed’ assumption – and implemented both 3D and 2D moisture tracing into an AGCM, which allowed us to make a direct quantitative comparison. Moreover, we implemented and evaluated two different 3D moisture tracing variants to account for the indeterminate degree of mixing that takes place between falling precipitation and the ambient water vapour.

We showed analytically that 2D moisture tracing is exact if the ‘well-mixed’ assumption holds; in this case neither horizontal advection nor the precipitation process are associated with errors due to the 2D approximation. Accordingly, the accuracy of the 2D approximation is highest where meteorological conditions are favourable of well-mixed conditions, and lowest where strong vertical inhomogeneities are present. We demonstrated that key atmospheric characteristics in this context are (I) the presence of directional shear, which generates vertical inhomogeneities, and (II) the frequency of deep convection, which acts to mix the atmosphere vertically. Overall, well-mixed conditions are seldom met and, hence, the 2D approximation is mostly associated with noticeable errors.

One can discern two kinds of errors introduced by the 2D approximation, namely (I) the omission of fast-recycling, which leads to an underestimation of local moisture in precipitation but does not greatly affect the spatial structure of the resulting patterns, and (II) the omission of layered horizontal advection, which can have a strong impact on the spatial structure of the resulting patterns and, hence, appears to be the more serious deficit of 2D moisture tracing. We find a different degree of fast-recycling also to be the main reason for differences between the two 3D moisture tracing variants, whereas layered advection is not a factor there. As a consequence, the (pattern distorting) errors introduced by the 2D approximation are generally larger than the (pattern conserving) uncertainties associated with 3D moisture tracing.

While the presence of fast-recycling is geographically not much constrained, strongly layered advection is a distinctive feature of the tropics with its thermally direct circulations;

the latter are suppressed in the extratropics where the Coriolis force gives rise to a certain vertical rigidity of the atmosphere. There are, of course, also in the tropics situations where the winds are only moderately sheared vertically and, if in combination with frequent vertical mixing, the errors resulting from the 2D approximation are as moderate as they tend to be in the extratropics. This is for example the case for the Amazon region in January. The rule however is that the 2D approximation is less appropriate in the tropics, in particular where strong directional shear combines with a low frequency of moist convective mixing.

An example for such a region is tropical western Africa (including the western Sahel), where in particular during the monsoon season (northern summer) the atmosphere's vertical structure is strongly layered and moist convective mixing does by far not suffice to maintain well-mixed conditions. Here, 2D moisture tracing strongly underestimates the amount of moisture originating from the tropical Atlantic that, in reality, is transported in the low-level monsoonal layer far into the African continent. Compensatingly, 2D moisture tracing overestimates the contribution to western Sahelian precipitation originating from beyond the Sahara.

We think that, due to its simplicity and straightforward applicability to different kinds of data, 2D moisture tracing is a useful approximation despite the errors that are introduced by the vertical integration. However, its application should largely be constrained to the extratropics, or, if applied to tropical regions, it should be made sure that the atmospheric conditions at the place and time are such that errors associated with the 2D approximation can be assumed to be small. Our study can be used as a basis for deciding when and where 2D moisture tracing can be considered a useful approximation.



Not everything that counts can be counted, and not everything that can be counted counts.

---

*(William Bruce Cameron)*

## Chapter 3

# Continental moisture recycling as a Poisson process

## **Abstract**

On their journey across large land masses, water molecules experience a certain number of precipitation-evaporation cycles (recycling events). Here we investigate analytically the frequency distributions of recycling events for the water molecules contained in a given air parcel. We show that, given the validity of certain simplifying assumptions, continental moisture recycling results in well-defined frequency distributions of recycling events, namely a Poisson distribution or a geometric distribution, depending on the assumptions.

We distinguish between two cases: in case (A) recycling events are counted since the water molecules were last advected across the ocean-land boundary. In case (B) recycling events are counted since the water molecules were last evaporated from the ocean. We show by means of simple scale analysis for case B that, given the conditions on Earth, realistic frequency distributions may be regarded as a mixture of a Poisson distribution and a geometric distribution. By contrast, in case A the Poisson distribution appears as a reasonable approximation. Our results demonstrate that continental moisture recycling can be interpreted as a Poisson process.

## 3.1 Introduction

Since the pioneering studies on the isotopic composition of precipitation and moisture recycling in the Amazon basin in the late 70's (Salati et al., 1979; Lettau et al., 1979), it has become conventional wisdom that tropical forests maintain a substantial fraction of their precipitation by their own evaporation. That continental evaporation contributes a large fraction to continental precipitation has been confirmed by a large number of studies since (e.g. Brubaker et al., 1993; Eltahir and Bras, 1994; Numaguti, 1999; van der Ent et al., 2010; Goessling and Reick, 2012). Moreover, it has been shown by means of climate model simulations that reduced continental evaporation rates, for example due to deforestation, result in less continental precipitation (e.g. Shukla and Mintz, 1982; Shukla et al., 1990; Werth and Avissar, 2002; Goessling and Reick, 2011). Recently, Spracklen et al. (2012) found evidence also from observations that moisture recycling is an important factor for the generation of continental rainfall.

So far, most studies dealing with continental moisture recycling focussed on determining the evaporative source regions of precipitation, for example the fraction of continental moisture in precipitation, using either atmospheric general circulation models (AGCMs) equipped with passive water vapour tracers (WVTs) (Numaguti, 1999; Bosilovich et al., 2002; Goessling and Reick, 2012), or using reanalysis data together with diagnostic moisture tracing algorithms (Yoshimura et al., 2004; van der Ent et al., 2010). Numaguti (1999) distinguished moisture not only by source regions (continental versus oceanic), but distinguished the continental fraction further according to the number of recycling events the water molecules have experience since they last evaporated from the ocean, where a recycling event comprises precipitation on and subsequent reevaporation from land. Numaguti (1999) noticed in one case that “from the first through the fourth generation the precipitation amount of the child generation is about 0.6 times that of the parent generation”. However, Numaguti (1999) did not attempt to explain what determines the shapes of the simulated frequency distributions (see in particular figure 14 in the paper).

To provide such an explanation is the goal of this paper. We show analytically that, given the validity of certain simplifying assumptions, the frequency distribution of continental

recycling events for the water molecules contained in a given air parcel attains either a Poisson distribution or a geometric distribution, depending on the assumptions.

## 3.2 Theory

The goal of the following derivations is to find simple analytical expressions for the frequency distribution of  $n$ , where  $n$  is the number of continental recycling events the water molecules contained in an air parcel have experienced either (A) since they were last advected across an ocean-land boundary, or (B) since they last evaporated from the ocean. To achieve this goal, we first consider how in general a moisture species  $i$  is transported in the atmosphere and how it is exchanged between the atmosphere and the surface (including the subsurface).

### 3.2.1 Exact transport equations

For convenience, in the following derivations we consider only one of the two horizontal dimensions, the second one being analogous. The partial differential equation that governs the temporal evolution of the specific concentration  $q_i$  [kg/kg] of moisture species  $i$  reads

$$\frac{\partial(\rho q_i)}{\partial t} + \frac{\partial(\rho q_i u)}{\partial x} + \frac{\partial(\rho q_i w)}{\partial z} = S_i \quad (3.1)$$

where  $\rho$  is air density [kg/m<sup>3</sup>],  $t$  is time [s],  $u$  [m/s] is wind speed in the horizontal dimension  $x$  [m],  $w$  [m/s] is wind speed in the vertical dimension  $z$  [m], and  $S_i$  is a non-advective source/sink term.

Following Goessling and Reick (2012), the vertical integral of Eq. (3.1) can be written in terms of the effective speed  $u_i^{\text{eff}}$  [m/s] at which  $q_i$  is horizontally transported. Using the notation  $\hat{\chi} = \int_0^\infty \rho \chi dz$  (where  $\chi$  can be any variable), with  $u_i^{\text{eff}} = \widehat{q_i u} / \hat{q}_i$  vertical integration gives

$$\frac{\partial \hat{q}_i}{\partial t} + \frac{\partial(\hat{q}_i u_i^{\text{eff}})}{\partial x} = E_i - P_i \quad (3.2)$$

where we substituted the vertical integral of  $S_i$  by the difference between surface evaporation  $E_i$  [kg/(m<sup>2</sup>·s)] and precipitation (including dew formation)  $P_i$  [kg/(m<sup>2</sup>·s)]. We can rewrite

Eq. (3.2) such that it resembles a Lagrangian formulation:

$$\frac{d\hat{q}_i}{dt} = E_i - P_i - \hat{q}_i \frac{\partial u_i^{\text{eff}}}{\partial x} \quad (3.3)$$

with  $d\hat{q}_i/dt = \partial\hat{q}_i/\partial t + u_i^{\text{eff}}(\partial\hat{q}_i/\partial x)$ .

### 3.2.2 The ‘well-mixed’ assumption

While Eqs. (3.2) and (3.3) are still exact, we now make the first approximation by assuming vertically well-mixed conditions, i.e. we assume that

$$f_i(t, x, z_1) = f_i(t, x, z_2) \quad \text{for all } t, x, z_1, z_2. \quad (3.4)$$

where  $f_i = q_i/q$  (and also, under well-mixed conditions,  $f_i = \hat{q}_i/\hat{q}$ ) and  $q$  is total specific moisture. This implies two simplifications, namely that (I) the species-dependent effective transport speed becomes  $u_i^{\text{eff}} = u^{\text{eff}} = \widehat{qu}/\hat{q}$  for all moisture species and (II) the precipitation term becomes  $P_i = f_i P$  where  $P$  is total precipitation (plus dew formation). For a comprehensive analysis of the errors that are introduced when well-mixed conditions are assumed in realistic situations, we refer the reader to Goessling and Reick (2012).

Since Eq. (3.3) likewise holds for  $q$  (omitting all indices  $i$ ), we can use Eq. (3.3) to derive the Lagrangian time derivative of  $f_i = \hat{q}_i/\hat{q}$ . Under well-mixed conditions we obtain the very simple expression

$$\begin{aligned} \frac{df_i}{dt} &= \frac{(E_i - f_i P - \hat{q}_i \frac{\partial u_i^{\text{eff}}}{\partial x}) \hat{q} - (E - P - \hat{q} \frac{\partial u^{\text{eff}}}{\partial x}) \hat{q}_i}{\hat{q}^2} \\ &= (\tilde{f}_i - f_i) \frac{E}{\hat{q}} \end{aligned} \quad (3.5)$$

where  $E$  is total surface evaporation and  $\tilde{f}_i = E_i/E$ . Note that  $P$  has dropped out here.

### 3.2.3 Species definition and the ‘steady-state’ assumption

In the above derivations we have not specified how the moisture species  $i$  are defined, but required only that the only sources and sinks of the moisture species are those associated

with surface evaporation and precipitation (including dew formation). One possible way to define different moisture species is to distinguish them according to their evaporative source region. In this case  $\tilde{f}_i$  would be either one or zero, depending on whether or not the considered air mass is located above the source region corresponding to species  $i$ . Instead, in the following we consider the case where moisture species are defined according to  $n$  – the number of recycling events the water molecules have experienced on their journey across the land masses.

As adumbrated at the beginning of this section, there are two natural alternatives how one can define  $n$ :

- case A:  $n$  is the number of recycling events a water molecule has experienced since it was last advected across an ocean-land boundary.
- case B:  $n$  is the number of recycling events a water molecule has experienced since it last evaporated from the ocean.

These two cases can roughly be characterised as intra-continental (A) and inter- or pan-continental (B) moisture recycling because in case B the recycling events can take place on different continents while this is forbidden in case A.

In either case  $\tilde{f}_n$  over land depends on the composition of the surface reservoir from which the water evaporates. The composition of the surface reservoir is determined by the composition of antecedent precipitation events and the intermediate redistribution within the reservoir. However, it is possible to circumvent an explicit treatment of the surface reservoir by assuming that over land

$$\tilde{f}_n = f_{n-1}, \quad n \in \mathbb{N} \tag{3.6a}$$

$$\tilde{f}_0 = 0. \tag{3.6b}$$

While Eq. (3.6b) is by definition of  $n$  generally valid over land, Eq. (3.6a) constitutes an approximation that becomes exact in two limit cases: The first one is given when evaporation is fed by water that precipitated immediately before re-evaporation. In reality, evaporation from intercepted water may often be close to this situation. The second limit

case is given when the system is in steady state, meaning that the atmospheric composition with respect to the moisture fractions  $f_n$  is temporally constant. When this is the case, the surface reservoir attains the same composition as the atmosphere above and, hence, the approximation defined by Eq. (3.6a) becomes exact. In reality, conditions that are not too far from such a steady-state situation may be given in tropical regions with weak variability of the meteorological conditions both at the daily and the seasonal time scale. In the following we denote the simplification given by Eq. (3.6a) the ‘steady-state’ assumption, keeping in mind that it is exact not only in steady state but also if evaporation is fed by water that precipitated immediately before.

### 3.2.4 The Poisson distribution as solution over land

With our specification of moisture species according to the number of continental recycling events ( $n$ ) and with the ‘steady-state’ assumption, which beside the ‘well-mixed’ assumption constitutes the second approximation we invoke, Eq. (3.5) becomes over land

$$\frac{df_n}{dt} = (f_{n-1} - f_n) \frac{E^c}{\hat{q}}, \quad n \in \mathbb{N} \quad (3.7a)$$

$$\frac{df_0}{dt} = -f_0 \frac{E^c}{\hat{q}} \quad (3.7b)$$

where  $E^c$  is total continental evaporation. For the system of ordinary differential equations given by Eqs. (3.7a-b) the following solution exists:

$$f_n = \frac{\lambda^n}{n!} e^{-\lambda}, \quad n \in \mathbb{N}_0 \quad (3.8)$$

where  $\lambda$  grows with time  $t$ :

$$\lambda(t) = \lambda(t_0) + \int_{t_0}^t \frac{E^c(t')}{\hat{q}(t')} dt'. \quad (3.9)$$

Equation (3.8) is a Poisson distribution, characterised by the only parameter  $\lambda$  which also is the mean value and the variance of the distribution. For Eq. (3.8) to be the actual solution of Eq. (3.7), it is necessary and sufficient that the initial state of the frequency distribution

is a Poisson distribution, i.e.  $f_n(t_0)$  must follow Eq. (3.8) with an arbitrary initial value  $\lambda(t_0)$ . If this condition is fulfilled, continental moisture recycling can be interpreted as an inhomogeneous Poisson process with the intensity  $E^c/\hat{q}$ , where inhomogeneous means that the intensity of the Poisson process varies as  $E^c$  and  $\hat{q}$  vary with time (for a general discussion of Poisson processes see e.g. Ross, 1983).

Whether  $f_n(t_0)$  is Poisson distributed depends on which of the cases A and B is considered. In case A,  $f_n(t_0)$  is indeed Poisson distributed with  $t_0$  being the moment of advection across the ocean-land boundary and  $\lambda(t_0)$  being equal to zero. This simply means that at  $t = t_0$  all water molecules have experienced zero recycling events ( $f_0(t_0) = 1$ ,  $f_n(t_0) = 0 \forall n > 0$ , which is a special case of Eq. 3.8). After  $t = t_0$ ,  $f_n$  develops as a Poisson distribution with  $\lambda$  growing according to Eq. (3.9) as long as the parcel's trajectory stays over land. Since Eq. (3.7) only holds over land, the solution loses validity when the parcel eventually leaves the continent. However, when the parcel is again advected across an ocean-land boundary, the solution regains validity starting again with  $\lambda = 0$ , and so forth.

### 3.2.5 Extension to the ocean (case B) and the high intensity limit

In contrast to case A, in case B there is no moment in time at which the frequency distribution of  $n$  is set to an initial Poisson distribution; a parcel crossing the ocean-land boundary contains water molecules with  $n > 0$ . This reflects the fact that some molecules have not been newly evaporated from the ocean but experienced recycling events earlier and then crossed the ocean without being lost from the atmosphere as precipitation. The prerequisites that are necessary for the specific solution given by Eq. (3.8) to be the actual solution to Eq. (3.7) are thus not given anymore. Approximating the frequency distribution of  $n$  with a Poisson distribution – when  $n$  is defined according to case B – hence entails additional errors because the initial state is not characterised by a Poisson distribution.

While Eqs. (3.7a-b) hold only for continental evaporation (given the ‘steady-state’ assumption), which is sufficient for case A, for case B it is necessary to extend the equations

so that they can be applied also over the ocean:

$$\tilde{f}_n = \begin{cases} f_{n-1} & \text{over land} \\ 0 & \text{over the ocean} \end{cases}, \quad n \in \mathbb{N} \quad (3.10a)$$

$$\tilde{f}_0 = \begin{cases} 0 & \text{over land} \\ 1 & \text{over the ocean.} \end{cases} \quad (3.10b)$$

Entering this into Eq. (3.5) gives as extension of Eqs. (3.7a-b) to the ocean

$$\frac{df_n}{dt} = (f_{n-1} - f_n) \frac{E^c}{\hat{q}} - f_n \frac{E^o}{\hat{q}}, \quad n \in \mathbb{N} \quad (3.11a)$$

$$\frac{df_0}{dt} = -f_0 \frac{E^c}{\hat{q}} + (1 - f_0) \frac{E^o}{\hat{q}} \quad (3.11b)$$

where  $E^o$  is total oceanic evaporation. Depending on the parcel's location, at least one of  $E^c$  and  $E^o$  is zero.

Still assuming vertically well-mixed and steady-state conditions, we now show that there are two limit cases for which also in case B the distribution of  $f_n$  can be obtained analytically. To this end we consider the integrated intensity  $\lambda^*$ , defined as

$$\lambda^* = \int_{t_0-T}^{t_0} (E/\hat{q}) dt \quad (3.12)$$

where  $T$  is the typical time it takes atmospheric air to cross either an ocean ( $T^o$ ) or a continent ( $T^c$ ). By relating the amount of evaporation, integrated along a trajectory from one coast to the next across an ocean or a continent, to the vertically integrated atmospheric moisture content,  $\lambda^*$  measures to what extent atmospheric moisture is replaced by newly evaporated moisture while the air is transported from one coast to the next.

The first limit case is the high intensity limit. It is given by  $\lambda^* \gg 1$ . In the high intensity limit, during an ocean crossing (almost) all water molecules originally contained in the air are replaced by newly evaporated water from the ocean for which by definition  $n = 0$  (note that, because the order of  $\hat{q}$  typically does not change, in this limit case it also holds that precipitation and evaporation are of the same order). Because thus  $f_0 \approx 1$  and  $f_{n>0} \approx 0$

at the ocean-land boundary, in the high intensity limit case B becomes equivalent to case A. This implies that the distribution of  $f_n$  evolves as a Poisson distribution with growing mean value (Eqs. 3.8 and 3.9) until, finally, the considered air parcel leaves the continent.

### 3.2.6 The geometric distribution as stationary solution in the low intensity limit

We now consider the low intensity limit which is given if  $\lambda^* \ll 1$ . In this limit a single crossing of an ocean or a continent does not much affect the distribution of  $f_n$ , and the latter becomes largely determined at time scales larger than  $T$ . In fact, it is now possible to treat oceanic and continental evaporation as if they occurred simultaneously. In mathematical terms this is consistent with the limit  $T \rightarrow 0$ , which is one way how to arrive at the low intensity limit. Treating oceanic and continental evaporation simultaneously requires to weight  $E^c$  and  $E^o$  in Eqs. (3.11a-b) according to  $T^c$  and  $T^o$ . Thus replacing  $E^c$  by  $\bar{E}^c = (T^c/(T^c + T^o))E^c$  and  $E^o$  by  $\bar{E}^o = (T^o/(T^c + T^o))E^o$ , and with  $\bar{E} = \bar{E}^c + \bar{E}^o$  and  $r^c = \bar{E}^c/\bar{E}$ , Eqs. (3.11a-b) become

$$\frac{df_n}{dt} = (r^c f_{n-1} - f_n) \frac{\bar{E}}{\hat{q}}, \quad n \in \mathbb{N} \quad (3.13a)$$

$$\frac{df_0}{dt} = (1 - r^c - f_0) \frac{\bar{E}}{\hat{q}}. \quad (3.13b)$$

Given  $\bar{E}/\hat{q} > 0$ , the only steady state solution of Eqs. (3.13a-b) reads

$$f_n = (r^c)^n (1 - r^c), \quad n \in \mathbb{N}_0 \quad (3.14)$$

and can easily be shown to be stable. Equation (3.14) is a geometric distribution with mean value  $r^c/(1 - r^c)$ .

The steady-state solution given by (3.14) (not to be confused with the ‘steady-state’ assumption formulated in Sect. 3.2.3), i.e. the geometric distribution, is attained and permanently maintained if  $r^c$  is globally constant. This condition is met if the low intensity limit (Eq. (3.12)) is formulated even more stringent as  $\lambda^{*,g} = \int_{t_0-T^g}^{t_0} (E/\hat{q}) dt \ll 1$ , where  $T^g$  is the typical time it takes air to travel global distances. In this case, the distribution

of  $f_n$  is a globally uniform geometric distribution with mean value  $r^{c,g}$ , where the latter is global land evaporation divided by total global evaporation.

### 3.3 From idealised to real conditions on Earth

#### 3.3.1 The intensity limits

While the intensity limits are irrelevant for case A, for case B we have shown the following: (I) In the high intensity limit the frequency distribution of  $n$  over land is a Poisson distribution with a mean value that grows as continental moisture evaporates into the considered air parcel (case B transitions into case A for the continental parts of the trajectories). (II) In the low intensity limit the frequency distribution of  $n$  is a stationary geometric distribution. We now investigate to what extent these two limits apply to real conditions on Earth by means of simple scale analysis.

Neglecting dry continental regions and ice-covered surfaces, typical values of  $E$  range between  $\sim 1 \text{ kg}/(\text{m}^2\text{d})$  in the high latitudes and  $\sim 5 \text{ kg}/(\text{m}^2\text{d})$  in the tropics. Because typical values of  $\hat{q}$  range between  $\sim 10 \text{ kg}/\text{m}^2$  in the high latitudes and  $\sim 50 \text{ kg}/\text{m}^2$  in the tropics, the intensity itself can be considered to be spatially more or less uniform at  $E/\hat{q} \approx 0.1/\text{d}$ . It is thus rather  $T$  which largely determines the order of  $\lambda^*$  (Eq. (3.12)).

We now estimate  $T$  exemplarily for air crossing the North Atlantic and for air crossing the tropical Pacific. For the easterlies above the tropical Pacific with  $u^{eff} \approx 5 \text{ m/s} \approx 5,000 \text{ km/d}$  and  $\Delta x \approx 15,000 \text{ km}$  one arrives at  $\lambda^* \approx 3$ . For the westerlies above the North Atlantic with  $u^{eff} \approx 10 \text{ m/s} \approx 1,000 \text{ km/d}$  and  $\Delta x \approx 5,000 \text{ km}$  one arrives at  $\lambda^* \approx 0.5$ . This suggests that the situation on Earth is somewhere between the two intensity limits.

The results of this simple scale analysis are consistent with studies where continental precipitation recycling ratios were quantified by means of numerical moisture tracing (e.g. Goessling and Reick, 2011, 2012). Considering the situation along a latitude within the northern summer extratropical westerlies, the fraction of continental moisture in precipitation significantly increases from west to east over the continents and decreases from west to east over the ocean basins (Figs. 1.2 and 2.8). The fact that the recycling ratio does not stay constant along the westerlies implies that the low intensity limit is not valid. On the

other hand, the high intensity limit seems to be an even worse approximation because the recycling ratio does by far not drop to zero over the ocean. The situation is slightly different in the tropics, in particular south of the equator. Air masses arriving at the eastern coasts of the continents located there – South America, Africa, and Australia – are characterised by recycling ratios that are very low compared to the maxima located close to western coasts. This suggests that here the high intensity limit is, if not an accurate, at least an instructive approximation.

The fact that conditions on Earth are somewhere between the two intensity limits suggests that real frequency distributions of  $n$  – when  $n$  is defined according to case B – can be interpreted as mixtures of Poisson distributions and geometric distributions. Moreover, depending on location and season, real distributions may be closer to either of the two analytical solutions. It must however be kept in mind that the use of two further simplifying assumptions causes additional discrepancies between real distributions and the theoretical solutions.

### **3.3.2 The ‘well-mixed’ assumption**

Independent of the cases A and B we had to introduce the ‘well-mixed’ assumption (Eq. 3.4) and the ‘steady-state’ assumption (Eq. 3.6a) in order to arrive at the analytical solutions. While in case B the use of these assumptions leads to discrepancies in addition to those due to the application of one of the two intensity limits, in case A these two assumptions are the only source of discrepancies between real distributions and the theoretical solution, which in this case is the Poisson distribution. In the following we discuss qualitatively how realistic the ‘well-mixed’ assumption and the ‘steady-state’ assumption are, focussing on case A and the Poisson distribution. The ‘well-mixed’ assumption is discussed in this section and the ‘steady-state’ assumption in the next section.

The applicability of the ‘well-mixed’ assumption was investigated in depth by Goessling and Reick (2012) in the context of 2D moisture tracing because the latter is based on the ‘well-mixed’ assumption. It was found that well-mixed conditions are seldom present in the atmosphere. In particular in the tropics, where horizontal winds often blow in different directions at different heights (directional vertical shear), the 2D approximation often leads

to substantial errors. By contrast, in the extratropics errors associated with 2D moisture tracing arise mostly from the neglect of fast-recycling and are rather moderate.

This suggests that in tropical regions with strong directional vertical shear of the winds, for example in western Africa during northern summer, real frequency distributions of  $n$  may significantly deviate from Poisson distributions. One can imagine that vertically sheared winds act to mix air masses horizontally. Even if one assumes that those different air masses exhibit Poisson-distributed  $f_n$ 's before horizontal mixing takes place, the horizontal mixing results in non-Poisson-distributed  $f_n$ 's because linear combinations of Poisson distributions (with different mean values) are not Poisson distributions. If air masses with strongly different mean values mix horizontally, the resulting frequency distributions can even be multimodal. However, even in such cases it may be admissible to interpret the resulting frequency distributions as linear combinations of Poisson distributions, corroborating that the process by which these distributions are generated is still a Poisson process.

In the extratropics horizontal mixing of air masses is weaker and, thus, horizontal advection is captured relatively well by the 2D approximation. This is true despite the fact that vertically well-mixed conditions are typically not given (Goessling and Reick, 2012). We thus expect that deviations from well-mixed conditions in the extratropics do not strongly distort the resulting frequency distributions of  $n$ . However, it still depends on the second simplification – the ‘steady-state’ assumption – whether real frequency distributions of  $n$  indeed resemble Poisson distributions.

### 3.3.3 The ‘steady-state’ assumption

First of all, it is important to recall that what we term the ‘steady-state’ assumption, given by Eq. (3.6a), is valid not only if the atmospheric composition with respect to the moisture fractions  $f_n$  is temporally constant (i.e. in steady-state), but also if evaporation is fed by precipitation that occurred immediately before.

In reality, the latter condition (fast evaporation) is approximately fulfilled in situations where evaporation is drawn from the surface skin reservoir, i.e. water that has been intercepted by leaves or retained by the uppermost millimeters of the soil. Skin evaporation rates can be substantial, in particular in warm climates with weak seasonality, and in some

cases contributes up to 50% to the total annual evaporation (Savenije, 2004). By contrast, if water from the deep soil is transpired by plants, the water can be several months (or more) old. Particularly large amounts of old water are transpired by deep-rooted forests that are located in tropical wet-dry or tropical monsoon climates during the dry season, but also by temperate or boreal forests during summer. In this case Eq. (3.6a) can be a poor approximation.

However, even if old water is evaporated Eq. (3.6a) can still be exact, namely if the precipitation that formed the old water had the same composition with respect to the moisture fractions  $f_n$  as the current atmospheric moisture. The ‘steady-state’ assumption is thus a reasonable approximation also for regions with weak seasonality of the frequency distribution of  $f_n$ , which may be the case for example in tropical rainforest climates.

In conclusion, these qualitative considerations suggest that (in case A) significant deviations from Poisson distributions occur globally, but for different reasons in the tropics and in the extratropics. For the tropics we expect that deviations arise mainly due to the invalidity of the ‘well-mixed’ assumption in combination with directional vertical shear of the horizontal winds, whereas the ‘steady-state’ assumption may often be considered acceptable. The opposite is the case for the extratropics where we expect that the invalidity of the ‘well-mixed’ assumption plays a minor role while the ‘steady-state’ assumption may be the main cause of deviations.

### 3.4 Final remarks

The arguments given in Sect. 3.3 are merely qualitative and are to some degree speculative. How realistic the analytical solutions derived in Sect. 3.2 actually are, and if the arguments in Sect. 3.3 are valid, could be assessed by means of numerical simulations. To this end one could modify a WVT-equipped AGCM such that the WVTs are not defined according to evaporative source regions, as it is usually the case (e.g. Koster et al., 1986; Jousaume et al., 1986; Bosilovich and Schubert, 2002; Goessling and Reick, 2012), but according to the number of continental recycling events ( $n$ ). As mentioned above, simulations of this kind have already been performed by Numaguti (1999), but in that study the resulting frequency

distributions were not investigated in much detail.

It seems however interesting to come back to the notice that “from the first through the fourth generation the precipitation amount of the child generation is about 0.6 times that of the parent generation”, which Numaguti (1999) found for (monthly averaged) moisture stemming originally from the North Indian Ocean when it precipitates in the eastern Tibet region. One may wonder how this notice relates to our analytical solutions—and indeed one of the solutions complies with such an exponential law: a geometric distribution with mean value 1.5 (compare Eq. 3.14). However, this distribution would entail that the above statement holds likewise for the zeroth and the fifth (and higher) generations, which obviously is not the case. By and large the distributions shown by Numaguti (1999) (Fig. 14 therein) resemble rather Poisson distributions than geometric distribution, even though an exponential law for subsequent generations ( $f_n = \text{const} \cdot f_{n-1}$ ) does not hold for Poisson distributions (Eq. 3.8). After all, Numaguti (1999)’s figures and notice do by far not suffice to assess the transferability of our theoretical solutions to real conditions on Earth. Instead, our results should be confronted with new more specific AGCM-WVT simulations.

Finally we think that, irrespective of the outcome of such simulations, our reflections on continental moisture recycling, and in particular the interpretation of continental moisture recycling as a Poisson process, are of scientific value in their own right—even if this value may be considered of rather academic nature.



The scientist is not a person who gives the right answers, he's one who asks the right questions.

---

*(Claude Lévi-Strauss)*

## Summary, conclusions, and outlook

## Summary and conclusions

### Chapter 1

In Chapter 1 I first used ECHAM6 in combination with an offline 2D moisture tracing scheme to simulate continental precipitation recycling ratios ( $R_c$ ). The simulated patterns agree well with the results of earlier studies:  $R_c$  increases from continental upwind to downwind coasts, with monthly-mean peak values reaching 80% and more in the eastern parts of central Eurasia during northern-hemisphere (NH) summer, and about 50% close to the western coasts of tropical South America and Africa throughout the year.

The main added value of Chapter 1 in comparison to earlier studies is to go an important step further by asking what these results tell us about the sensitivity of precipitation to continental evaporation. To come to an answer I simulated how climate responds to the complete suppression of continental evaporation, using the same AGCM that I used before to generate the input data for the offline 2D moisture tracing scheme. The complete suppression of continental evaporation results in strongly reduced precipitation rates over most of the continents, with the most severe drying occurring in Eurasia and North America during NH-summer.

While the drying of the continents suggests that reduced continental moisture recycling plays an important role, the spatial pattern of the response within the continents does not agree with the pattern of  $R_c$ : the latter increases from upwind to downwind coasts, but the reduction of precipitation in response to suppressed continental evaporation tends to be stronger in the upwind parts of the continents, in particular in Eurasia and North America during NH-summer.

This mismatch is due to the active role of water in the atmosphere. While I found some evidence that positive local coupling contributes to the response, a strong influence of changes in the large-scale circulation is obvious. Most of all, the missing latent cooling of the land surface by evaporation, amplified by more solar heating due to reduced cloud cover, leads to stronger ‘thermal lows’ over the continents. This is most pronounced during NH-summer in Eurasia and North America where it leads to substantially attenuated westerlies and thus a more continental climate in the western parts of these large land masses.

### Key findings of Chapter 1

- Due to water's active role in the atmosphere, continental evaporation affects precipitation not only via moisture recycling but also via local coupling and via the large-scale circulation.
- The complete suppression of continental evaporation leads to severely reduced precipitation rates over the continents. The spatial pattern of the response however does not correlate well with the pattern of continental precipitation recycling ratios because changes in the large-scale circulation dominate the response.
- At the continental scale, moisture recycling estimates can thus not be used to infer the sensitivity of precipitation to modified evaporation.
- It remains an open question whether moisture recycling estimates are more useful indicators at smaller spatial scales, where the influence of changes in the large-scale circulation should be less dominant.

## Chapter 2

To investigate the significance of the vertical dimension in the context of atmospheric moisture tracing, in Chapter 2 I first examined the ‘well-mixed’ assumption – the basis of 2D moisture tracing – from a theoretical point of view. I showed that the 2D-approximation is exact if the atmosphere is well-mixed vertically. If by contrast vertical inhomogeneities exist, the 2D-approximation leads to inaccurate results for two reasons, namely (I) because the composition of precipitation with respect to different tracer species depends on the height at which the precipitation forms, and (II) because the horizontal advection term becomes erroneous. The severity of the latter effect grows with the degree to which the atmospheric winds are vertically sheared.

To complement the theoretical analysis, I conducted numerical experiments for which I implemented passive water vapour tracers (WVTs) into ECHAM6. The results of the online 3D moisture tracing (which I implemented in two variants, see below) reveal that moisture from different source regions is scarcely well-mixed vertically. This already indicates that

## *Summary, conclusions, and outlook*

2D moisture tracing must be associated with some errors. To quantify these errors directly, I compared the results obtained with the online 3D moisture tracing with results obtained with a 2D scheme. In order to make sure that differences between the results arise only from the 2D approximation (and not from e.g. numerical issues), I did not use an offline 2D scheme as in Chapter 1, but an online variant of 2D moisture tracing that I obtained by modifying the 3D implementation. The modification required to achieve this reduction is to artificially mix all moisture species in the vertical after every model time-step.

The large-scale patterns of continental recycling ratios ( $R_c$ ) obtained with the 3D scheme(s) and the 2D scheme are overall similar. This justifies *ex post* the use of the 2D approximation in Chapter 1 where the focus is on large-scale patterns. Closer inspection of the differences between the results reveals a qualitative difference between the tropics and the extratropics: errors of the 2D scheme are largest in the tropics, where the atmospheric flow field is often characterised by strong directional vertical shear of the winds due to the presence of thermally direct circulations. The more moderate errors occurring in the extratropics are mainly due to neglecting fast-recycling, meaning that the contribution of local (continental) evaporation to local (continental) precipitation is slightly underestimated.

In Chapter 2 I investigated further how accurate 2D moisture tracing is when it is applied to smaller-scale regions. In this summary I only want to highlight the results I obtained for the evaporative sources for precipitation in the western Sahel – a region where the horizontal winds are particularly strongly sheared in the vertical. According to the results obtained with the 2D approximation, 40 % of the region’s precipitation stem from the Mediterranean and its surroundings and only 4 % from the tropical and southern Atlantic. By contrast, 3D moisture tracing reveals that the contributions from the two source regions are approximately equal. This implies that the results published by Keys et al. (2012) contain unjustifiably large errors.

Finally, I drew attention to the fact that online 3D moisture tracing is associated with some uncertainty – even if the underlying AGCM is assumed to be “perfect”. The reason is that AGCMs operate only with net exchange fluxes of water molecules between precipitation and the ambient water vapour because only the net evaporation/condensation terms are relevant for the physical system. For a moisture tracing scheme to be precise, it is however

necessary to know about the gross terms which are not provided by the AGCM. To quantify the maximum uncertainty associated with this issue, I implemented two 3D tracing variants in which the gross terms are assumed to be either large (variant 3D-s) or small (variant 3D-w). I found that the differences between results obtained with these two 3D variants are smaller than the errors introduced by the 2D approximation. The main uncertainty relates to the degree of fast-recycling that is significantly different between the two 3D variants. However, vertically sheared winds that cause the most severe errors when the 2D approximation is used do not lead to significant differences between the two 3D variants.

### **Key findings of Chapter 2**

- The accuracy of 2D moisture tracing depends on the degree to which the atmosphere is well-mixed vertically with respect to moisture species from different evaporative source regions.
- Well-mixed conditions are typically not met in the atmosphere because vertical mixing is not strong enough to nullify vertical inhomogeneities arising from surface evaporation and vertically sheared winds.
- Errors of 2D moisture tracing are largest in the tropics because the tropical atmosphere often features strong directional vertical shear of the horizontal winds due to thermally direct circulations.
- Apart from the neglect of fast-recycling, 2D moisture tracing gives reasonable results in the extratropics. This is true despite invalidity of the ‘well-mixed’ assumption because horizontal winds in the extratropics tend to point in vertically rather uniform directions.
- Online 3D moisture tracing bears uncertainties because the degree to which precipitation mixes with the ambient water vapour is not provided by AGCMs.

## **Chapter 3**

In Chapters 1 and 2 I distinguished only between continental and oceanic moisture. By contrast, in Chapter 3 I subdivided the continental fraction of atmospheric moisture fur-

## *Summary, conclusions, and outlook*

ther, based on the number of recycling events the water molecules have experienced either since they were last advected across the ocean-land boundary (case A) or since they last evaporated from the ocean (case B). I showed analytically that, given the validity of certain simplifying assumptions, the frequency distribution of recycling events attains the form of one of two theoretical solutions—either a Poisson distribution or a geometric distribution, depending on the assumptions and whether case A or case B is considered.

Two assumptions are necessary to arrive at either of the two theoretical solutions. The first of these is the ‘well-mixed’ assumption that I discussed in depth in Chapter 2. The second is the ‘steady-state’ (or ‘fast-evaporation’) assumption. Given the latter, the composition of the continental (sub-)surface moisture (and hence the land evaporation) with respect to recycling events does not need to be treated explicitly, but can be related in a simple way to the composition of the atmospheric moisture.

If the number of recycling events is considered to be zero for all water molecules at the moment they are advected across the ocean-land boundary (case A), the two above assumptions suffice to enable an analytical solution: the frequency distribution of recycling events for a given air mass travelling over a continent attains a Poisson distribution. The Poisson distribution is completely determined by its mean value which grows gradually from zero at the upwind coast to finite values within the continent until, finally, the solution loses validity at the moment the air is advected across the downwind coast to the ocean.

For case B, however, I showed that the above solution is only valid if a third condition is met, namely the high intensity limit. The latter implies that the moisture contained in an air mass is exchanged much more than once while the air mass crosses an ocean basin or a continent. In other words, the high intensity limit implies that the evaporation flux integrated over the time it takes air to travel continental distances by far exceeds the air’s vertically integrated moisture content. In this case a Poisson distribution is attained in case B as in case A. By contrast, in case B another solution is attained if the low intensity limit holds. The low intensity limit implies that the alternation between land and ocean of an air mass occurs much faster than it takes to exchange the atmospheric moisture by surface fluxes. The resulting frequency distribution is a (stationary) geometric distribution.

On Earth, the evaporation flux integrated along a typical air mass trajectory across a

continent or an ocean basin is of the same order as the atmosphere's vertically integrated moisture content. This means that neither the low intensity limit nor the high intensity limit can be considered a realistic approximation. Instead, this suggests that actual frequency distributions of recycling events can be thought of as mixtures of Poisson distributions and geometric distributions. However, shifting the focus to case A, the Poisson distribution is indeed a reasonable approximation, where the accuracy depends on the extent to which the actual conditions deviate from the 'well-mixed' assumption and the 'steady-state' assumption. Regarding these assumptions I argued based on qualitative arguments that, while the 'well-mixed' assumption may be appropriate in the extratropics but less appropriate in the tropics, the opposite seems to be the case for the 'steady-state' assumption.

In contrast to the first two chapters, it is not so obvious to what extent the results of Chapter 3 constitute an advancement of our understanding of evaporation-precipitation coupling. My interpretation of continental moisture recycling as a Poisson process may still find some further application in the future, and apart from this I perceive this interpretation as a scientific achievement in its own right.

### Key findings of Chapter 3

- The frequency distribution ( $f$ ) of continental recycling events ( $n$ ) for the water molecules contained in an air parcel attains – given the validity of certain simplifying assumptions – either a Poisson distribution with mean value  $\lambda$  or a geometric distribution with mean value  $r^c/(1 - r^c)$ :

$$\text{Poisson distribution: } f_n = \frac{\lambda^n}{n!} e^{-\lambda} \quad , \quad n \in \mathbb{N}_0$$

$$\text{geometric distribution: } f_n = (r^c)^n (1 - r^c), \quad n \in \mathbb{N}_0$$

- If recycling events are counted since the water molecules last evaporated from the ocean (case B), the requirements for neither of the two solutions are met on Earth. Actual frequency distributions thus appear as mixtures of a Poisson distribution and a geometric distribution.
- If recycling events are counted since the water molecules were last advected across the ocean-land boundary (case A), the Poisson distribution appears as a reasonable approximation. Continental moisture recycling can thus be interpreted as a Poisson process.

## **Further research opportunities**

There are promising opportunities to conduct further research based on each of the three chapters that constitute my dissertation. In the following I will delineate three possibilities as to how, building on my work, our understanding of continental moisture recycling and evaporation-precipitation coupling could be further advanced.

### **Opportunity 1: Transferring the approach of Chapter 1 to smaller scales**

In Chapter 1 I demonstrated that, at the continental scale, source-sink relations of atmospheric moisture (i.e. recycling estimates) cannot be used to infer the sensitivity of precipitation to evaporation. I argued that changes of the large-scale circulation rather than effects due to moisture recycling dominate the response to modified evaporation rates. But it remains an open question whether recycling estimates are more useful indicators at smaller, i.e. more realistic, scales, even though studies on local coupling give rise to some doubts.

One could take the approach I used in Chapter 1 and apply it to smaller spatial scales. One would thus (I) define some interesting evaporative source region, (II) use an AGCM with WVTs to trace the moisture from this source region, (III) again use the AGCM to simulate how precipitation responds when evaporation rates in the source region are modified, (IV) compare the results of the tracing with the simulated response to see to what extent the response can be attributed to moisture recycling, and (V) investigate in how far local coupling and the large-scale circulation contribute to the response. Of course this procedure could be repeated for a number of regions of different spatial extent to get most out of the approach. Investigations of the above delineated kind would be an important step toward the “missing link” I pointed out in the Introduction, and would bring us closer to an answer regarding the question “What do moisture recycling estimates tell us”?

It is important to note that I suggest using an AGCM with WVTs (i.e. online 3D moisture tracing) instead of a 2D scheme such as the one I used for Chapter 1. I showed in Chapter 2 that the errors associated with the 2D approximation can be considered acceptable if the focus is on continental-scale patterns only. This is not the case anymore when smaller scales are investigated, as the example of the western Sahel impressively revealed.

**Opportunity 2: (a) Developing an online 3D moisture tracing scheme with realistic precipitation-water vapour mixing rates, and/or (b) developing a pseudo tracing method that maximizes the relevance of the results for evaporation-precipitation coupling**

I argued in Chapter 2 that online 3D moisture tracing is associated with uncertainties because the gross evaporation and condensation rates that determine the degree of mixing between precipitation and the ambient water vapour are not provided by AGCMs. Instead of trying to develop a scheme based on gross evaporation and condensation rates that are as realistic as possible, I implemented two variants, one of which features very high gross rates (“strong (instantaneous) mixing”, 3D-s), the other only the net rates (“weak mixing”, 3D-w). I then showed that the two variants indeed lead to significantly different results, mostly due to the different degrees of fast-recycling they diagnose.

It should be possible to narrow down the uncertainty associated with this issue and develop an online 3D moisture tracing scheme that utilises more realistic gross rates. The latter can in principle be deduced based on the simple relation  $C = rhR$ , where  $C$  and  $R$  are the gross rates of condensation and re-evaporation and  $rh$  is the air’s relative humidity (e.g. Silberberg et al., 1996). However, this relation cannot easily be applied in an AGCM because the spatial resolution of the latter is much coarser than the scale at which the relevant processes, in particular moist convection, take place. One would therefore have to come up with sophisticated parameterisations that are incorporated into and/or communicate with the already existing parameterisations handling the relevant subgrid-scale processes.

Finally, it would be interesting to investigate whether or not the source-sink relations established with such an improved WVT scheme are also more meaningful when it comes to inferring the sensitivity of precipitation to evaporation. Given the results of Chapter 1, I speculate that potential improvements in this respect – if present at all – are negligible compared to the modulation of the “recycling only”-response caused by the active role of water, i.e. by local coupling and the large-scale circulation. By contrast, it may be possible to come up with a pseudo moisture tracing method that in some yet-to-be-devised way accounts for the effects arising from water’s active role. Such a method would lead to pseudo source-sink relations that are worse compared to ordinary source-sink relations

regarding the question of which paths water takes in the atmosphere, but would be more telling regarding the sensitivity of precipitation to evaporation. Compared to the other two rather clearly delineated research opportunities, this one is the least explicit and by far the most challenging.

**Opportunity 3: Confronting the analytical solutions of Chapter 3 with explicitly simulated frequency distributions**

In Chapter 3 I had to introduce simplifying assumptions in order to arrive at the analytical solutions for the frequency distribution of continental recycling events. For case A (recycling events are counted since the water molecules were last advected across the ocean-land boundary) I found that the accuracy of the analytical solution – the Poisson distribution – depends on the adequacy of two assumptions, namely the ‘well-mixed’ assumption and the ‘steady-state’ assumption. For case B (recycling events are counted since the water molecules last evaporated from the ocean) I found that, even if the two above mentioned assumptions are perfectly valid, neither of the two limit cases – the Poisson distribution in the high intensity limit and the geometric distribution in the low intensity limit – are attained because the conditions on Earth are somewhere between these limit cases.

It is possible to simulate frequency distributions of continental recycling events explicitly with an AGCM that is equipped with WVTs (e.g. ECHAM6 with the WVT scheme I implemented as described in Chapter 2). One would have to modify the implementation such that WVT species are not distinguished by their evaporative source region, but by the number of recycling events. It would also be necessary – if the ‘steady-state’ assumption is not applied – to treat the continental (sub-)surface reservoirs explicitly. In fact, exactly this has already been done by Numaguti (1999). However, in that study the frequency distributions were not further investigated.

Once these feasible modifications are implemented, one could quantify the extent to which the explicitly simulated frequency distributions deviate from the theoretical solutions. Moreover, one could investigate the influence of the assumptions that were necessary for the theoretical solutions one by one. To this end one could artificially enforce the validity of either the ‘well-mixed’ assumption (which would correspond to the 2D tracing variant in Chapter

2), or the ‘steady-state’ assumption (by relating the composition of the land evaporation to the composition of the atmospheric water vapour), or both. Finally, one could simulate the two cases A and B separately, giving in total 8 (2x2x2) simulations that could be analysed to assess the realism of the analytical solutions.

## **What have we learned?**

The title of my dissertation raises expectations that we should by now have learned something about continental moisture recycling and evaporation-precipitation coupling. And indeed, among other things we have learned that continental moisture recycling can be interpreted as a Poisson process, that the ‘well-mixed’ assumption scarcely holds but 2D moisture tracing nevertheless gives reasonable results in the extratropics – while this cannot be said of the tropics –, and that source-sink relations of atmospheric moisture are not necessarily useful indicators for the sensitivity of precipitation to evaporation.

However, a reader with particular interest in the exact nature of the mechanisms by which evaporation affects precipitation due to water’s role as an *active* component of the atmosphere may find his or her expectations unfulfilled. Regarding my investigations on continental moisture recycling as a Poisson process, I would even go so far as to say that they contribute hardly anything to the question of how precipitation responds to modified evaporation. A sceptic might simply concur with Cameron’s declaration that “not everything that can be counted counts”. To me, however, finding that continental moisture recycling can be interpreted as a Poisson process is a valuable contribution to the science of global-scale hydrology in its own right. And who knows, at some point someone may pick up my ideas on counting water molecules and derive something that is of more direct relevance to the question of evaporation-precipitation coupling.

By contrast, the work I presented in Chapters 1 and 2 is of direct relevance to current and future research not only on moisture recycling *per se*, but also on evaporation-precipitation coupling in a more general sense. Moreover, to formulate the title of Chapter 1 as a question – “What do moisture recycling estimates tell us?” – was a conscious decision: I want to call attention to a knowledge gap, a missing link, that was previously not perceived as such. To

identify and expose this missing link is the main purpose of Chapter 1 – the partial answer I gave comes second. I proposed two in my view promising ways in which, building on the results of Chapters 1 and 2, one could advance towards a more comprehensive answer (opportunities 1 and 2). It will however be a long time before one can say with confidence that we entirely understand how evaporation-precipitation coupling works. The blame lies with the complexity of water's active role in the atmosphere.



# Bibliography

- Beljaars, A. C. M.; Viterbo, P.; Miller, M. J., and Betts, A. K. The anomalous rainfall over the United States during July 1993: Sensitivity to land surface parameterization and soil moisture anomalies. *Monthly Weather Review*, 124(3):362–383, 1996.
- Benton, G. S.; Blackburn, R. T., and Snead, V. O. The role of the atmosphere in the hydrologic cycle. *EOS Trans. AGU*, 31:61–73, 1950.
- Bosilovich, M. G. On the vertical distribution of local and remote sources of water for precipitation. *Meteorol. Atmos. Phys.*, 80:31–41, 2002.
- Bosilovich, M. G. and Schubert, S. D. Water vapor tracers as diagnostics of the regional hydrologic cycle. *J. Hydrometeor.*, 3:149–165, 2002.
- Bosilovich, M. G.; Sud, Y.; Schubert, S. D., and Walker, G. K. GEWEX CSE sources of precipitation using GCM water vapor tracers. *Global Energy and Water Cycle Experiment NEWS*, 3:6–7, 2002.
- Brubaker, K. L.; Entekhabi, D., and Eagleson, P. S. Estimation of continental precipitation recycling. *J. Clim.*, 6:1077–1089, 1993.
- Budyko, M. I. Climate and Life. *Int. Geophys. Ser.*, 18, 1974.
- Burde, G. I. Bulk recycling models with incomplete vertical mixing. Part I: Conceptual framework and models. *Journal of climate*, 19(8):1461–1472, 2006.
- Burde, G. I. and Zangvil, A. The Estimation of Regional Precipitation Recycling. Part II: A New Recycling Model. *J. Climate*, 14:2509–2527, 2001.
- Danielson, E.W.; Levin, J., and Abrams, E. *Meteorology*. WCB/McGraw-Hill, 2003.

## Bibliography

- Dansgaard, W. Stable isotopes in precipitation. *Tellus*, 16(4):436–468, 1964.
- Dee, D.P.; Uppala, S.M.; Simmons, A.J.; Berrisford, P.; Poli, P.; Kobayashi, S.; Andrae, U.; Balmaseda, M.A.; Balsamo, G.; Bauer, P., and others, . The ERA-Interim reanalysis: Configuration and performance of the data assimilation system. *Quarterly Journal of the Royal Meteorological Society*, 137(656):553–597, 2011.
- Dirmeyer, P. Interactive comment on “Analyzing precipitation sheds to understand the vulnerability of rainfall dependent regions” by P. W. Keys et al. *Biogeosciences Discussions*, 8:C4544–C4546, 2011.
- Dirmeyer, P. A. and Brubaker, K. L. Characterization of the global hydrologic cycle from a back-trajectory analysis of atmospheric water vapor. *Journal of Hydrometeorology*, 8(1): 20–37, 2007.
- Dirmeyer, P. A.; Koster, R. D., and Guo, Z. Do global models properly represent the feedback between land and atmosphere? *Journal of Hydrometeorology*, 7(6):1177–1198, 2006.
- Dirmeyer, P. A.; Schlosser, C. A., and Brubaker, K. L. Precipitation, recycling, and land memory: An integrated analysis. *Journal of Hydrometeorology*, 10(1):278–288, 2009.
- Dirmeyer, P.A. and Brubaker, K.L. Contrasting evaporative moisture sources during the drought of 1988 and the flood of 1993. *Journal of geophysical research*, 104:19, 1999.
- Eltahir, E. A. B. and Bras, R. L. Precipitation recycling in the Amazon basin. *Quarterly Journal of the Royal Meteorological Society*, 120(518):861–880, 1994.
- Findell, K. L. and Eltahir, E. A. B. An analysis of the soil moisture-rainfall feedback, based on direct observations from Illinois. *Water Resources Research*, 33(4):725–735, 1997.
- Findell, K. L. and Eltahir, E. A. B. Atmospheric controls on soil moisture-boundary layer interactions. Part I: Framework development. *Journal of Hydrometeorology*, 4(3):552–569, 2003a.
- Findell, K. L. and Eltahir, E. A. B. Atmospheric controls on soil moisture-boundary layer interactions. Part II: Feedbacks within the continental United States. *Journal of Hydrometeorology*, 4(3):570–583, 2003b.
- Findell, K. L.; Gentine, P.; Lintner, B. R., and Kerr, C. Probability of afternoon precipitation in eastern United States and Mexico enhanced by high evaporation. *Nature Geoscience*, 4(7):434–439, 2011.

- Fitzmaurice, J. A. A critical analysis of bulk precipitation recycling models, 2007. Ph.D. thesis, Massachusetts Institute of Technology.
- Garratt, J.R. *The atmospheric boundary layer*. Cambridge University Press, Cambridge, 1992.
- Goessling, H. F. and Reick, C. H. What do moisture recycling estimates tell us? Exploring the extreme case of non-evaporating continents. *Hydrology and Earth System Sciences*, 15(10):3217, 2011. **(reproduced in Chapter 1 of this dissertation)**.
- Goessling, H. F. and Reick, C. H. Atmospheric water vapour tracers and the significance of the vertical dimension. *Atmospheric Chemistry and Physics Discussions*, acp-2012-743, 2012. **(reproduced in Chapter 2 of this dissertation)**.
- Hagemann, S.; Arpe, K., and Roeckner, E. Evaluation of the Hydrological Cycle in the ECHAM5 Model. *J. Climate*, 19:3810–3827, 2006.
- Hohenegger, C.; Brockhaus, P.; Bretherton, C. S., and Schaer, C. The soil moisture-precipitation feedback in simulations with explicit and parameterized convection. *Journal of Climate*, 22(19):5003–5020, 2009.
- Hou, A.Y. and Lindzen, R.S. The Influence of Concentrated Heating on the Hadley Circulation. *Journal of the Atmospheric Sciences*, 49(14):1233–1241, 1992.
- IPCC *Climate change 2007: the physical science basis: contribution of Working Group I to the Fourth Assessment Report of the Intergovernmental Panel on Climate Change*. Cambridge University Press, 2007.
- Jöckel, P.; von Kuhlmann, R.; Lawrence, M.G.; Steil, B.; Brenninkmeijer, C.A.M.; Crutzen, P.J.; Rasch, P.J., and Eaton, B. On a fundamental problem in implementing flux-form advection schemes for tracer transport in 3-dimensional general circulation and chemistry transport models. *Quarterly Journal of the Royal Meteorological Society*, 127(573):1035–1052, 2001.
- Joussaume, S.; Sadourny, R., and Vignal, C. Origin of precipitating water in a numerical simulation of July climate. *Ocean-Air Interact.*, 1:43–56, 1986.
- Keys, P.W.; van der Ent, R.J.; Gordon, L.J.; Hoff, H.; Nikoli, R., and Savenije, H.H.G. Analyzing precipitation sheds to understand the vulnerability of rainfall dependent regions. *Biogeosciences*, 9:733–746, 2012.

## Bibliography

- Kiehl, J.T. and Trenberth, K.E. Earth's annual global mean energy budget. *Bulletin of the American Meteorological Society*, 78(2):197–208, 1997.
- Kleidon, A. and Heimann, M. Assessing the role of deep rooted vegetation in the climate system with model simulations: mechanism, comparison to observations and implications for Amazonian deforestation. *Climate Dynamics*, 16:183–199, 2000.
- Koster, R.; Jouzel, J.; Suozzo, R.; Russell, G.; Broecker, W.; Rind, D., and Eagleson, P. Global sources of local precipitation as determined by the Nasa/Giss GCM. *Geophys. Res. Lett.*, 13(2):121–124, 1986.
- Koster, R. D.; Dirmeyer, P. A.; Guo, Z.; Bonan, G.; Chan, E.; Cox, P.; Gordon, C. T.; Kanae, S.; Kowalczyk, E.; Lawrence, D.; Liu, P.; Lu, C. H.; Malyshev, S.; McAvaney, B.; Mitchell, K.; Mocko, D.; Oki, T.; Oleson, K.; Pitman, A.; Sud, Y. C.; Taylor, C. M.; Versegny, D.; Vasic, R.; Xue, Y., and Yamada, T. Regions of strong coupling between soil moisture and precipitation. *Science*, 305(5687):1138, 2004. doi: 10.1126/science.1100217.
- Lettau, H.; Lettau, K., and Molion, L. C. B. Amazonia's Hydrologic Cycle and the Role of Atmospheric Recycling in Assessing Deforestation Effects. *Mon. Weather Rev.*, 107(3): 227–238, 1979.
- Lin, S.-J. and Rood, R.B. Multidimensional flux-form semi-Lagrangian transport schemes. *Monthly Weather Reviews*, 124:2046–2070, 1996.
- Nordeng, T. E. Extended versions of the convection parametrization scheme at ECMWF and their impact upon the mean climate and transient activity of the model in the tropics. Technical report, Research Department Technical Memorandum, ECMWF, Reading, UK, 1994.
- Numaguti, A. Origin and recycling processes of precipitating water over the Eurasian continent: Experiments using an atmospheric general circulation model. *J. Geophys. Research*, 104:1957–1972, 1999.
- Pal, J. S. and Eltahir, E. A. B. Pathways relating soil moisture conditions to future summer rainfall within a model of the land-atmosphere system. *Journal of Climate*, 14(6):1227–1242, 2001.
- Press, W. H.; Teukolsky, S. A.; Vetterling, W. T., and Flannery, B. P. *Numerical recipes: the art of scientific computing*. Cambridge Univ Pr, 2007. ISBN 0521880688.
- Raddatz, T. J.; Reick, C.H.; Knorr, W.; Kattge, J.; Roeckner, E.; Schnur, R.; Schnitzler, K. G.; Wetzell, P., and Jungclaus, J. Will the tropical land biosphere dominate the

- climate-carbon cycle feedback during the twenty-first century? *Clim. Dyn.*, 29:565–574, 2007.
- Roeckner, E.; Baeuml, G.; Bonaventura, L.; Brokopf, R.; Esch, M.; Giorgetta, M.; Hagemann, S.; Kirchner, I.; Kornblueh, L.; Manzini, E.; Rhodin, A.; Schlese, U.; Schulweida, U., and Tompkins, A. The atmospheric general circulation model ECHAM5. Part I: Model description. Technical Report 349, Max Planck Institute for Meteorology, Hamburg, Germany, 2003.
- Ross, S.M. *Stochastic processes*, volume 23. John Wiley & Sons New York, 1983.
- Rowntree, P. R. and Bolton, J. A. Simulation of the atmospheric response to soil moisture anomalies over Europe. *Quarterly Journal of the Royal Meteorological Society*, 109(461): 501–526, 1983. ISSN 1477-870X.
- Saeed, F.; Hagemann, S., and Jacob, D. Impact of irrigation on the South Asian summer monsoon. *Geophysical Research Letters*, 36(20):L20711, 2009.
- Salati, E.; Dall'Olio, A.; Matsui, E., and Gat, J. R. Recycling of water in the Amazon basin: an isotopic study. *Water Resources Research*, 15(5):1250–1258, 1979.
- Salvucci, G. D.; Saleem, J. A., and Kaufmann, R. Investigating soil moisture feedbacks on precipitation with tests of Granger causality. *Advances in water resources*, 25(8-12): 1305–1312, 2002.
- Savenije, H. H. G. New definitions for moisture recycling and the relation with land-use changes in the Sahel. *J. Hydrol.*, 167:57–78, 1995.
- Savenije, H.H.G. The importance of interception and why we should delete the term evapotranspiration from our vocabulary. *Hydrological Processes*, 18(8):1507–1511, 2004.
- Schär, C.; Luethi, D.; Beyerle, U., and Heise, E. The soil-precipitation feedback: A process study with a regional climate model. *Journal of Climate*, 12(3):722–741, 1999. ISSN 1520-0442.
- Seneviratne, S. I.; Corti, T.; Davin, E. L.; Hirschi, M.; Jaeger, E. B.; Lehner, I.; Orlowsky, B., and Teuling, A. J. Investigating soil moisture-climate interactions in a changing climate: A review. *Earth-Science Reviews*, 99(3-4):125–161, 2010. ISSN 0012-8252.
- Shukla, J. and Mintz, Y. Influence of land-surface evapotranspiration on the Earth's climate. *Science*, 215:1498–1501, 1982.

## Bibliography

- Shukla, J.; Nobre, C., and Sellers, P. Amazon deforestation and climate change. *Science*, 247(4948):1322–1325, 1990.
- Silberberg, M.S.; Duran, R.; Haas, C.G., and Norman, A.D. *Chemistry: The Molecular Nature of Matter and Change*. Mosby, 1996.
- Sodemann, H.; Wernli, H., and Schwierz, C. Sources of water vapour contributing to the Elbe flood in August 2002 – A tagging study in a mesoscale model. *Quarterly Journal of the Royal Meteorological Society*, 135(638):205–223, 2009.
- Spracklen, D. V.; Arnold, S. R., and Taylor, C. M. Observations of increased tropical rainfall preceded by air passage over forests. *Nature*, 2012. advance online publication.
- Stevens, B. Atmospheric moist convection. *Annu. Rev. Earth Planet. Sci.*, 33:605–643, 2005.
- Stohl, A. and James, P. A Lagrangian analysis of the atmospheric branch of the global water cycle. Part I: Method description, validation, and demonstration for the August 2002 flooding in Central Europe. *Journal of Hydrometeorology*, 5(4):656–678, 2004.
- Taylor, C. M.; Parker, D. J., and Harris, P. P. An observational case study of mesoscale atmospheric circulations induced by soil moisture. *Geophysical Research Letters*, 34, 2007.
- Taylor, C. M.; Gounou, A.; Guichard, F.; Harris, P. P.; Ellis, R. J.; Couvreur, F., and De Kauwe, M. Frequency of Sahelian storm initiation enhanced over mesoscale soil-moisture patterns. *Nature Geoscience*, 2011.
- Tiedtke, M. A comprehensive mass flux scheme for cumulus parameterization in large-scale models. *Monthly Weather Review*, 117(8):1779–1800, 1989.
- Trenberth, K. E. Atmospheric Moisture Recycling: Role of Advection and Local Evaporation. *J. Climate*, 12:1368–1381, 1999.
- van den Hurk, B. J. J. M. and Blyth, E. WATCH/LoCo Workshop. 25–27 June 2008. De Bilt, The Netherlands. *GEWEX news*, pages 12–14, 2008.
- van den Hurk, B. J. J. M. and van Meijgaard, E. Diagnosing land-atmosphere interaction from a regional climate model simulation over West Africa. *Journal of Hydrometeorology*, 11(2):467–481, 2010.
- van der Ent, R. J. and Savenije, H. H. G. Length and time scales of atmospheric moisture recycling. *Atmos. Chem. Phys*, 11:1853–1863, 2011.

- van der Ent, R. J.; Savenije, H. H. G.; Schaeffli, B., and Steele-Dunne, S. C. Origin and fate of atmospheric moisture over continents. *Water Resour. Res.*, 46, 2010.
- Werth, D. and Avissar, R. The local and global effects of Amazon deforestation. *J. Geophys. Res.*, 107(D20):8087, 2002.
- Yoshimura, K.; Oki, T.; Ohte, N., and Kanae, S. Colored moisture analysis estimates of variations in 1998 Asian monsoon water sources. *J. Meteorol. Soc. Jpn.*, 82(5):1315–1329, 2004.



## Acknowledgements

A large number of great people made the work in hand possible. First of all, I am indebted to Christian Reick and Martin Claussen, who made a superb job of supervising and guiding me and my research. In this context I am also grateful to Andreas Chlond who chaired my advisory panel. For continuous support with modelling issues I heartily thank Veronika Gayler, Reiner Schnur, Thomas Raddatz, and Sebastian Rast. For proofreading, reviewing, and editing I am grateful to Robert Sutcliffe, Andreas Chlond, Cathy Hohenegger, Sebastian Rast, Rudi van der Ent, Paul Dirmeyer, and Bart van den Hurk. I also thank people at the European Centre for Medium-range Weather Forecast for a fertile summer course, and Omar Bellprat, Sonia Seneviratne, and Christoph Schär for supporting my visit at the ETH Zürich.

For organisational support and further help I am very grateful to Antje Weitz and Cornelia Kampmann, the good souls of the International Max Planck Research School on Earth System Modelling that I was part of, and to Barbara Zinecker and Sylvia Houston, the good souls of the ‘Land in the Earth System’ department. Further, I thank the staff at the Max Planck Institute for Meteorology’s administration and Central IT Services, and the staff at the German Climate Computing Center (DKRZ) where I conducted my numerical simulations. For vivid discussions, some more and some less research-related, I warmly thank my ‘roommates’ Sebastian Bathiany, Jessica Engels and Fabio Cresto-Aleina.

Last but not least I am very grateful to my parents and parents-in-law for their unceasing support, and – most of all – to my dear wife Steffi: By bearing the greater share of raising our three wonderful daughters, she – a scientist herself – made and makes it possible that I can run free in my enthusiasm about natural science. As a token of gratitude I dedicate this doctoral thesis to her.



# Appendix A

## Supplementary material for Chapter 1

## A.1 Effect of different averaging methods on recycling estimates

Since former studies showing continental recycling ratios used different methods to aggregate (average) recycling ratios over time, we show in Fig. A.1 the differences that arise from different averaging methods (compare Sect. 1.4 in the main text).

For every time step one has a field of continental recycling ratios ( $R_c$ ). There are two ways to average them over time, either uniformly:

$$\langle R_c \rangle_\tau = \sum_{t=t_1}^{t_N} \left( \frac{1}{N} \cdot R_c(t) \right) \quad (\text{A.1})$$

or weighted according to the precipitation rate  $p(t)$ :

$$\langle R_c \rangle_\pi = \sum_{t=t_1}^{t_N} \left( \frac{p(t)}{\sum_{t'=t_1}^{t_N} p(t')} \cdot R_c(t) \right). \quad (\text{A.2})$$

Please note that  $\langle R_c \rangle_\pi$  is not defined at locations that do not receive any precipitation in the considered time interval.

While the uniformly weighted mean  $\langle R_c \rangle_\tau$  (Eq. A.1) represents the average fraction of recycled (continental) moisture in precipitable water, the precipitation-weighted mean  $\langle R_c \rangle_\pi$  (Eq. A.2) corresponds to the fraction of recycled (continental) moisture in precipitation. The resulting difference is large if (and only if) precipitation and  $R_c$  covary significantly in time. The difference plots in Fig. A.1 reveal that the two methods yield very similar results for monthly means, meaning that precipitation and  $R_c$  do not strongly covary at the monthly time scale. However, differences are considerably larger for annual means, meaning that precipitation and  $R_c$  covary much more at the annual time scale.

In the strongly seasonal northern extratropics an interesting aspect can be seen from the differences between the annual means (bottom right): Since  $R_c$  is high in northern summer and low in northern winter, regions that receive more precipitation in summer are red in the figure (e.g. eastern/northern Asia and Canada:  $\langle R_c \rangle_\pi$  is larger than  $\langle R_c \rangle_\tau$ ) and

A.1 Effect of different averaging methods on recycling estimates

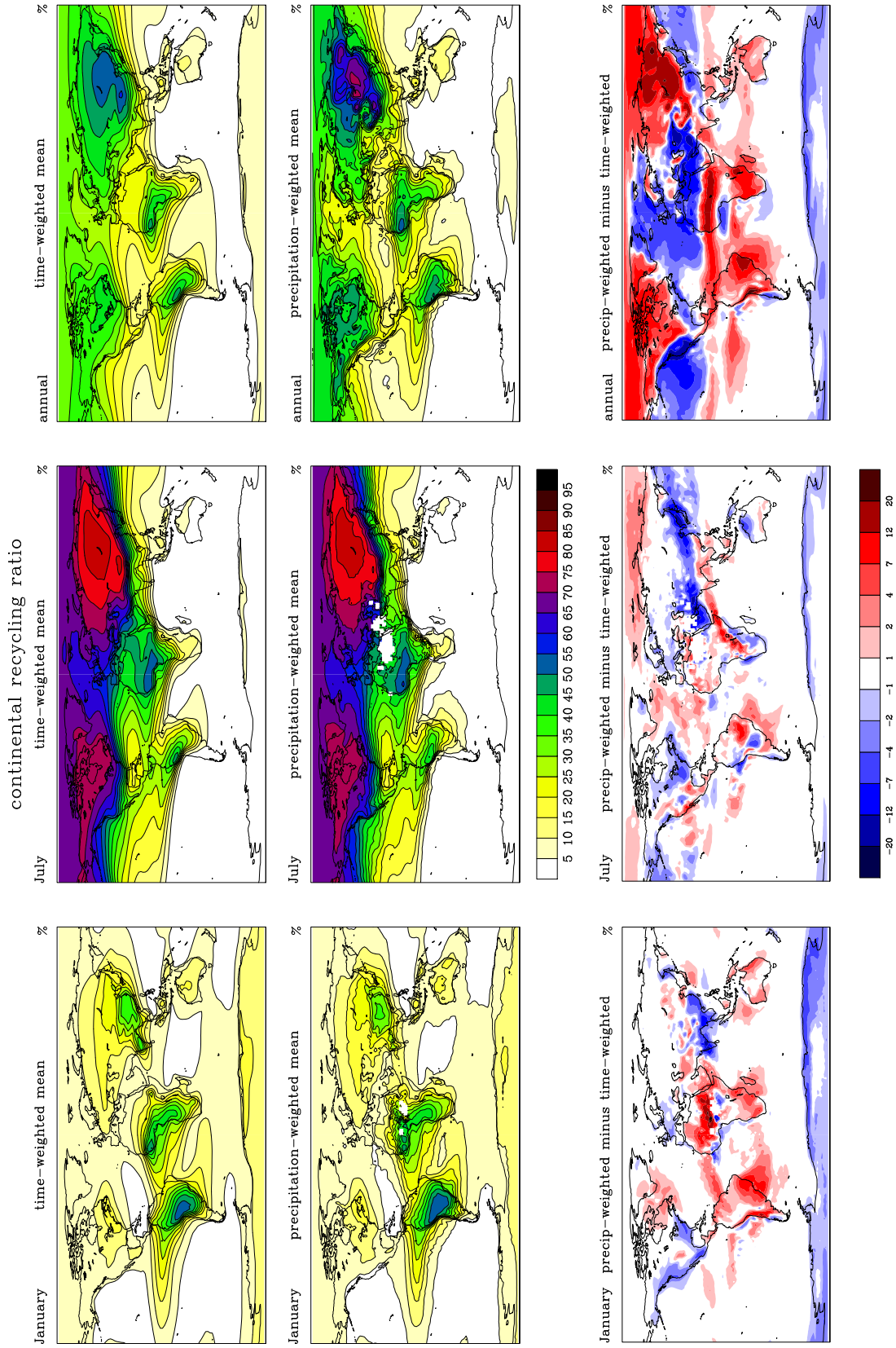


Figure A.1: Comparison of continental recycling ratios ( $R_c$ ) that have been aggregated differently over time. Left column: January. Middle column: July. Right column: annual. Top row: Uniformly weighted time-means ( $\langle R_c \rangle_\tau$  in Eq. A.1). Middle row: Precipitation-weighted time-means ( $\langle R_c \rangle_\pi$  in Eq. A.2). Bottom row: Difference between the precipitation-weighted and the uniformly weighted time-means.

regions that receive more precipitation in winter are blue (e.g. the North Atlantic and the Mediterranean Basin:  $\langle R_c \rangle_\pi$  is smaller than  $\langle R_c \rangle_\tau$ ).

The patchy white grid cells occurring in the panels showing  $\langle R_c \rangle_\pi$  (middle row) are spots where there is no precipitation in any single time step of the 30 months used for the analysis. Infrequent precipitation events (i.e. low sample sizes) are also one reason why the fields of precipitation-weighted values are less smooth than the fields of the simple uniformly weighted means. Note that in chap. 1 we show only  $\langle R_c \rangle_\pi$ , as Bosilovich et al. (2002), Yoshimura et al. (2004), and van der Ent et al. (2010), while Numaguti (1999) shows  $\langle R_c \rangle_\tau$ .

## **A.2 Simulations with an alternative moist-convection scheme**

To address the uncertainty associated with the parameterisation of moist convection, we show in Fig. A.2 how precipitation responds to the suppression of continental evaporation when the original Tiedtke mass-flux scheme is used instead of the standard scheme of the MPI-ESM (see Sects. 1.3.1 and 1.5 in the main text).

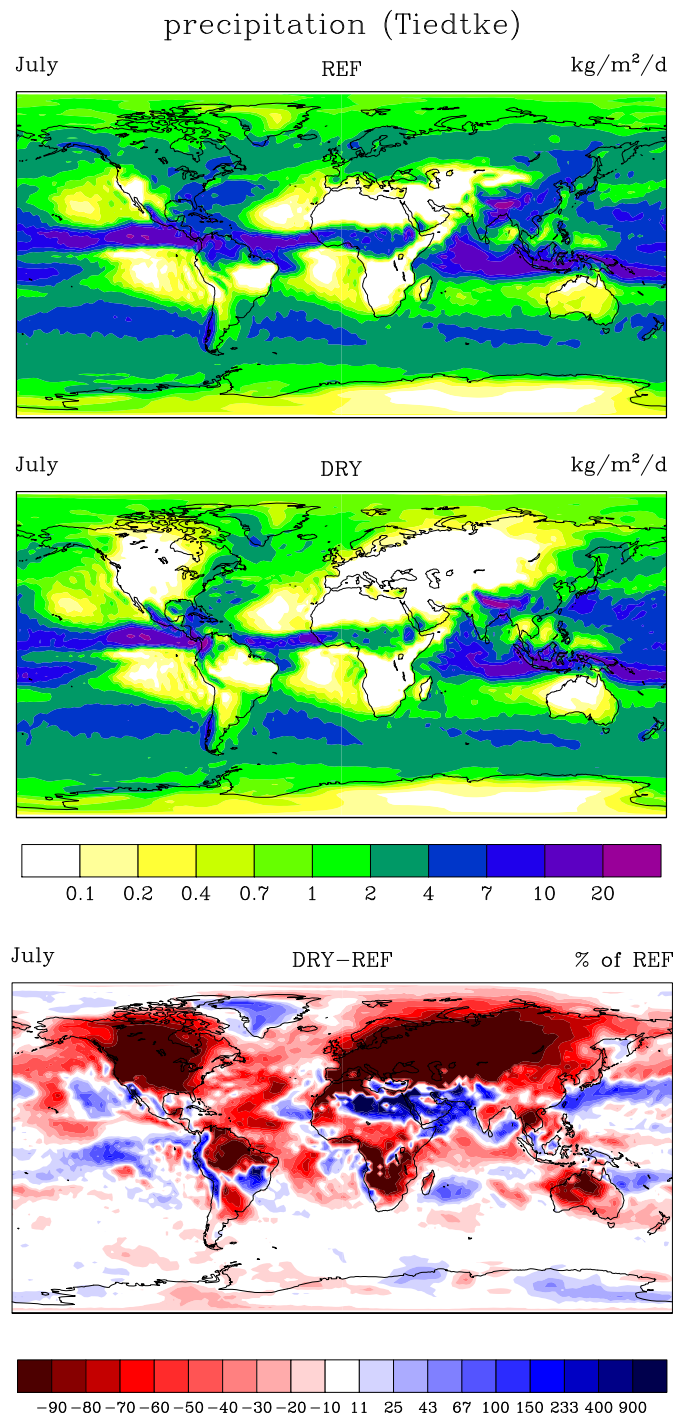


Figure A.2: Precipitation ( $\text{kg m}^{-2} \text{d}^{-1}$ ) with the Tiedtke convection scheme in July in the REF experiment (top), in the DRY experiment (middle), and the difference between the two (bottom, %). The values of the blue part of the colour scale of the difference plot equate to (10 %, 20 %, ..., 90 %) in relation to the DRY experiment. The corresponding figure in the main text showing the results with the standard scheme of the MPI-ESM is Fig. 1.4.

## **A.3 Results from the standard moist-convection scheme for January**

In the main text we focus on the results for July (Sect. 1.5, Figs. 1.4, 1.5, 1.6, 1.7, 1.9, and 1.10), where continental evaporation and, hence, moisture recycling are most pronounced. Figures A.3–A.8 show the corresponding situation for January.

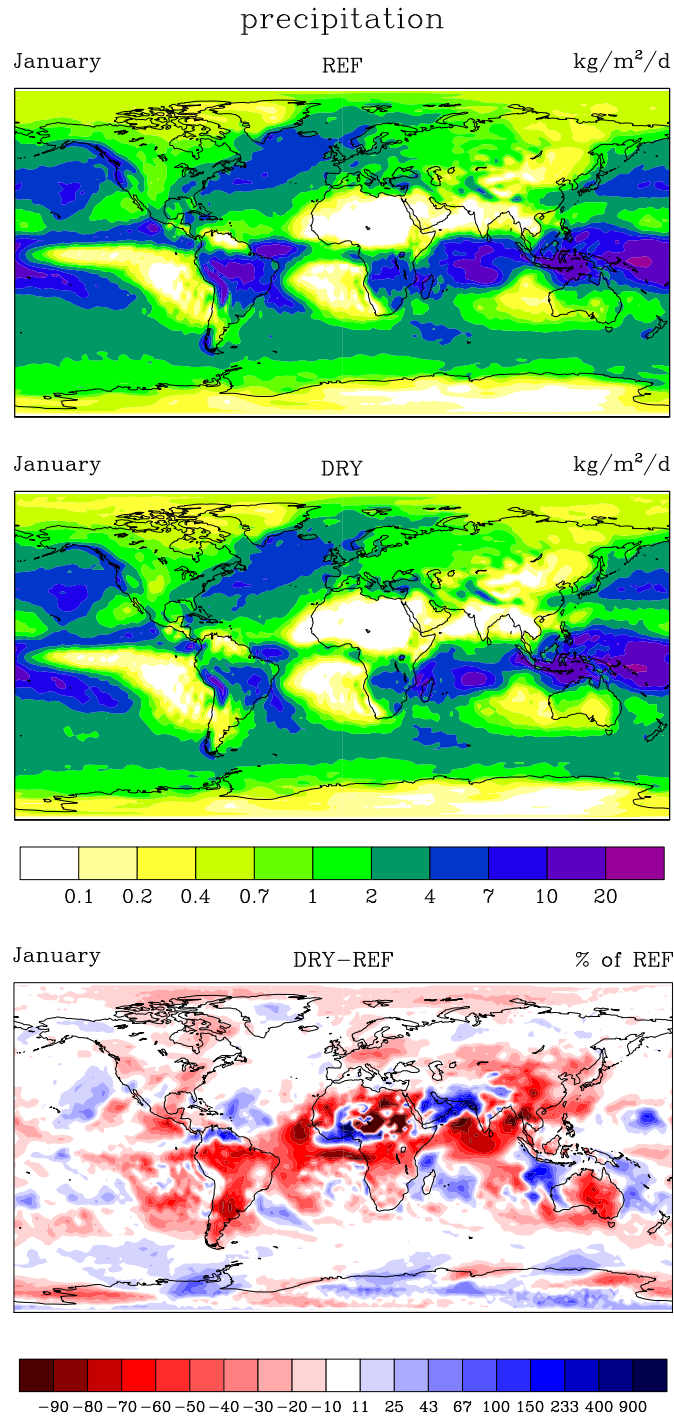


Figure A.3: Precipitation ( $\text{kg m}^{-2} \text{d}^{-1}$ ) with the standard convection scheme in January in the REF experiment (top), in the DRY experiment (middle), and the difference between the two (bottom, %). The values of the blue part of the colour scale of the difference plot equate to (10 %, 20 %, ..., 90 %) in relation to the DRY experiment. The corresponding figure in the main text showing the results for July is Fig. 1.4.

A.3 Results from the standard moist-convection scheme for January

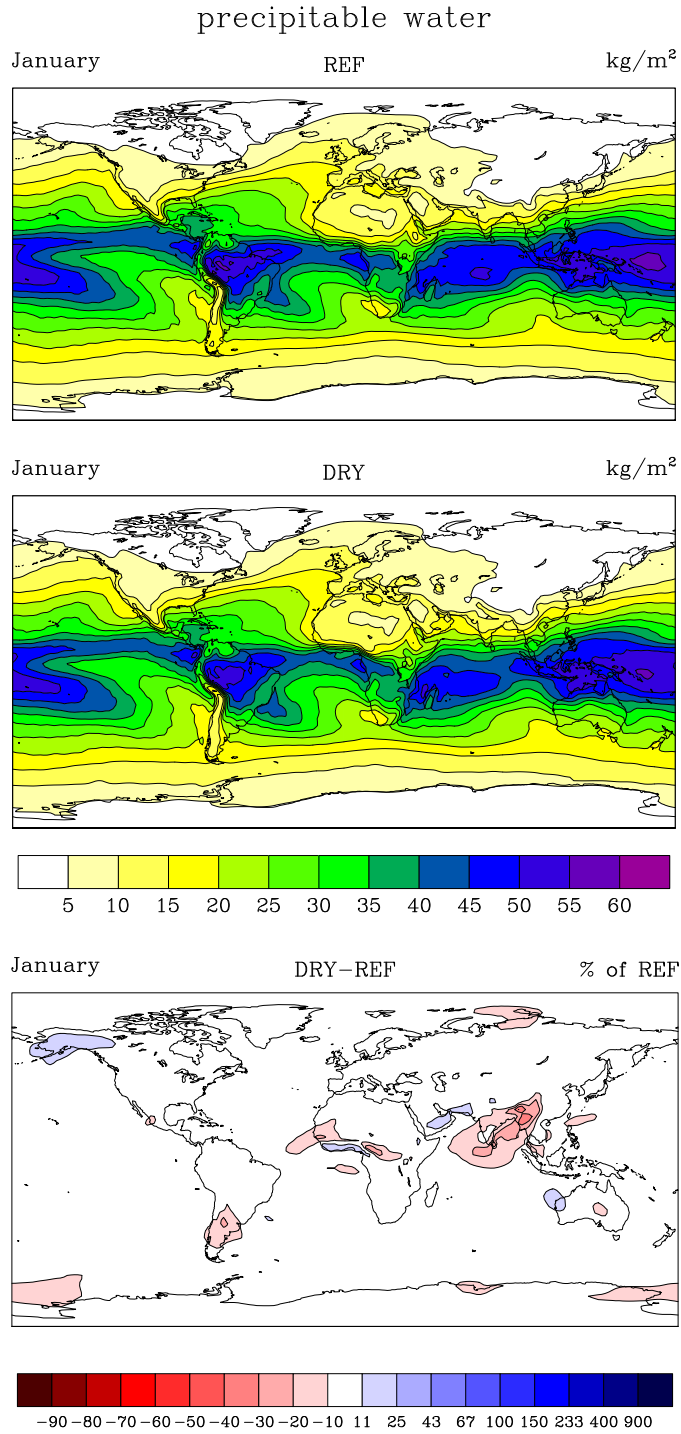


Figure A.4: Precipitable water ( $\text{kg m}^{-2}$ , vapour + liquid + ice) with the standard convection scheme in January in the REF experiment (top), in the DRY experiment (middle), and the difference between the two (bottom, %). The values of the blue part of the colour scale of the difference plot equate to (10%, 20%, ..., 90%) in relation to the DRY experiment. The corresponding figure in the main paper showing the results for July is Fig. 1.5.

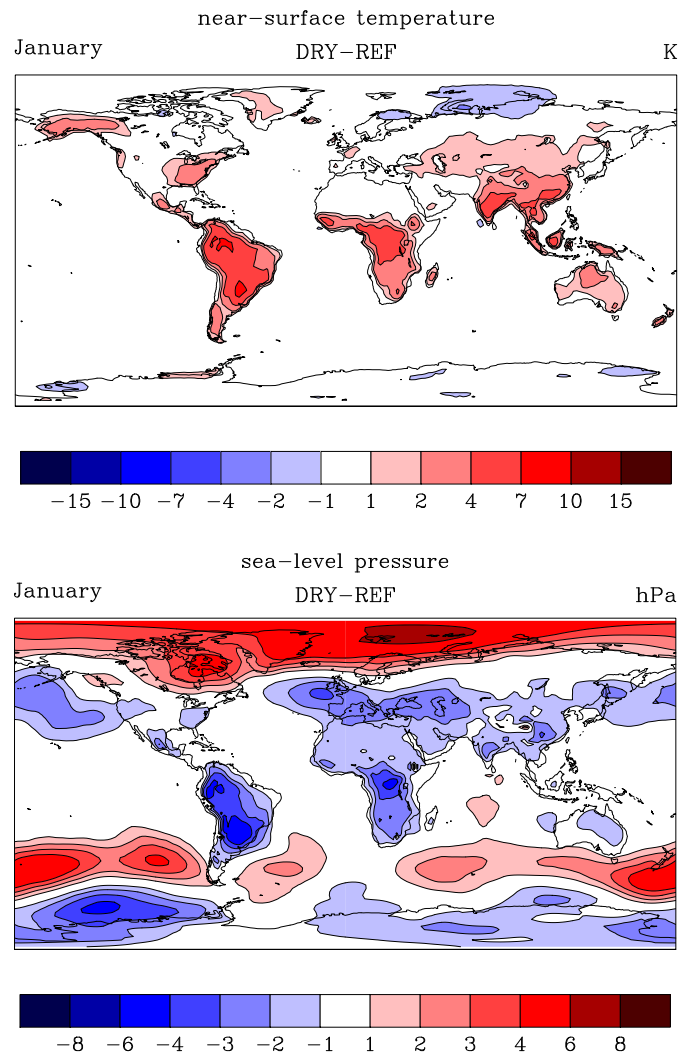


Figure A.5: Top: Difference in near-surface (2m) temperature in January (K, DRY-REF). Bottom: Difference in pressure reduced to sea-level in July (hPa, DRY-REF). Both with the standard convection scheme. The corresponding figure in the main text showing the results for July is Fig. 1.6.

### A.3 Results from the standard moist-convective scheme for January

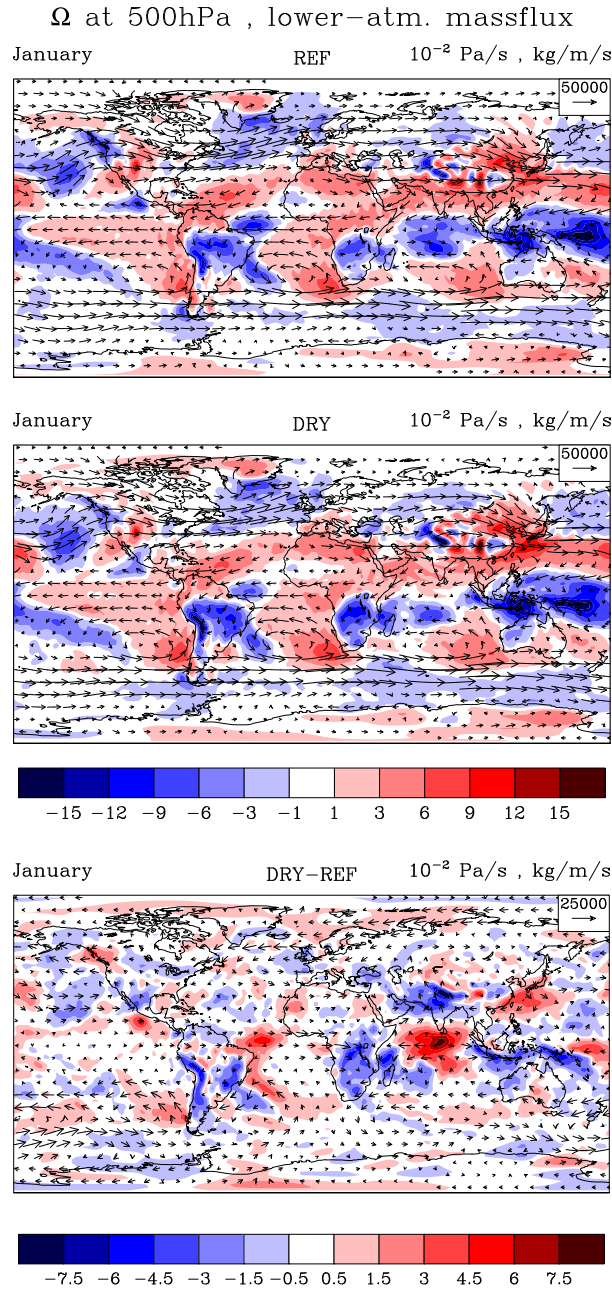


Figure A.6: Vertical velocity ( $\Omega$ ) at 500 hPa (colours,  $\text{Pa s}^{-1}$ ) and horizontal total mass flux in the lowest 13 model levels (arrows,  $\text{kg m}^{-1} \text{s}^{-1}$ ) with the standard convection scheme in January in the REF experiment (top), in the DRY experiment (middle), and the difference between the two (bottom). The lowest 13 model levels correspond approximately to the lower half of the atmosphere. Hence, the vertical velocity at 500 hPa approximately corresponds to the divergence of the shown mass flux. Note that the scale for both  $\Omega$  and the mass flux are changed by a factor 2 in the bottom panel to make the differences better visible. The corresponding figure in the main text showing the results for July is Fig. 1.7.

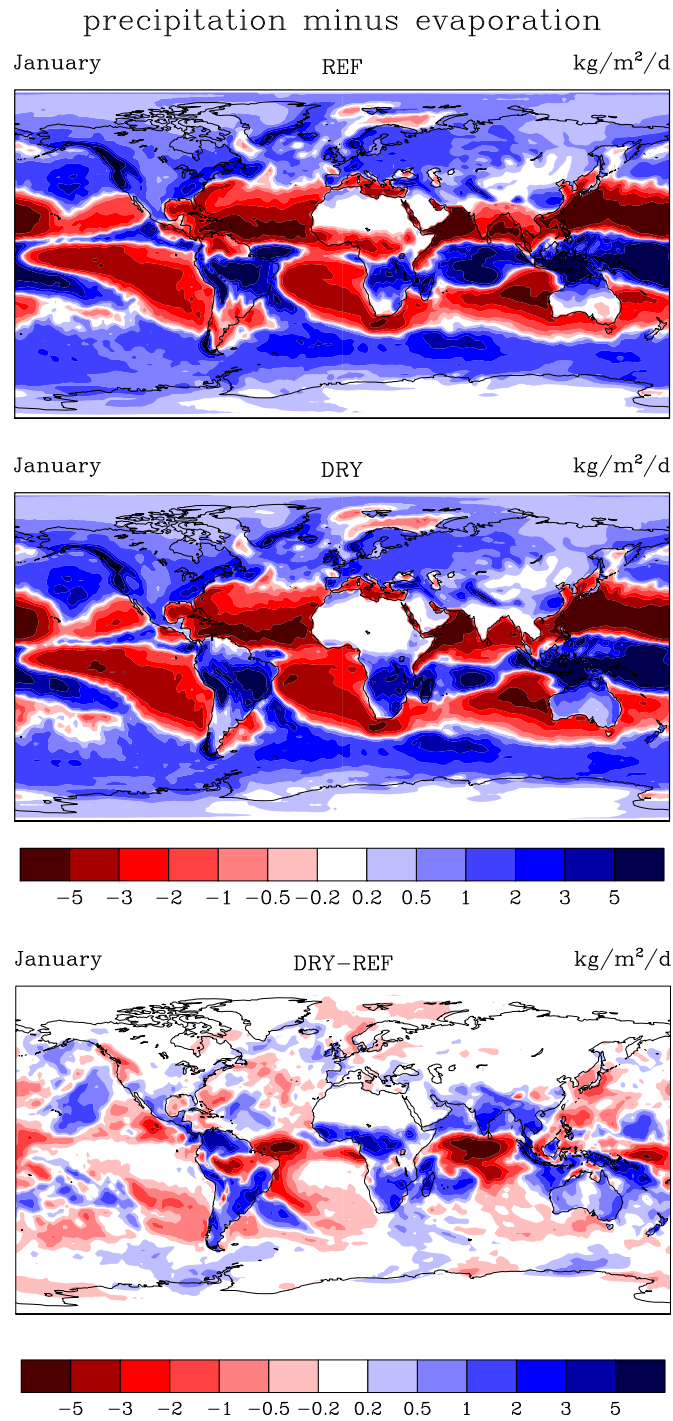


Figure A.7: Precipitation minus evaporation ( $\text{kg m}^{-2} \text{d}^{-1}$ ) with the standard convection scheme in January in the REF experiment (top), in the DRY experiment (middle), and the difference between the two (bottom). The corresponding figure in the main text showing the results for July is Fig. 1.9.

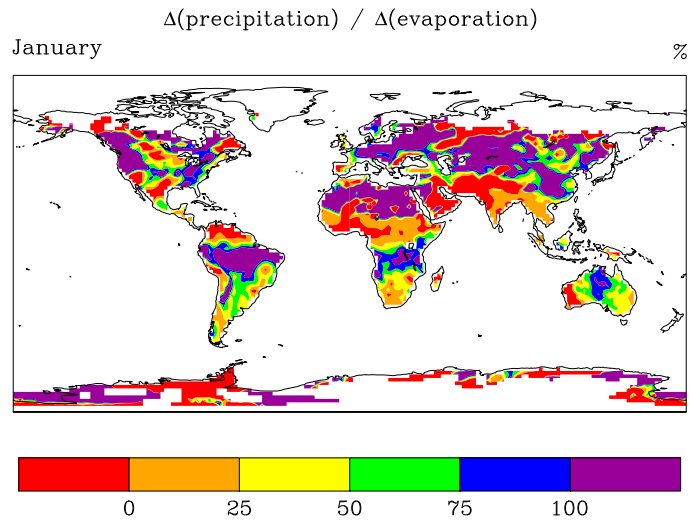


Figure A.8: The response of precipitation in relation to the imposed evaporation decrease ( $\frac{P_{REF}-P_{DRY}}{E_{REF}}$ , %) with the standard convection scheme in January. Violet indicates over-compensation (the land becomes a weaker moisture sink), blue, green, yellow and orange indicate incomplete compensation (precipitation still decreases, but the land becomes a stronger moisture sink or weaker moisture source), and red indicates amplification (precipitation increases and hence adds to the evaporation decrease). Continental regions with negative evaporation (= dew) in the REF experiment are left white. The corresponding figure in the main text showing the results for July is Fig. 1.10.





